AWARD NUMBER: W81XWH-16-1-0566

TITLE: Polycaprolactone-collagen Composite Biomaterials for Mandible Regeneration

PRINCIPAL INVESTIGATOR: Brendan Harley

RECIPIENT: UNIVERSITY OF ILLINOIS
GRANTS AND CONTRACTS OFFICE
06 S WRIGHT ST STE 364
URBABA, IL 61801-3649

REPORT DATE: October 2021

TYPE OF REPORT: Annual

PREPARED FOR: U.S. Army Medical Research and Development Command
Fort Detrick, Maryland 21702-5012

REPORT DOCUMENTATION PAGE

Form Approved
OMB No. 0704-0188

1. REPORT DATE	2. REPORT TYPE	3. DATES COVERED
OCTOBER 2021	Annual	30SEPT2020 - 29SEPT2021

4. TITLE AND SUBTITLE

Polycaprolactone-collagen Composite Biomaterials for Mandible Regeneration

5a. CONTRACT NUMBER
W81XWH-16-1-0566

5b. GRANT NUMBER
USAMRMC 1464004

5c. PROGRAM ELEMENT NUMBER

6. AUTHOR(S)

Brendan Harley

E-Mail: bharley@illinois.edu

5d. PROJECT NUMBER

5e. TASK NUMBER

5f. WORK UNIT NUMBER

7. PERFORMING ORGANIZATION NAME(S) AND ADDRESS(ES)
UNIVERSITY OF ILLINOIS
GRANTS AND CONTRACTS OFFICE
506 S WRIGHT ST STE 364
URBABA, IL 61801-3649

8. PERFORMING ORGANIZATION REPORT NUMBER

9. SPONSORING / MONITORING AGENCY NAME(S) AND ADDRESS(ES)

U.S. Army Medical Research and Development Command
Fort Detrick, Maryland 21702-5012

10. SPONSOR/MONITOR'S ACRONYM(S)

11. SPONSOR/MONITOR'S REPORT NUMBER(S)

12. DISTRIBUTION / AVAILABILITY STATEMENT

Approved for public release; distribution is unlimited

13. SUPPLEMENTARY NOTES

14. ABSTRACT

Our primary objective is to demonstrate approaches to create mechanically robust, patient-customized biomaterials for large, load-bearing maxillofacial bone defects. To do this, we are developing approaches to integrate a biomolecule decorated collagen scaffold with micro-scale porosity into a mechanically-robust polymeric frame generated via 3D-printing with macro-porosity. Through the second year of this project we have completed the design, fabrication, as well as mechanical and in vitro osteogenesis testing of multiple elements of the final composite biomaterial design. We identified a PLA-collagen composite that could support robust mesenchymal stem cell (MSC) viability, osteogenic differentiation, and new mineral synthesis while rendering it shape-fitting to improve conformal contact with the wound margin. We have advanced multiple strategies to incorporate biomolecular signals into the collagen scaffold via transient sequestration, covalent attachment, and through included zinc ions that enhance osteogenic activity. Ongoing efforts are completing biomolecule incorporation and release experiments to facilitate long-term (>7 day) biomolecule bioavailability via mineral-based factor sequestration chemistries. Our efforts are essential for our goal to identify a shelf-stable, patient customizable biomaterial that can be seeded with autologous MSCs to regenerate large CMF bone defects.

15. SUBJECT TERMS

Biomaterial, composite, collagen, growth factor release, osteogenesis

16. SECURITY CLASSIFICATION OF:			17. LIMITATION OF ABSTRACT	18. NUMBER OF PAGES	19a. NAME OF RESPONSIBLE PERSON
a. REPORT	b. ABSTRACT	c. THIS PAGE			USAMRDC
Unclassified	Unclassified	Unclassified	Unclassified	94	19b. TELEPHONE NUMBER *(include area code)*

Table of Contents

INTRODUCTION:

Severe craniomaxillofacial (CMF) injuries are prevalent after a wide range of acute and chronic injuries, are typically large in size, and are characterized by significant loss of hard and soft tissue. Our primary objective is to demonstrate a novel approach for creating mechanically robust, patient-customized biomaterials for large, load-bearing maxillofacial bone defects. We address a fundamental bottleneck in CMF biomaterial design. Constructs must balance very real considerations regarding mechanical competence and load bearing, the need to fit complex defect geometries unique to each patient, and biotransport of nutrients within the construct during healing. To do this, we are developing approaches to integrate a biomolecule decorated collagen scaffold with micro-scale porosity into a mechanically-robust polymeric frame generated via 3D-printing with macro-porosity. We are first validating the osteogenic potential of growth factor decorated composite (Aim 1). We are evaluating the influence of composite structural properties on mesenchymal stem cell (MSC) osteogenesis in vitro and will subsequently establish whether, and to what extent, selective incorporation and release of the growth factors BMP-2/VEGF, the mineral zinc, or modifications to scaffold glycosaminoglycan (GAG) content enhances osteogenesis. Next, we will examine the quality and kinetics of mandible bone regeneration using the composite in critically-sized mandibular ramus defects in the Yorkshire pig (Aim 2). The larger goal of this program is to identify a shelf-stable, patient customizable biomaterial that can be seeded with autologous MSCs intraoperatively and immediately implanted in order to regenerate large, load-bearing CMF bone defects.

KEYWORDS:

Biomaterial, composite, collagen, growth factor release, osteogenesis

OVERALL PROJECT SUMMARY:

Through the forth year of this project, we have made significant progress in addressing tasks and milestones associated with Major Tasks 1 and 2. Our efforts are on track to meet the goals of the entire research project, which are to validate the osteogenic potential of the biomolecule decorated collagen composites via tiered in vitro and in vivo assays. However, during the past year we had significant time where laboratory shut down in response to the novel coronavirus stalled in person laboratory work. While this in person shut down actually facilitated data analysis and manuscript preparation for the vast majority of in vitro studies, we were unable to initiate the in vivo porcine mandible regeneration studies. To complete the in vivo animal component of the proposed work we have requested and received a No Cost Extension (through 9/30/2021).

MAJOR TASK 1: Composite Fabrication

The primary goals associated with Major Task 1 are:

- Fabricate PCL cages for collagen-PCL composites
- Fabricate library of collagen-PCL composites and growth factor modified composites for in vitro testing

Key Milestones associated with Major Task 1 are:

- Biophysical characterization of mineralized collagen scaffolds and PCL-collagen composites
- Biophysical and functional characterization of growth factor loading/elution

MAJOR TASK 2: In vitro osteogenesis assays

The primary goals associated with Major Task 2 are:

- Assess mechanisms by which the mineralized collagen scaffold accelerate MSC osteogeneic differentiation and matrix biosynthesis.

Key Milestones associated with Major Task 2 are:

- Identify the degree to which BMP-2, VEGF, and growth factor sequestering chemistries incorporated within the collagen scaffolds increase MSC osteogenic differentiation.

Summary of Results, Progress and Accomplishments with Discussion:

PRIOR WORK (reported in YR2 annual report). First generation composite biomaterials for CMF repair. A significant challenge to improving the quality and speed of craniomaxillofacial bone regeneration are competing design requirements for a biomaterial platform: porosity required for cell recruitment and adequate biotransport; mechanical strength that is significantly reduced by the inclusion of pores; shape-fitting to improve conformal contact and osseointegration between the implant and the defect. With USMRMC funding, we developed a new class of collagen composite biomaterial. We leveraged 3D printing tools to create macro-scale poly (lactic acid) (PLA) reinforcement frames that can be integrated into the collagen suspension prior to lyophilization, resulting in a multiscale scaffold-fiber composite. A critical advance associated with this work was demonstrating an approach to render the composite shape-fitting to address an unmet clinical need: the need for close conformal contact between

biomaterial implant and the surrounding wound site. We showed selective removal of circumferential fiber segments from the PLA frame could yield a composite that was deformable radially yet retained sufficient spring-back capacity to increase the required push-out force. These findings confirm that the addition of even small volume fractions (~10% v/v) of polymeric mechanical reinforcement are sufficient to increase composite mechanical strength and address the current translational limitation of the mineralized collagen scaffold (compressive moduli < 1MPa). We completed biophysical and vitro MSC osteogenic activity characterization [1].

PRIOR WORK (reported in YR3 annual report). Zinc-modified scaffolds promote scaffold osteogenic activity. Implant osteoinduction and subsequent osteogenic activity are critical events that need improvement for regenerative healing of large craniofacial bone defects. While preliminary data was reported in the Year 2 Annual report, in the past year we successfully completed our study of incorporation of zinc ions into the mineralized collagen scaffold to accelerate MSC osteogenesis. Zinc is an essential trace element in skeletal tissue and bone, with soluble zinc being shown to promote osteogenic differentiation of porcine adipose derived stem cells. We augmented the mineral content of a class of mineralized collagen scaffolds under development for craniomaxillofacial bone regeneration via the inclusion of zinc ions to promote osteogenesis in vitro. Zinc sulfate was added to a mineralized collagen-glycosaminoglycan precursor suspension then freeze dried to form a porous biomaterial. We reported biophysical parameters of zinc functionalized scaffolds via imaging (scanning electron [2]microscopy), mechanical testing (compression), and compositional (X-ray diffraction, inductively coupled plasma mass spectrometry) analyses. Zinc-functionalized scaffolds display morphological changes to the mineral phase and altered elastic modulus without substantially altering the composition of the brushite phase or removing the micro-scale pore morphology of the scaffold. These scaffolds also display zinc release kinetics on the order of days to weeks and promote successful growth and pro-osteogenic capacity of porcine adipose derived stem cells cultured within these zinc scaffolds. Taken together, we believe that zinc functionalized scaffolds provide a unique platform to explore strategies to improve in vivo osteogenesis in craniomaxillofacial bone injuries models [3].

Mineralized collagen scaffolds fabricated with amniotic membrane matrix increase osteogenesis under inflammatory conditions. Defects in craniofacial bones occur congenitally, after high-energy impacts, and during the course of treatment for stroke and cancer; improved regenerating healing likely requires addressing challenges associated with the inflammatory environment surrounding the injury. We have adapted the mineralized collagen scaffold under development as part of this project, already capable of supporting significant osteogenic differentiation and matrix biosynthesis in the absence of osteogenic media or supplemental proteins, to include amniotic membrane matrix derived from placentas (Fig. 1). We report increased mechanical properties of a mineralized collagen–amnion scaffold and investigated osteogenic differentiation and mineral deposition of porcine adipose-derived stem cells within these scaffolds as a function of inflammatory challenge. Incorporation of amniotic membrane matrix promotes osteogenesis similarly to un-

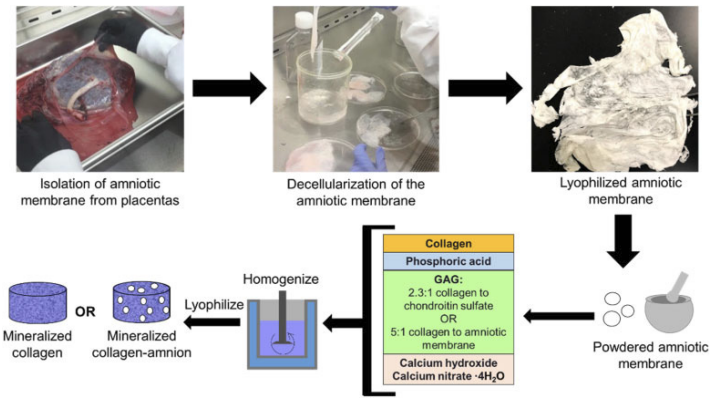

Fig. 1. Isolation of amniotic membrane from placentas and synthesis of mineralized collagen and mineralized collagen–amnion scaffolds.

modified mineralized collagen scaffolds, and increases in mineralized collagen–amnion scaffolds under inflammatory challenge. Together, these findings suggest that a mineralized collagen–amnion scaffold may provide a beneficial environment to aid craniomaxillofacial bone repair, especially in the course of defects presenting significant inflammatory complications. See appendix: [2].

Anisotropic mineralized collagen scaffolds accelerate osteogenic response in a glycosaminoglycan-dependent fashion. Regeneration of critically-sized craniofacial bone defects requires a template to promote cell activity and bone remodeling. However, induced regeneration becomes more challenging with increasing defect size. Methods of repair using allografts and autografts have inconsistent results, attributed to age-related regenerative capabilities of bone. We adapted the mineralized collagen scaffold under development as part of this project seeking scaffold technologies to promote craniomaxillofacial bone regeneration as an alternative to repair. We hypothesized modifying the pore anisotropy and glycosaminoglycan content of the scaffold will improve cell migration, viability, and subsequent bone formation (Fig. 2). Using anisotropic and isotropic scaffold variants, we first tested the role of pore orientation on human mesenchymal stem cell (MSC) activity. We subsequently explored the role of glycosaminoglycan content, notably chondroitin-6-sulfate, chondroitin-4-sulfate, and heparin sulfate on mineralization. We found that while short term MSC migration and activity was not affected by pore orientation, increased bone mineral synthesis was observed in anisotropic scaffolds. Further, while scaffold glycosaminoglycan content did not impact cell viability, heparin sulfate and chondroitin-6- sulfate containing variants increased mineral formation at the late stage of in vitro culture, respectively. Overall, these findings show scaffold microstructural and proteoglycan modifications represent a powerful tool to improve MSC osteogenic activity. See appendix: [4].

Stiffness of Nanoparticulate Mineralized Collagen Scaffolds Triggers Osteogenesis via Mechanotransduction and Canonical Wnt Signaling. As part of our further optimization of scaffold biophysical properties to support craniofacial bone regeneration, we examined the role of carbodiimide crosslinking induced stiffening of the mineralized scaffold on MSC osteogenic activity. We reported that the use of carbodiimide crosslinking increases scaffold elastic modulus 10-fold. Moreover, we examined two aspects of MSC osteogenic differentiation in response to scaffold stiffening. Both crosslinked and non-crosslinked scaffolds are capable of autogenously activating the canonical BMPR signaling pathway with phosphorylation of Smad1/5. Interestingly, human mesenchymal stem cells cultured on crosslinked scaffolds display significantly elevated expression of the major mechanotransduction mediators YAP and TAZ expression, coincident with β-catenin activation in the canonical Wnt signaling pathway. Inhibiting YAP/TAZ activation reduces osteogenic expression, mineralization,

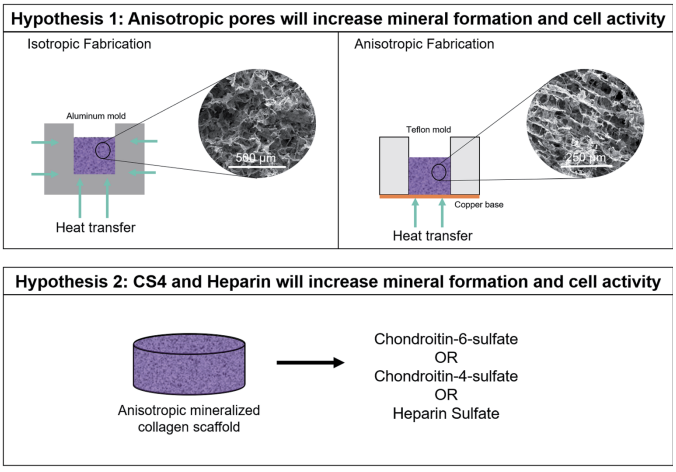

Fig. 2. *Hypothesis 1: anisotropic pores will have greater mineral formation and cell activity than isotropic pores. The different molds used during freeze drying to fabricate isotropic and anisotropic mineralized collagen scaffolds is demonstrated. Hypothesis 2: chondroitin-4-sulfate and heparin sulfate will have greater mineral formation and cell activity than scaffolds containing chondroitin-6-sulfate. Anisotropic scaffolds containing the same amount of chondroitin-6-sulfate, chondroitin-4-sulfate, or heparin sulfate are compared.*

and β-catenin activation in crosslinked scaffolds moreso thatn non-crosslinked. These results indicate that increasing scaffold stiffness via carbodiimide crosslinking induces osteogenic differentiation via the mechanotransduction mediators YAP/TAZ and the canonical Wnt signaling pathway, whereas the canonical BMPR signaling pathway is activated independent of scaffold stiffness. This adds an important observation regarding alterations to the mineralized collagen scaffold to maximally support MSC osteogenesis. See appendix: [5].

Sequential sequestrations increase the incorporation and retention of multiple growth factors in mineralized collagen scaffolds. Over the past year we completed analysis of, and successfully published a manuscript describing, the use of non-covalent growth factor sequestration methods to improve the bioactivity of our mineralized collagen scaffold. This is a major element of the proposed efforts in this project and has been a project that took almost two years to complete. Here, growth factor signaling has the potential to coordinate the behavior of multiple cell types following an injury, and effective alteration of growth factor availability within a biomaterial can be critical for accelerating bone healing. During this project we have optimized the design parameter of a mineralized collagen scaffolds to facilitate cell invasion and MSC osteogenesis. Here we describe the use of modified simulated body fluid treatments to enable sequential sequestration of bone morphogenic protein 2 and vascular endothelial growth factor into the mineral phase of these mineralized collagen scaffolds (Fig. 3). This approach is unlike traditional crosslinking based methods for incorporating growth factors; we have now showed as part of this project optimization of scaffold structure (pore anisotropy [4]), scaffold composition (glycosaminoglycan content [4]; incorporation of amnionic membrane[2]), and crosslinking[5] to support beneficial MSC osteogenic activity. Hence, incorporation of growth factors must be performed in a manner orthogonal to those efforts. Here we show that sequential exposure to biomolecules of interest and simulated body fluid can be used to sequester 60–90% of growth factor from solution into the mineral phase without additional crosslinking treatments. This approach allows high levels of retention for both individual growth factors (>94%) or multiple growth factors (>88%) that can be layered into the material via sequential sequestration steps. Sequentially sequestering growth factors allows prolonged release of growth factors in vitro (>94%) and suggests the potential to improve healing of large-scale bone injury models in vivo. Future work will utilize this sequestration method to induce

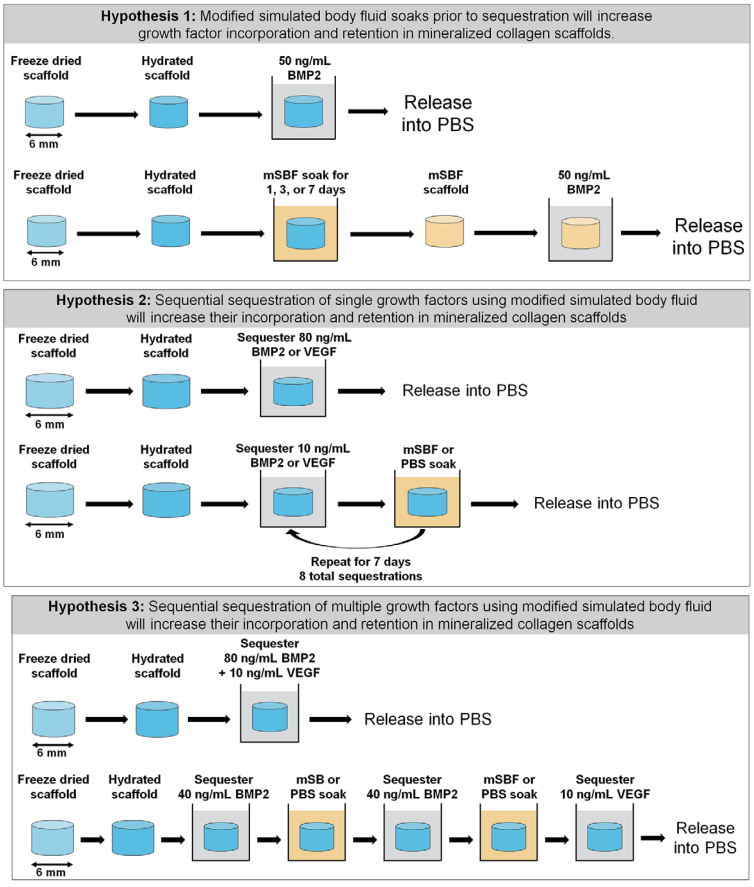

Fig. 3. Hypothesis 1: Growth factor sequestration with varying modified simulated body fluid (mSBF) treatments. Hypothesis 2: Sequential sequestration of individual growth factors (BMP2 or VEGF). Hypothesis 3: Sequential sequestration of multiple growth factors (BMP2 and VEGF) versus sequentially sequestered BMP2 then VEGF.

cellular activities critical to bone healing such as vessel formation and cell migration. See appendix: [6].

Inclusion of a 3D-printed mesh improves mechanical and osteogenic performance of a mineralized collagen scaffold. During this project we have reported on the concept of incorporating polymer-based reinforcement meshes into the mineralized collagen scaffold to increase the mechanical performance of the resulting composite. In work recently submitted[7] we showed the degradation byproducts and acidic release from the printed polymer structures have limited negative impact on the viability of mesenchymal stem cells but may be chosen to actively promote osteogenic activity. Inclusion of a mesh (Fig. 5) formed from Hyperelastic Bone^{TM} bioinks generates a reinforced composite with significantly improved mechanical performance (elastic modulus, push-out strength). Composites formed from the mineralized collagen scaffold and either Hyperelastic Bone supported human bone-marrow derived mesenchymal stem cell osteogenesis and mineral biosynthesis. Strikingly, composites reinforced with Hyperelastic Bone mesh elicited significantly increased secretion of osteoprotegerin, a soluble glycoprotein and endogenous inhibitor of osteoclast activity. These results suggest that architected meshes can be integrated into collagen scaffolds to boost mechanical performance and actively instruct cell processes that aid osteogenicity; specifically, secretion of a factor crucial to inhibiting osteoclast-mediated bone resorption. Future work beyond the scope of this project will focus on further adapting the polymer mesh architecture to confer improved shape-fitting capacity as well as to investigate the role of polymer reinforcement on MSC-osteoclast interactions as a means to increase regenerative potential.

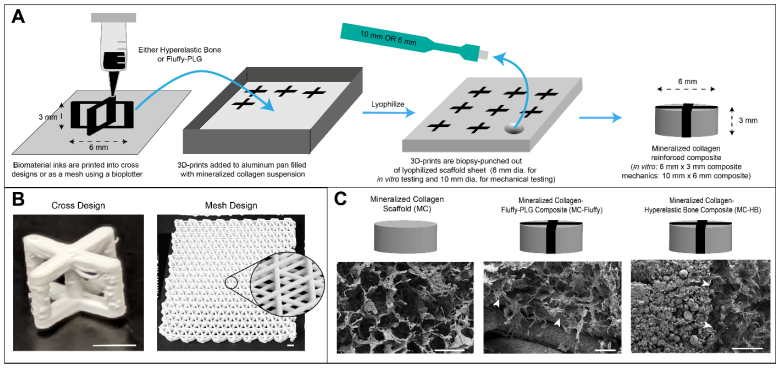

Fig. 5. Fabrication of composites used in vitro and for mechanical testing. *(A) Hyperelastic Bone and Fluffy-PLG were 3D printed in "cross designs" for in vitro testing or as a mesh for mechanical testing. Cross prints were printed individually and added to a continuous mineralized collagen suspension in an aluminum mold. After the addition of multiple prints, the entire mold was freeze-dried and a 6 mm biopsy punch was used to remove scaffold and 3D-print together. Mesh reinforced composites were fabricated by adding the entire mesh to the aluminum mold with mineralized collagen suspension and biopsy punching 10 mm diameter composites after lyophilization. Mesh 3D-prints were printed with either 2 mm or 3 mm line spacing. (B) Images of cross design and mesh 3D-prints, scale bar represents 3 mm. (C) SEM images of mineralized collagen scaffold and cross design reinforced composites and acronyms used to represent the groups in the study. Scale bar represents 150 µm and white arrows indicate interface between the mineralized collagen and 3D-printed reinforcing structures.*

Adapting the design of conformal fitting polymeric reinforcement cages to meet translational challenges. During Year 3 of this project, we reported [1] a polymer fiber reinforcement strategy for the mineralized collagen scaffold. As stiffness requirements for confined CMF bone defects are lower (5-10 MPa[8]) than for segmental bone defects, we prioritized biomaterial innovations to improve conformal contact with the defect margin. The initial composite used a PLA-fiber array to create conformal fitting design elements for our scaffold. In the past year we adapted the design of the reinforcing cage for the porcine CMF defect model. This requires a more robust PCL-based bioink for comparison to results reported outside of this project that used a high-density PCL reinforcing strategy. We have fabricated

prototype PCL reinforcement cages with conformal-fitting geometries and received ACURO approval for animal studies of PCL-reinforced mineralized collagen scaffolds in a porcine mandible defect. We have developed proof-of-concept for a novel composite based on the mechanical performance of low-density Voronoi foams (Fig. 6). These open cell foams pack to fill space and their random nature (absence of regularity) affords a simple approach to define mechanical performance independent of foam geometry.[9,10] Under load, the fibers that define the pores of these foams bend elastically during the first ~10% applied strain then buckle plastically.[9] Mechanical performance of these meshes is controlled by overall relative density (ρ^*/ρ_s; ρ^*, density of the porous material; ρ_s, density of the solid phase) not pore geometry, making them ideal for maintaining mechanical properties despite being cut/shaped. So rather than requiring a global optimization process, Voronoi foams can be rapidly generated to meet defined mechanical benchmarks.

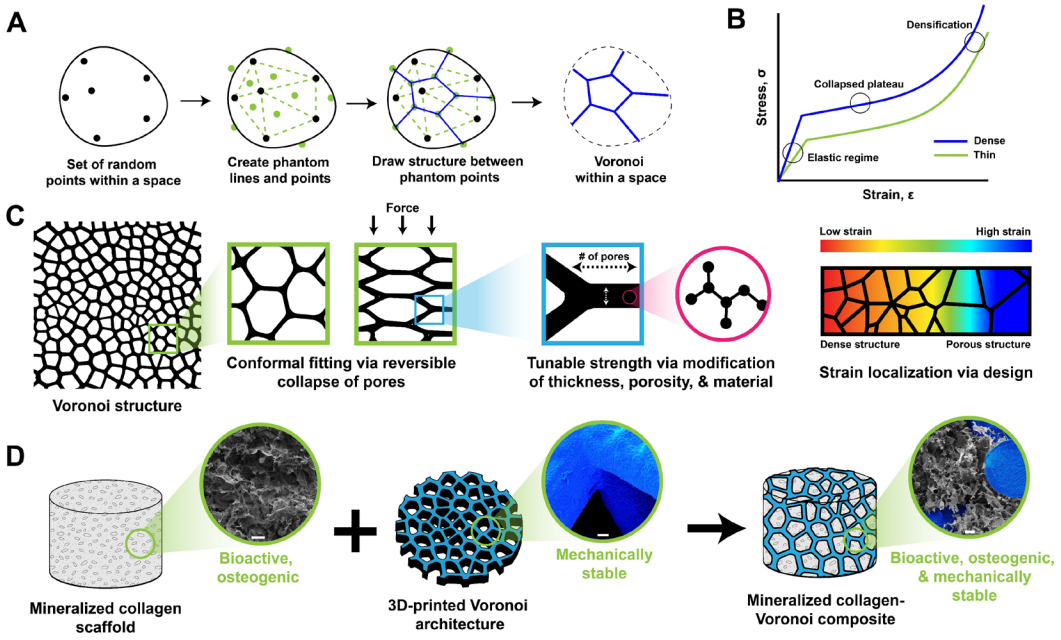

Fig. 6. Tough and tunable Voronoi structures. *(A) Creating a Voronoi structure within any space. First, a set of "seed" points are added to the space. Then phantom lines (green) are drawn between these points, with phantom points (green) in the middle of these areas. Finally, the lines of the Voronoi structure (blue) are drawn between the phantom lines connecting the phantom points. (B) Representative stress-strain curve of foams, such as Voronoi structures. These structures are characterized by a linear elastic regime, a collapsed plateau, and densification. Increasing the density of Voronoi structures increases the modulus (elastic regime). (C) Voronoi structures can be added to any size or shape design and can achieve conformal fitting by the reversible collapse of pores. Additionally, the thickness of the individual struts in the architecture and the material it is comprised of can lead to tunable strength and elasticity. Finally, strain can easily be localized by printing these designs with regions of variable porosity or density of material. (D) The goal of this study was to incorporate tunable Voronoi 3D-printed architectures into mineralized collagen scaffolds for use in bone repair. Mineralized collagen scaffolds off excellent bioactivity and osteogenic properties due to the mineral, glycosaminoglycans, collagen, and porous nature of this material, however, this porosity also lends to these being very soft structures and more difficult to handle in bone repair situations. 3D-printed Voronoi structures offer a mechanically stable material with tunable mechanics, however, the macro-scale porosity and print material may not be as osteogenic as mineralized collagen scaffolds. Combined together, mineralized collagen and 3D-printed Voronoi structures have the ability to promote osteogenesis while also maintaining strength. Scale bar represents 100 μm.*

The mechanical performance of architected Voronoi foams is predictably dependent on print parameters (porosity, strut thickness) that can be defined by generative design algorithms (Fig. 7). As predicted, the porosity and thickness of printed Voronoi structures altered the Young's Modulus, all decreasing the Young's Modulus as density decreased. Due to the random structure of Voronoi designs, these by nature should be isotropic; however, in all of our tests we noticed some degree of anisotropy, as two or more sides had different moduli. This could be attributed to the small size of these designs and the large point spacing (i.e. 10 mm cubes with 4 mm point spacing). We hypothesize that a larger design, such as sheets of Voronoi structures, would result in a more isotropic structure, and CMF defects are typically 25 mm or larger in size. Voronoi computation models used to relate moduli to predictive equations have used a minimum of 27 cells to accurately assess isotropy 66, suggesting the differences in modulus may be due to an insufficient number of pores in that axis of compression.

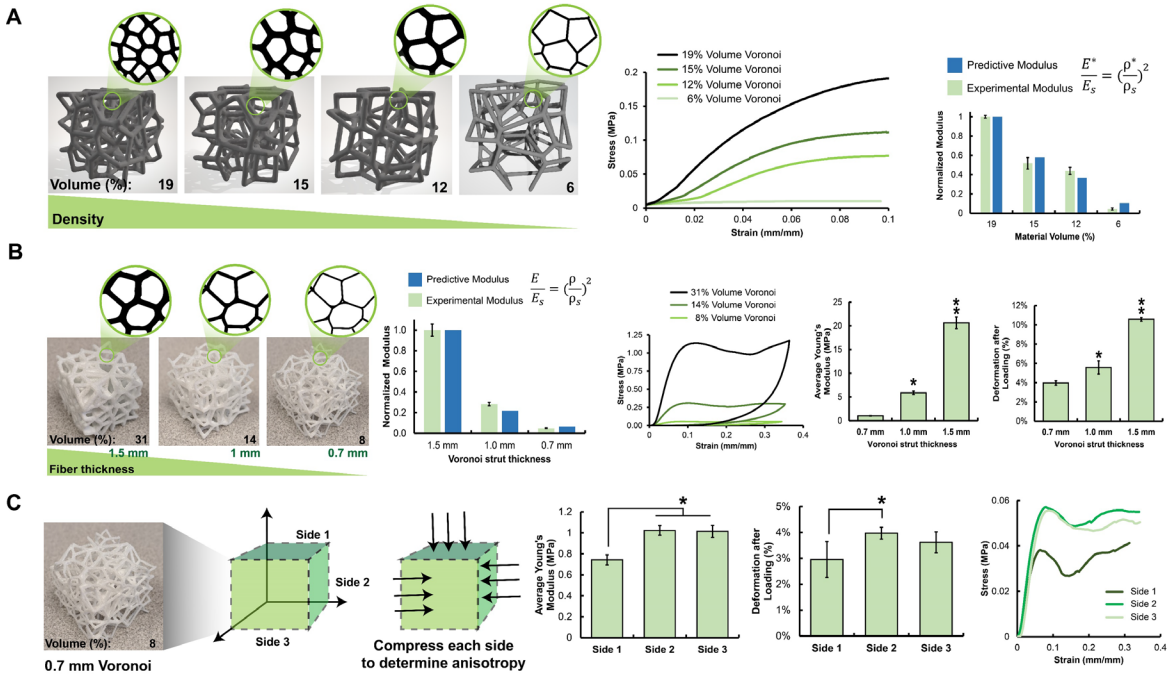

Fig. 7. Tuning stiffness through Voronoi density and material thickness. *(A) Four Voronoi designs (10 mm cubes) of different porosities altered by changing the architecture were fabricated by 3D-printing photopolymerized resin. Designs were compressed and the stress-strain profiles were recorded, and as the volume % material of the design increased, the stiffness increased. The modulus of the four designs was compared to a predictive modulus for Voronoi architectures. (B) Three of the same Voronoi design (25 mm cubes) with different material thicknesses were 3D-printed using polycaprolactone. The modulus of these designs were tested against a predictive modulus for Voronoi architectures. Samples were loaded and unloaded compressively and the stress-strain profiles were recorded. The average modulus and deformation after loading increased with increasing strut thickness. ** indicates the 1.5 mm group was significantly ($p < 0.05$) greater than all other groups. * indicates the 1.0 mm group was significantly ($p < 0.05$) greater than all other groups. (C) Analyzing anisotropy in 0.7 mm thickness Voronoi designs printed with polycaprolactone and 8% volume material (25 mm cubes). Each of the sides of one Voronoi design (x, y, z axis) were loaded and unloaded under compression and the modulus and deformation after loading were examined. * indicates which group(s) were significantly ($p < 0.05$) greater than another group. Differences in the modulus between sides of the same design can indicate anisotropy. Data expressed as average ± standard deviation (n=6).*

Local changes to Voronoi mesh architecture enable localized control over composite deformation (Fig. 8). We designed a biphasic 3D-print with a porous and dense region and were able to successfully combine this with mineralized collagen scaffolds to create a composite material, and further compared this to a composite with only one reinforced phase (porous). The compression of the biphasic 3D-print and

composite demonstrated stress-strain profiles of two different density materials, and DIC analysis demonstrated that strain is concentrated at the porous region. Compared to Voronoi composites with one phase, stress localization was randomly throughout the material. Upon comparing to the predictive modulus, this was fairly accurate for the dense structure, but not as accurate for the porous portion, most likely due to the analysis of the stress-strain curve portions and these combined structures leading to an altered moduli.

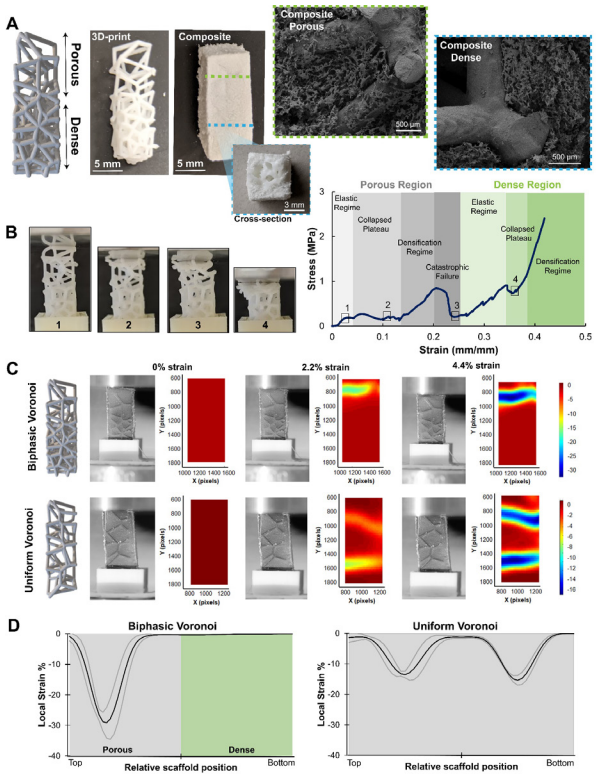

Fig. 8. Localizing strain through biphasic Voronoi design. *(A) Biphasic Voronoi designs were 3D-printed with photopolymerized resin into designs with a distinctly porous region and dense region. These were combined with mineralized collagen scaffolds to create a composite material. SEM images demonstrate the integration of the 3D-print with the surrounding mineralized collagen in the dense region (blue) and porous region (green). (B) Biphasic Voronoi 3D-prints were compressed and the stress-strain profile was recorded. The stress-strain profile was comprised of two different curves, whereas the porous region first compressed until failure (grey), and then the dense region was compressed (green), outlined on the stress-strain profile with matching images of the 3D-print under compression. (C) Biphasic Voronoi and mineralized collagen composites were compared to uniform Voronoi mineralized collagen composites, with the uniform region being the same throughout as the porous region of the biphasic Voronoi. These were compared under compression and further Digital Image Correlation to map strain regions and create contour plots. At 0%, 2.2%, and 4.4% global applied strain, images of the composite are alongside representative strain localization images, with blue representing the greatest strain. (D) Line scans of the strain on biphasic Voronoi composite and uniform Voronoi composite were created from Digital Image Correlation data. Average strain at a global applied 4.4% strain was plotted as a function of position for each sample, with the average (black line) and standard deviation (interval contained by gray lines) of strain magnitude along the entire length of each scaffold. The porous region is demonstrated by a grey background and the dense region with green (n=6).*

KEY RESEARCH ACCOMPLISHMENTS (cumulative):

The overall goal of this project is to develop a novel composite collagen biomaterial to improve the quality and speed of craniomaxillofacial bone regeneration. The major elements of the project are to demonstrate design modifications to an existing mineralized collagen scaffold in order to:

- Create a polymer-scaffold composite that exhibits improved compressive strength (vs. the scaffold alone) as well as conformal fitting capacity to aid the composite to fit Against the wound margins of irregular defect geometries.
- Demonstrate material and cytokine delivery innovations that accelerate cell infiltration into the scaffold as well as subsequent osteogenic differentiation and angiogenic activity.
- Validate improvements to this scaffold via assessment of the quality and kinetics of new bone formation in a porcine mandibular defect model.

Key accomplishments to date to meet these challenges:

- Demonstrating multi-scale composite reinforcement paradigm for mineralized collagen scaffolds to address acute clinical needs for biomaterials with improved macro-scale compressive strength and conformal fitting within the defect margins [1].

- Confirming incorporation of a polymeric reinforcement frame does not negatively influence the osteogenic capabilities of porcine adipose stem cells within the multi-scale composite [1].
    - NOTE: This finding extends beyond previous publications that examined the activity of human and rabbit bone marrow derived MSCs in the mineralized collagen scaffold alone [11,12] or that only confirmed adMSC viability in one design variant of a collagen-PCL composite [13].

- Developing and characterizing a novel zinc-functionalized variant of the mineralized collagen scaffold at the core of this CMF bone regeneration project. We confirmed zinc can be incorporated into and released from the scaffold microstructure. We showed incorporation of zinc improved scaffold mechanical properties, and that while zinc incorporation alters microscale mineral morphology of the scaffold it does not affect the Brushite phase of the calcium phosphate deposits. We showed zinc-functionalized scaffolds accelerate adMSC proliferation and metabolic health while maintaining osteogenic differentiation and mineral deposition capacity [3].

- In addition to long standing analysis of MSC-osteogenesis within mineralized collagen scaffolds, we have showed the mineralized collagen scaffold may also alter activity of osteoclasts [14,15], and motivates ongoing efforts to better investigate scaffold-osteoclast-MSC interactions in the context of matrix remodeling.

- We demonstrated the use of cyclodextrin-based transient sequestration of growth factors within the scaffold could enhance BMP-2 mediated osteogenic differentiation [16]. While short term growth factor retention may accelerate cell recruitment, cyclodextrin studies are now motivating current exploration of mineral-linked growth factor retention as an alternative means to delivery growth factors within the collagen scaffold.

- We demonstrated the use of nanostructured mineral-based sequestration of growth factors within the scaffold to enhance the bioavailability of BMP-2 and VEGF (manuscript in preparation). Ongoing efforts will: 1) define the long-term biological efficacy of growth factor retention; and 2) identify the VEGF loading paradigm that efficiently activates

vascular cell activity. These efforts are expected to be early in Year 4 of this project and are necessary prior to in vivo testing of a final scaffold composite in a porcine mandibular defect.

- We completed design and manufacture of a novel PCL polymeric reinforcement cage. The original PCL cage structure detailed in the motivation for this project contained high (>30% vol/vol) polymer. We previously reported a fiber-based design to improve strength and conformal fitting of a composite, but this relied on PLA-fibers. We have completed adaptation of the PLA design to the additive manufacturing technology required to fabricate PCL structures. This PCL design has the dual capacity to improve the compressive strength of scaffold-PCL composites while also providing the opportunity to enhance conformal-fitting capacity of the resulting implants (manuscript in preparation).

- We have adapted the structure of the mineralized collagen scaffold, creating a new class of anisotropic mineralized collagen scaffolds. We are defined the role of scaffold anisotropy (the inclusion of aligned tracks of pores) to aid MSC osteogenesis and infiltration into the material as a means to accelerate healing.

- We have identified a variant of the mineralized collagen scaffold that contains amniotic matrix as a portion of its organic composition to improve cell activity in response to inflammatory challenge.

- We identified proteoglycans (heparin sulfate and chondroitin-6-sulfate) that can be incorporated into the mineralized collagen scaffold to maximize mineral formation in vitro.

- Defined sequestration efficiency and release kinetics for VEGF and BMP-2 in the mineralized scaffold using a mineral phase patterning approach that avoids covalent growth factor attachment.

- We showed chemical crosslinking of the mineralized collagen scaffold to increase scaffold stiffness does not affect scaffold-mediated activation of canonical BMPR signaling required for MSC osteogenic differentiation. However, stiffer crosslinked scaffolds promote MSC osteogenic differentiation via the mechanotransduction mediators YAP/TAZ and the canonical Wnt signaling pathway.

- We showed architected meshes can be integrated into collagen scaffolds to passively boost mechanical performance and actively instruct cell processes that aid osteogenicity; specifically, secretion of a factor crucial to inhibiting osteoclast-mediated bone resorption. Notably, the mechanical performance of architected Voronoi foams is predictably dependent on print parameters (porosity, strut thickness) that can be defined by generative design algorithms. Further, local changes to Voronoi mesh architecture enable localized control over composite deformation.

CONCLUSION:

Successful biomaterial implants to improve regenerative healing must meet a number of design requirements that are often in conflict with each other. They must be biocompatible, meet micro-scale mechanical needs to promote osteogenesis as well as macro-scale requirements for a mechanically robust implant, be bioresorbable, and conformal fitting within irregular defects to improve osseointegration. Through the third year of this project we have completed the design, fabrication, as well as mechanical and in vitro osteogenesis testing of a conformal fitting mineralized composite for CMF defect repair applications. We have demonstrated multiple means to incorporate and release growth factors from the scaffold. And we have shown incorporation of zinc ions into the scaffold mineral phase is a powerful stimulus to increase MSC proliferation and metabolic health. The ability to increase close contact between the biomaterial implant and the host bone as well as incorporate pro-osteogenic factors (i.e., zinc) is particularly important for improving cell recruitment and subsequent osseointegration between host and implant. We have developed alternative methods to leverage mineral-based sequestration of growth factors within the mineralized collagen scaffold without the need for chemical crosslinking. We have also defined the role of scaffold anisotropy, modification of scaffold glycosaminoglycan content, and inclusion of amnion derived matric on guiding MSC osteogenesis. We have developed a Voronoi-based approach to create exotic polymeric reinforcement designs to address challenges of complex defect geometries (submitting intellectual property filing and working to complete a manuscript reporting this technology). We have shut down and restarted our laboratory in response to the novel coronavirus pandemic, received formal ACURO Animal Use approval for our in vivo trials, and are awaiting ACURO re-approval of our updated campus IACUC-approved animal protocol so that we may initiate in-person operating room efforts required to execute those in vivo trials. We expect this work to generate significant enthusiasm in the regenerative medicine and biomaterials community regarding a new paradigm for orthogonally manipulating multiple design criteria to create biomaterials for large, load bearing craniofacial defects. Impact will be primarily in basic sciences associated with the design of regenerative biomaterials.

PUBLICATIONS, ABSTRACTS, AND PRESENTATIONS:

a. List all manuscripts submitted for publication during the period covered by this report resulting from this project.

(1) *Lay Press:*
Nothing to report

(2) *Peer-Reviewed Scientific Journals:*
Accepted/Published:

M.J. Dewey, A.V. Nosatov, K. Subedi, R. Shah, A. Jakus, B.A.C. Harley, 'Inclusion of a 3D-printed Hyperelastic Bone mesh improves mechanical and osteogenic performance of a mineralized collagen scaffold,' Acta Biomater., 121:224-36, 2021. PMCID: PMC7856202.

M.J. Dewey and B.A.C. Harley, 'Biomaterial design strategies to address obstacles in craniomaxillofacial bone repair,' RSC Adv., 11(29):17809-27, 2021. PMCID: PMC8443006. NOTE: review article which heavily cites work supported by this grant.

M.J. Dewey and B.A.C. Harley, 'Principles of Bone Tissue Engineering,' in B. Mahadik and J. Fisher (eds.) Bone Tissue Engineering: Bench to Bedside Using 3D Printing, 2021.

In preparation

M.J. Dewey, R. Sun Han Chang, A.V. Nosatov, K. Janssen, S.J. Crotts, S.J. Hollister, B.A.C. Harley, 'Tunable Voronoi reinforcements for mechanically stable implants to repair craniomaxillofacial bone defects,' in preparation.

(3) *Invited Articles:*
Nothing to report

(4) *Abstracts:*
Nothing to report

b. List presentations made during the last year (international, national, local societies, military meetings, etc.).

B.A.C. Harley, 'Building tissues – engineering complexity through biomaterial design,' University of Florida, Depts. of Chemical Engineering and Biomedical Engineering, 10/2020 (virtual).

B.A.C. Harley, 'Building tissues – engineering complexity through biomaterial design,' University of Washington, Dept. of Bioengineering, 12/2020

B.A.C. Harley, 'Building tissues – engineering complexity through biomaterial design,' University of Toronto, Donnelly Centre for Cellular and Biomolecular Research, 1/2021 (virtual).

B.A.C. Harley, 'Building tissues – engineering complexity through biomaterial design,' University of British Columbia, School of Biomedical Engineering Research Symposium,

2/2021 (virtual; rescheduled from 6/2020 due to coronavirus).

B.A.C. Harley, ‘Building tissues – engineering complexity through biomaterial design,’ Mayo Clinic, NeuroOncology Rounds, 2/2021 (virtual).

B.A.C. Harley, ‘Building tissues – engineering complexity through biomaterial design,’ Notre Dame, Dept. of Aerospace and Mechanical Engineering, 3/2021 (virtual).

B.A.C. Harley, ‘Building tissues – engineering complexity through biomaterial design,’ Clemson Award for Basic Science, Society for Biomaterials Annual Meeting, 4/2021 (virtual).

B.A.C. Harley, ‘Building hierarchy: engineering porous scaffolds for regenerative medicine,’ Invited Keynote, Tissue and Cell Engineering Society Annual Meeting, 7/2021 (virtual).

B.A.C. Harley, ‘Building tissues – engineering complexity through biomaterial design,’ Washington University in St. Louis, Dept. of Bioengineering, 11/2021.

INVENTIONS, PATENTS AND LICENSES:

Marley Dewey, Brendan Harley, Daniel Weisgerber, ‘Adaptable PLA fiber reinforcement for conformal fitting,’ submitted, Nov. 2017.

Marley Dewey, Brendan Harley, Rebecca Hortensius, Simona Slater, ‘Mineralized Collagen Scaffolds combined with the Amniotic Membrane derived from placentas to address inflammation in Craniomaxillofacial Bone Regeneration,’ submitted, July, 2018.

Marley Dewey, Brendan Harley, Justine Lee, Ramille Shah, Adam Jakus, ‘Bioactive collagen composites for musculoskeletal tissue repair,’ submitted, September, 2020.

REPORTABLE OUTCOMES:

Mineralized collagen scaffolds fabricated with amniotic membrane matrix increase osteogenesis under inflammatory conditions. We have reported a process to incorporate amniotic derived extracellular matrix into a mineralized collagen scaffold to form a mineralized collagen–amnion composite biomaterial We reported inclusion of amniotic membrane matrix increases scaffold mechanicial properties without affecting the osteogenic capacity of porcine adipose-derived stem cells in the mineralized collagen scaffold. Incorporation of amniotic membrane matrix promotes increased osteogenic capacity in response to inflammatory media challenge. Mineralized collagen–amnion scaffold may provide a beneficial environment to aid craniomaxillofacial bone repair, especially in the course of defects presenting significant inflammatory complications.

Anisotropic mineralized collagen scaffolds accelerate osteogenic response in a glycosaminoglycan-dependent fashion. We have adapted the lyophilization process used to fabricate porous collagen scaffold, incorporating a directional solidification approach to generate anisotropic mineralized collagen scaffolds containing aligned tracks of ellipsoidal pores. Notably, while pore anisotropy did not increase short term human mesenchymal stem cell (MSC) migration, anisotropic scaffolds promoted increased bone mineral synthesis in vitro. Further, altering scaffold glycosaminoglycan content to contain heparin sulfate or chondroitin-6-sulfate further increased mineral formation in vitro. These findings show scaffold microstructural and proteoglycan modifications represent a powerful tool to improve MSC osteogenic activity.

Sequential sequestrations increase the incorporation and retention of multiple growth factors in mineralized collagen scaffolds. We have developed a process to decorate mineralized collagen scaffolds with activity inducing growth factors after scaffold fabrication. We showed sequential exposure to modified simulated body fluid treatments enable sequential sequestration of bone morphogenic protein 2 and vascular endothelial growth factor into mineralized collagen scaffolds without additional chemical crosslinking steps. This method allows scaffolds to: 1) sequester 60–90% of growth factor from solution without additional crosslinking treatments; and 2) retain high levels of individual (>94%) or multiple (>88%) growth factors that can be layered into the material via sequential sequestration steps. Sequentially sequestering growth factors allows prolonged release in vitro (>94%) and suggests the potential to improve healing of large-scale bone injury models in vivo.

Stiffness of Nanoparticulate Mineralized Collagen Scaffolds Triggers Osteogenesis via Mechanotransduction and Canonical Wnt Signaling. We report the consequences of chemical crosslinking of mineralized collagen scaffolds on human mesenchymal stem cell (MSC) osteogenicity. Carbodiimide crosslinking increases the mechanical stiffness of the scaffolds. Mineralized collagen scaffolds activate canonical BMPR signaling pathways regardless of crosslinking status. However, stiffer crosslinked mineralized collagen scaffolds promote MSC osteogenic differentiation via the mechanotransduction mediators YAP/TAZ and the canonical Wnt signaling pathway. These finding provide important information regarding modification to scaffold properties to improve the efficiency of osteogenic differentiation in the absence of exogenous growth factors, a key requirement to aid surgical practicality.

Tough and tunable scaffold-hydrogel composite biomaterial for soft-to-hard musculoskeletal tissue interfaces. We reported a process to incorporate a hydrogel based zone adjacent to mineralized collagen scaffold to reduce localized strain concentrations that occur at the interface between biomaterials with dissimilar mechanical properties. While this work was largely focused on tendon-to-bone enthesis repair, mechanical mismatch exists

between mineralized collagen scaffolds and the defect margin of craniofacial bone defects, suggesting the potential use of adaptations to this technology to aid implant integration into complex craniomaxillofacial bone defects.

Tunable Voronoi reinforcements for mechanically stable implants to repair craniomaxillofacial bone defects. The design of biomaterial implants to induce regenerative healing of musculoskeletal defects often requires they address multi-scale mechanical challenges. Notably, material porosity, essential for cell-infiltration and diffusive transport, and mechanics, to promote surgical handling and implant stability, are often in direct conflict. Craniomaxillofacial bone defects occur congenitally, often after high-energy impacts, and are large and irregularly shaped. We have recently described a mineralized collagen scaffold able to promote bone formation in vivo and mineralization by mesenchymal stem cell differentiation in vitro. However, while cell bioactivity and oxygen/nutrient biotransport in these porous scaffolds scale with material porosity, mechanical performance scales inversely with porosity and is insufficient for large-scale clinical adoption. We reported an innovative scaffold-mesh composite biomaterial that uses modular polymer reinforcement elements based on Voronoi structures and a scalable generative design paradigm to create a collagen-mesh composite able to conformally fit complex defect geometries. We showed Voronoi reinforced composites fit a predictive moduli equation, create biphasic composites to localize strain during loading, and create 2D and 3D composite sheets that can be rapidly shaped and which provide conformal fitting capacity. Voronoi based composite biomaterials offer unique potential as a biomaterial that can be rapidly shaped intraoperatively to conformally fit complex defects unique for individual patients while also actively accelerating bone regeneration.

Future reportable outcomes:

1. Completion of analysis of the role of Voronoi-based scaffold reinforcement frames to aid surgical practicality.
2. Initiation and completion of tiered in vivo craniomaxillofacial bone regeneration studies

OTHER ACHIEVEMENTS:

Degrees obtained by personnel supported by this award:

Nothing to report this year.

Fellowships awarded to personnel supported by this award:

Nothing to report this year.

Additional honors awarded to personnel supported by this award:

Marley Dewey

2020; Annual Innovation Award for Outstanding Ph.D. Thesis, Chakrapani Family Trust, Dept. of Materials Science and Engineering, University of Illinois.

REFERENCES:

1. Dewey MJ, Johnson EM, Weisgerber DW, Wheeler MB, Harley BAC, Shape-fitting collagen-PLA composite promotes osteogenic differentiation of porcine adipose stem cells. *J Mech Behav Biomed Mater*, 95:21-33, 2019.
2. Dewey MJ, Johnson EM, Slater ST, Milner DJ, Wheeler MB, Harley BAC, Mineralized collagen scaffolds fabricated with amniotic membrane matrix increase osteogenesis under inflammatory conditions. *Regen Biomater*, 7(3):247-258, 2020.
3. Tiffany AS, Gray DL, Woods TJ, Subedi K, Harley BAC, The inclusion of zinc into mineralized collagen scaffolds for craniofacial bone repair applications. *Acta Biomaterialia*, 93:86-96, 2019.
4. Dewey MJ, Nosatov AV, Subedi K, Harley B, Anisotropic mineralized collagen scaffolds accelerate osteogenic response in a glycosaminoglycan-dependent fashion. *RSC Adv*, 10:15629-41, 2020.
5. Zhou Q, Lyu S, Bertrand AA, Hu AC, Chan CH, Ren X, Dewey MJ, Tiffany AS, Harley BAC, Lee JC, Stiffness of nanoparticulate mineralized collagen scaffolds triggers osteogenesis via mechanotransduction and canonical Wnt signaling. *Macromol Biosci*, 2020.
6. Tiffany AS, Dewey MJ, Harley BAC, Sequential sequestrations increase the incorporation and retention of multiple growth factors in mineralized collagen scaffolds. *RSC Adv*, 10:26982-96, 2020.
7. Dewey MJ, Nosatov AV, Subedi K, Shah R, Jakus A, Harley BAC, Inclusion of a 3D-printed Hyperelastic Bone mesh improves mechanical and osteogenic performance of a mineralized collagen scaffold. *Acta Biomaterialia*, 121:224-236, 2021.
8. Zhang D, George OJ, Petersen KM, Jimenez-Vergara AC, Hahn MS, Grunlan MA, A bioactive “self-fitting” shape memory polymer scaffold with potential to treat cranio-maxillo facial bone defects. *Acta Biomaterialia*, 10(11):4597-4605, 2014.
9. Gibson LJ, Ashby MF, Harley BA. Cellular materials in nature and medicine. Cambridge, U.K.: Cambridge University Press; 2010.
10. Gibson LJ, Ashby MF. Cellular solids: structure and properties. 2nd ed. Cambridge, U.K.: Cambridge University Press; 1997.
11. Weisgerber DW, Caliari SR, Harley BAC, Mineralized collagen scaffolds induce hMSC osteogenesis and matrix remodeling. *Biomater Sci*, 3(3):533-42, 2015.
12. Ren X, Bischoff D, Weisgerber DW, Lewis MS, Tu V, Yamaguchi DT, Miller TA, Harley BA, Lee JC, Osteogenesis on nanoparticulate mineralized collagen scaffolds via autogenous activation of the canonical BMP receptor signaling pathway. *Biomaterials*, 50:107-14, 2015.
13. Weisgerber DW, Erning K, Flanagan C, Hollister SJ, Harley BAC, Evaluation of multi-scale mineralized collagen-polycaprolactone composites for bone tissue engineering. *J Mech Behav Biomed Mater*, 61:318-327, 2016.
14. Ren X, Zhou Q, Foulad D, Dewey MJ, Bischoff D, Miller TA, Yamaguchi DT, Harley BAC, Lee JC, Nanoparticulate mineralized collagen glycosaminoglycan materials directly and indirectly inhibit osteoclastogenesis and osteoclast activation. *J Tissue Eng Regen Med*, 13(5):823-34, 2019.
15. Ren X, Zhou Q, Foulad D, Tiffany AS, Dewey MJ, Bischoff D, Miller TA, Reid RR, He T-C, Yamaguchi DT, Harley BAC, Lee JC, Osteoprotegerin reduces osteoclast resorption activity without affecting osteogenesis on nanoparticulate mineralized collagen scaffolds. *Sci Adv*, 5(6):eaaw4991, 2019.
16. Grier WK, Tiffany AS, Ramsey MD, Harley BAC, Incorporating β-cyclodextrin into collagen scaffolds to sequester growth factors and modulate mesenchymal stem cell activity. *Acta Biomaterialia*, 76:116-125, 2018.

APPENDICES:

Please find appended original copies of the following work:

Quad Chart:

Year 5 Quarter 4 Quad Chart

Peer-Reviewed Scientific Journals:

M.J. Dewey, A.V. Nosatov, K. Subedi, R. Shah, A. Jakus, B.A.C. Harley, 'Inclusion of a 3D-printed Hyperelastic Bone mesh improves mechanical and osteogenic performance of a mineralized collagen scaffold,' Acta Biomater., 121:224-36, 2021. PMCID: PMC7856202.

M.J. Dewey and B.A.C. Harley, 'Biomaterial design strategies to address obstacles in craniomaxillofacial bone repair,' RSC Adv., 11(29):17809-27, 2021. PMCID: PMC8443006. NOTE: review article which heavily cites work supported by this grant.

M.J. Dewey and B.A.C. Harley, 'Principles of Bone Tissue Engineering,' in B. Mahadik and J. Fisher (eds.) Bone Tissue Engineering: Bench to Bedside Using 3D Printing, 2021.

Technology Disclosures:

None

Polycaprolactone-collagen composite biomaterials for mandible regeneration

USAMRMC 1464004
W81XWH-16-1-0566

PI: Brendan Harley **Org:** University of Illinois at Urbana-Champaign **Award Amount:** $800,000

Study/Product Aim(s)

Our goal is to demonstrate that integrating a mineralized collagen scaffold within a macroporous PCL construct will generate a multi-scale composite that enhances adipose-derived MSC osteogenesis and subsequent bone regeneration. Our aims:

Aim 1: Validate the osteogenic potential of growth factor decorated collagen-PCL composites.

Aim 2: Examine the quality and kinetics of mandible bone regeneration using the collagen-PCL composite.

Approach

We a polycaprolactone (PCL) support cage into a mineralized collagen scaffold to form a PCL-collagen composite. We will define the improvement in adipose-derived mesenchymal stem cell osteogenesis in response to the release of growth factors (BMP-2 and VEGF) from the collagen scaffold, as well as regenerative potential of the growth factor decorated collagen-PCL composite in a porcine model of mandibular defect.

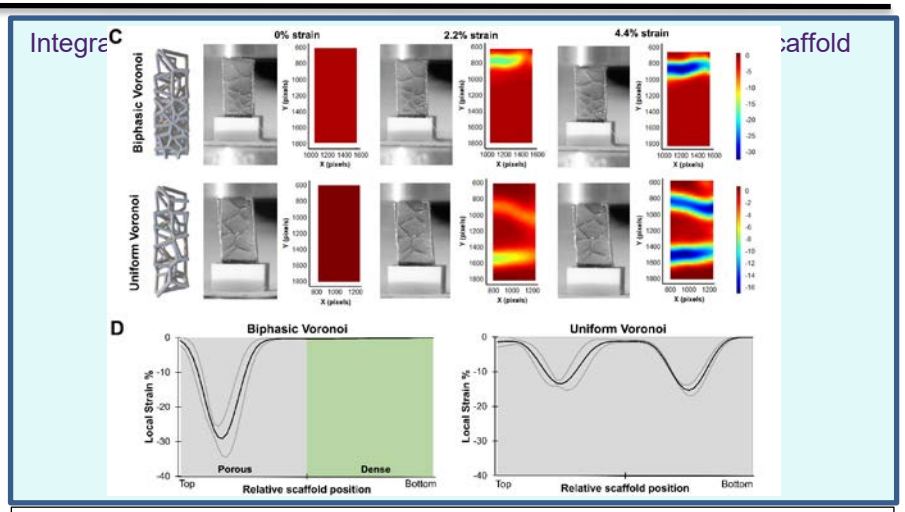

Accomplishments: We completed analysis of local strain profiles in an experimental set of PCL fiber reinforcement cages that can be added into the collagen scaffold to improve implant conformal fitting. We show it possible to locally alter deformation profiles to aid conformal fitting.

Timeline and Cost

Activities / CY	16	17	18	19
Fabrication, biophysical characterization of growth-factor decorated collagen-PCL composites				
In vitro osteogenic activity of growth-factor decorated collagen-PCL composites				
Determine kinetics of mandibular healing via growth-factor decorated collagen-PCL composites				
Define improved quality of mandibular healing using growth-factor decorated collagen-PCL composites				
Estimated Budget ($K)	**$30k**	**$200k**	**$340k**	**$230k**

Updated: 20 Oct 2021

Goals/Milestones

CY16 Goal – Collagen-PCL composite fabrication
- ☑ Fabricate initial library of collagen-PCL composites

CY17 Goal – In vitro osteogenesis assessment
- ☑ Biophysical characterization of composites
- ☑ Define growth factor elution from collagen-PCL composites

CY19 Goal – In vivo bone regeneration assays
- ☑ Quantify degree of enhanced osteogenic potential of adMSCs within BMP-2 and VEGF decorated collagen-PCL composites
- ☑ Finalize design criteria for collagen-PCL composites for *in vivo* implantation and initiate subcritical and critical defect models

CY20 Goal – Quantify quality and kinetics of mandible regeneration
- ☑ Complete structural, biomolecular, and growth factor optimization of scaffold.
- ☐ Identify collagen-PCL variant that displays high quality bone repair.

Comments/Challenges/Issues/Concerns

- We requested a no cost extension to initiate/complete the in vivo component of the project (we have retained sufficient budget for the work).

Budget Expenditure to Date

Projected Expenditure: $725,000
Actual Expenditure: $703,742.40

Acta Biomaterialia 121 (2021) 224–236

Contents lists available at ScienceDirect

Acta Biomaterialia

journal homepage: www.elsevier.com/locate/actbio

Inclusion of a 3D-printed Hyperelastic Bone mesh improves mechanical and osteogenic performance of a mineralized collagen scaffold

Marley J. Dewey[a], Andrey V. Nosatov[a], Kiran Subedi[b,c], Ramille Shah[c], Adam Jakus[c], Brendan A.C. Harley[a,d,e,*]

[a] Dept. of Materials Science and Engineering, University of Illinois at Urbana-Champaign, Urbana, IL 61801, United States
[b] College of Agriculture and Environmental Sciences, North Carolina Agriculture and Technical State University, Greensboro, NC 27411, United States
[c] Dimension Inx, Chicago, IL 60616, United States
[d] Dept. of Chemical and Biomolecular Engineering, University of Illinois at Urbana-Champaign, Urbana, IL 61801, United States
[e] Carl R. Woese Institute for Genomic Biology, University of Illinois at Urbana-Champaign, Urbana, IL 61801, United States

ARTICLE INFO

Article history:
Received 29 August 2020
Revised 17 November 2020
Accepted 17 November 2020
Available online 21 November 2020

Keywords:
Mineralized collagen
Craniomaxillofacial
Bone repair
3D-printing
Shape-fitting
3D-paints

ABSTRACT

Regenerative repair of craniomaxillofacial bone injuries is challenging due to both the large size and irregular shape of many defects. Mineralized collagen scaffolds have previously been shown to be a promising biomaterial implant to accelerate craniofacial bone regeneration *in vivo*. Here we describe inclusion of a 3D-printed polymer or ceramic-based mesh into a mineralized collagen scaffold to improve mechanical and biological activity. Mineralized collagen scaffolds were reinforced with 3D-printed Fluffy-PLG (ultraporous polylactide-co-glycolide co-polymer) or Hyperelastic Bone (90wt% calcium phosphate in PLG) meshes. We show degradation byproducts and acidic release from the printed structures have limited negative impact on the viability of mesenchymal stem cells. Further, inclusion of a mesh formed from Hyperelastic Bone generates a reinforced composite with significantly improved mechanical performance (elastic modulus, push-out strength). Composites formed from the mineralized collagen scaffold and either Hyperelastic Bone or Fluffy-PLG reinforcement both supported human bone-marrow derived mesenchymal stem cell osteogenesis and new bone formation. This was observed by increased mineral formation in Fluffy-PLG composites and increased cell viability and upregulation of *RUNX2*, *Osterix*, and *COL1A2* genes in both composites. Strikingly, composites reinforced with Hyperelastic Bone mesh elicited significantly increased secretion of osteoprotegerin, a soluble glycoprotein and endogenous inhibitor of osteoclast activity. These results suggest that architectured meshes can be integrated into collagen scaffolds to boost mechanical performance and actively instruct cell processes that aid osteogenicity; specifically, secretion of a factor crucial to inhibiting osteoclast-mediated bone resorption. Future work will focus on further adapting the polymer mesh architecture to confer improved shape-fitting capacity as well as to investigate the role of polymer reinforcement on MSC-osteoclast interactions as a means to increase regenerative potential.

Statement of significance

Craniofacial bone defects occur due to trauma, congenital abnormalities, and during the course of surgical treatments for stroke and cancer. Clinically-available technologies for craniofacial reconstruction are non-regenerative. We report inclusion of polymer mesh generated via 3D-printing into a mineralized collagen scaffold under development for craniofacial bone regeneration. Scaffold-mesh composites improved mechanical performance and mesenchymal stem cell activity, notably secretion of osteoprotegerin, a soluble glycoprotein and endogenous inhibitor of osteoclast activity. These findings suggest the exciting possibility to co-optimize the composition and architecture of an integrated polymer mesh to both passively aid surgical-practicality and actively accelerate regenerative healing.

https://doi.org/10.1016/j.actbio.2020.11.028
1742-7061/

1. Introduction

There is a clinical need to improve surgical repair of craniomaxillofacial bone defects. Osseous defects of the skull occur secondary to trauma, congenital abnormalities, or after resection to treat stroke, cerebral aneurysms, or cancer [1,2]. CMF defects can occur in all age ranges; cleft palate birth defects, trauma from battlefield injuries, and multiple missing teeth or oral cancer which can cause loss of jaw bone [3]. Battlefield injuries are a special class of CMF injuries, with greater than 25% of all survivable battlefield injuries in recent military conflicts in southwest Asia (Operation Iraqi Freedom, Operation Enduring Freedom) classified as maxillofacial or neck trauma, with greater than 50% attributed to explosives [4,5]. These types of injuries result in poor healing outcomes due to infection, inadequate healing of the defect, and fixation failures [6]. Current standard of care for these defects is cranioplasty, or calvarial reconstruction, which prioritize cerebral protection over regeneration [7]. Cranioplasties are common (>35,000/yr in the US; incl. >10,000 cleft palate repairs) [8], but current clinical materials have significant shortcomings. Autologous or allogenic bone remains a gold standard [9], but are limited by access to autologous bone [10], donor site morbidity, surgical complications after cancellous autografts or cadaveric allografts (10-40%) [11], and difficulty fitting irregular defects, as well as inconsistent repair [12]. Alloplastic materials are plagued by complications such as extrusion, high cost, and high infection rates (5-12x more complications than autologous transplant) [13,14].

These drawbacks motivate tissue engineering solutions to potentiate calvarial bone regeneration, notably metal, ceramic, and polymer-based scaffolds. Significant challenges remain, notably optimization of biomaterial strength, osteogenic activity, and ability to fit complex defect geometries. Mechanical stability and the ability to limit micromotion at the host-implant interface is crucial to the healing outcome and can directly affect osseointegration and bone regeneration [15]. Surgical practicality is a key factor in biomaterial design and implementation. Notably, there is significant intraoperative time required to shape implants to fit irregular defects, adding time and expense that becomes even more challenging for high risk defects (radiation, previous infection) [9,16]. Drawbacks of currently available clinical materials highlight the urgent need for scalable solutions that prioritize calvarial bone regeneration through the ability to fit complex defect geometries and avoid micromotion. This suggests a need to identify scalable materials that contain a precise repeating unit structure similar to a mesh to improve reproducibility, achievable through 3D-printing.

Mineralized collagen scaffolds have been developed as a biomaterial implant to promote *in vivo* bone formation and *in vitro* mineral formation [17–21]. Recent work by our own laboratory has identified a mineralized collagen scaffold variant that does not need additional osteogenic supplements such as osteogenic media or Bone Morphogenic Protein-2 (BMP-2) in order to differentiate mesenchymal stem cells (MSCs) towards the osteoblastic lineage [22,23]. These osteoprogenitors and their progeny produce a secretome to accelerate osteogenic specification, promote vascular remodeling, and suppress inflammatory damage [24], making them highly translational. We recently showed that MSC-osteoprogenitors seeded in this mineralized collagen scaffold secrete osteoprotegerin (OPG) a soluble glycoprotein and endogenous inhibitor of osteoclastogenesis and osteoclast activity; further, osteoclasts show reduced activity in response to the osteoprogenitor seeded scaffold [25]. These results suggest this mineralized scaffold may both increase MSC-osteogenesis and inhibit osteoclast activity [26]. However, despite these biological advantages the high-porosity of these scaffolds renders them mechanically weak. Successful clinical use requires the biomaterial also be surgically practical. Specifically that they be readily customized to fit complex three-dimensional defects and strong enough to withstand physiological loading [9,27].

Beyond general mechanical strength, poor conformal contact between the biomaterial and wound margin significantly inhibits cell recruitment, angiogenesis, regenerative healing and greatly increases the risk of graft resorption [28]. Implants with improved conformal contact to the host bone can limit micromotion and may improve osseointegration and regenerative healing [15]. This can be accomplished by developing shape-fitting implants that can conformally fit to the host defect site. Approaches to aid shape-fitting include the use of temperature sensitive polymers that can be shaped intraoperatively to fit complex defect sites [29,30]. Recently, our laboratory has looked to adapt three-dimensional printing approaches to create biomaterial composites with improved mechanical strength and shape-fitting capacity. Notably, we embed a mechanically-robust polymer mesh with millimeter-scale porosity into the mineralized collagen scaffold with micron-scale porosity [31]. We generated a first generation polycaprolactone (PCL) structure to form a PCL-collagen composite; this composite accelerated sub-critical defect repair in a porcine mandible defect [31,32]. However, these PCL cages were mechanically rigid, and had no design elements to improve conformal fitting. We recently reported a 3D-printed poly(lactic-acid) based fiber with reduced percent polymer content and modifications to the fiber architecture to improve conformal fitting [33]. However, both approaches considered the polymer reinforcement phase of the composite as a passive reinforcement design rather than an active component of the biological response.

Here, we describe *in vitro* characterization of a new class of composite biomaterials. We define our composite as a mineralized collagen scaffold reinforced with a microporous mesh 3D-printed from Hyperelastic Bone® or Fluffy-PLG (Dimension Inx, LLC, from here on Hyperelastic Bone® will be denoted Hyperelastic Bone). Fluffy-PLG is comprised of medical-grade poly(L-lactide-co-glycolide), with ≥95% internal porosity and elastic properties (2.7 ± 0.8 MPa Elastic Modulus) sufficient to form a self-supporting mesh [34], and is capable of supporting cell proliferation *in vitro* and vascularization *in vivo* [34,35]. Hyperelastic Bone is comprised of 90 wt% calcium phosphate, specifically synthetic medical-grade hydroxyapatite, and 10 wt% poly(lactide-co-glycolide); Hyperelastic Bone 3D-prints have separately been shown to induce MSC osteogenic differentiation *in vitro* and new bone formation *in vivo* [36–39]. We incorporate two different print architectures into mineralized collagen to create Hyperelastic Bone and Fluffy-PLG composites, one cross-design to facilitate rapid *in vitro* experiments, and one mesh design to better represent fabrication designs more relevant for eventual clinical translation of a composite architecture. We investigate whether inclusion of 3D-printed architectures into a mineralized collagen scaffold to create reinforced composites improves mechanical performance (stiffness, conformal fitting capacity). We subsequently examined whether inclusion of a Fluffy-PLG or Hyperelastic Bone mesh provides biological advantage via degradation by-products to improve osteogenic response of human mesenchymal stem cells (hMSCs) within the mineralized collagen scaffold. These studies therefore consider inclusion of architectured cellular structures into mineralized collagen scaffolds to provide significant mechanical and biological advantage for regenerative medicine applications.

* Corresponding author at: Dept. of Chemical and Biomolecular Engineering, Carl R. Woese Institute for Genomic Biology, University of Illinois at Urbana-Champaign, 110 Roger Adams Laboratory, 600 S. Mathews Ave., Urbana, IL 61801, United States.

E-mail addresses: ksubedi@ncat.edu (K. Subedi), bharley@illinois.edu (B.A.C. Harley).

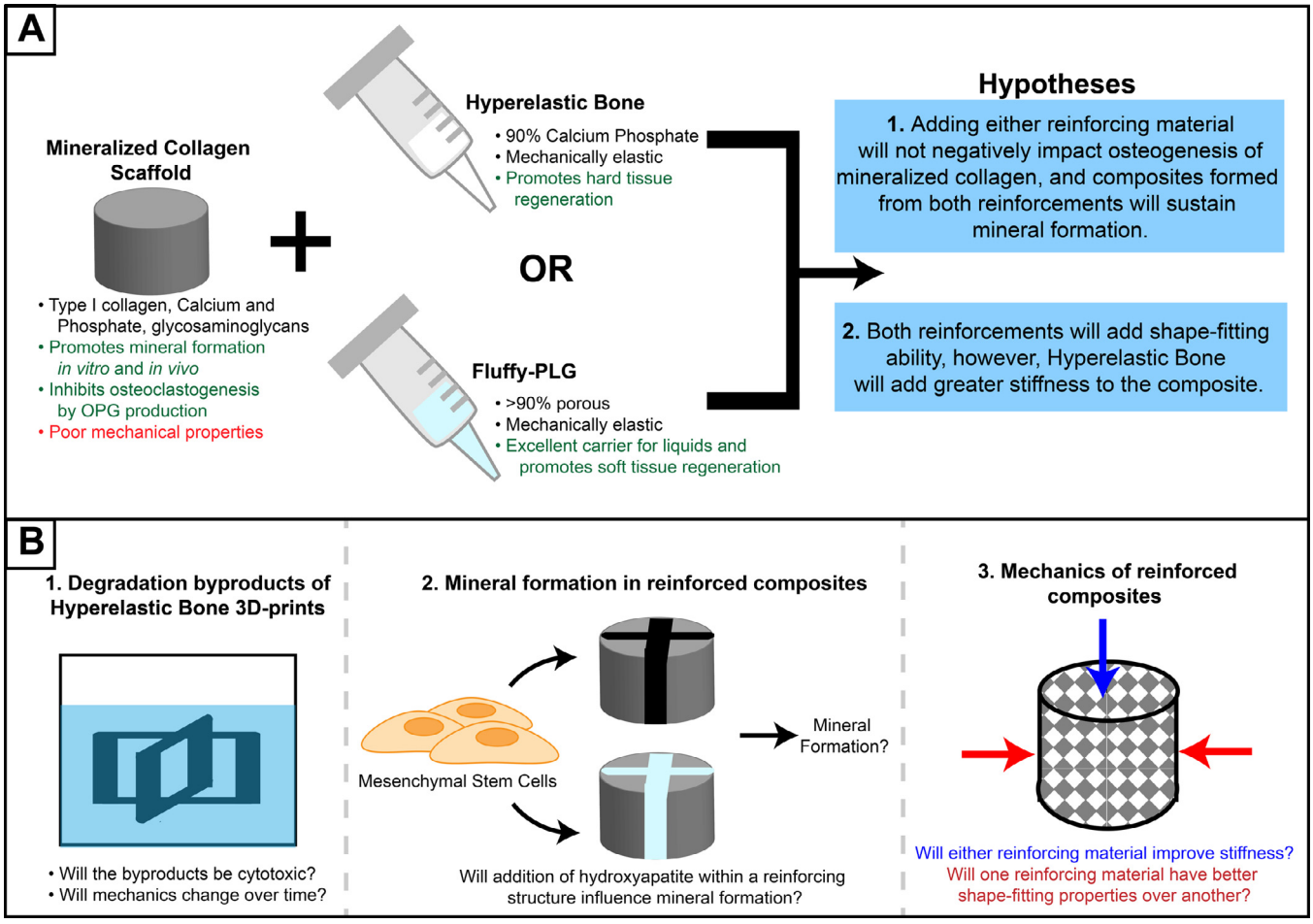

Fig. 1. Experimental outline. Mineralized collagen scaffolds promote bone repair, however, these have poor mechanical properties including lack of shape-fitting behavior. (A) We examined incorporating reinforcing structures 3D-printed from either Hyperelastic Bone or Fluffy-PLG, to the mineralized collagen scaffolds. We investigated (1) if addition of the reinforcing structures could increase the osteogenic response, and if the 3D-printed structure containing calcium phosphate would promote bone formation over the one without and (2) the influence of the 3D-printed structures on scaffold mechanical properties (i.e. compressive properties and shape-fitting). (B) Steps of the experiment to answer the study questions.

2. Materials and methods

2.1. Experimental design

Composites were fabricated from mineralized collagen scaffolds combined with reinforcing support architectures 3D-printed from Hyperelastic Bone or Fluffy-PLG 3D-paints (Dimension Inx LLC, Illinois, USA) (Fig. 1A). Throughout this study we compared the three material groups: mineralized collagen scaffolds (MC) on their own, mineralized collagen composites reinforced with 3D-printed Hyperelastic Bone, and mineralized collagen composites reinforced with 3D-printed Fluffy-PLG (MC-Fluffy). Although nano- and microstructurally distinct, 3D-printed Fluffy-PLG and Hyperelastic Bone are based on the same polylactide-co-glycolide (PLG), with the only compositional difference being addition of 90wt% calcium phosphate mineral in the Hyperelastic Bone. Studies of the effect of degradation products (released lactic and glycolic acid; changes in pH; calcium and phosphorous release) or degradation induced changes in mechanical performance (elastic modulus) was evaluated for 3D-printed Hyperelastic Bone. *In vitro* testing of hMSC osteogenesis and mineral formation was performed using mineralized collagen scaffolds as a function of the inclusion of 3D-printed, reinforcing Hyperelastic Bone or Fluffy-PLG the form of a cross-design (Fig. 1B). Overall mechanical performance (elastic modulus; shape-fitting ability) was performed on reinforced composites with a 3D-printed mesh design, and was evaluated via compression and push-out tests to determine if inclusion of the reinforcing structures improve mechanical properties of the mineralized collagen scaffolds (Fig. 1B).

2.2. 3D-printing Hyperelastic Bone and Fluffy-PLG fiber arrays

Hyperelastic Bone and Fluffy-PLG 3D-Paints were provided by Dimension Inx LLC and 3D-printed using a Manufacturing Series 3D-BioPlotter (EnvisionTEC, Michigan, USA). Constructs used for degradation studies and *in vitro* culture were printed as cross designs, symmetrical crosses 6 mm in diameter and 3 mm in height with a 0.7 mm feature thickness (Fig. 2) using a 27 Ga nozzle at a speed of 2-5 mm/s dependent on solution viscosity, a room temperature stage and deposition, and low print speeds to accommodate the fine structure of the print [34,35,39]. These structures display low polymer volume fractions within the resulting composite (13.61 v/v%). Hyperelastic Bone 3D-prints were stored in the dark at 4°C until use while Fluffy-PLG 3D-prints were stored at -80°C until use, per manufacturer instructions. A 3D-printed mesh design was used to reinforcement mineralized collagen scaffolds for mechanical testing. These were prepared and printed by Dimension Inx LLC as square sheets at 70 mm/s (60 mm on a side; 6 mm

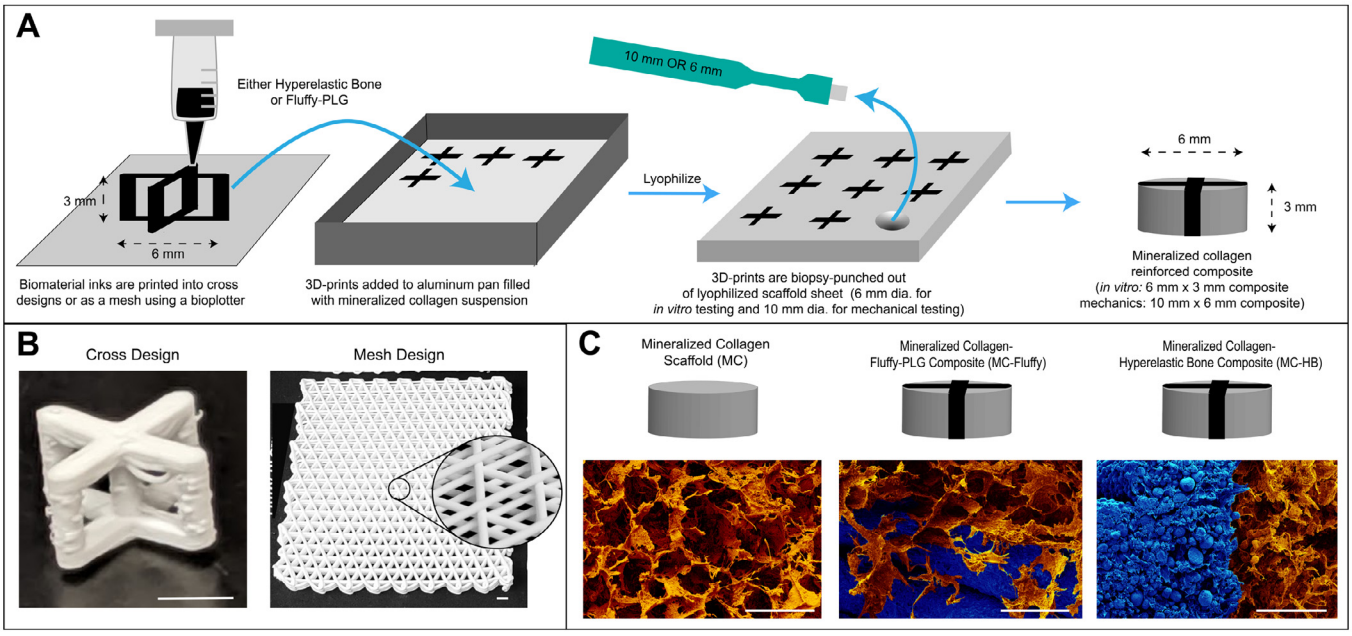

Fig. 2. Fabrication of composites used *in vitro* and for mechanical testing. (A) 3D-paints were 3D printed in "cross designs" for *in vitro* testing or as a mesh for mechanical testing. Cross prints were printed individually and added to a continuous mineralized collagen suspension in an aluminum mold. After the addition of multiple prints, the entire mold was freeze-dried and a 6 mm biopsy punch was used to remove scaffold and 3D print together. Mesh composites were fabricated by adding the entire mesh to the aluminum mold with mineralized collagen suspension and biopsy punching 10 mm diameter composites after lyophilization. Mesh prints were printed with either 2 mm or 3 mm line spacing. (B) Images of cross and mesh 3D prints, scale bar represents 3 mm. (C) SEM images of mineralized collagen scaffold and composites. Scale bar represents 200 μm and images are false-colored to demonstrate collagen (orange) and 3D-print (blue). Raw SEM images can be viewed in Supp. Fig. 3.

thick), with a standardized 120° angle [35]. 3D-printed reinforcing meshes were printed with Fluffy-PLG and prepared with two distinct feature sizes (2 mm or 3 mm line spacing). However, Hyperelastic Bone 3D-printed meshes were only tested for 2 mm line spacing (3 mm line spacing composites were not stable with regard to handling and manipulation due to the large structural pore size relative to the small, comprising fiber diameters). A 2 mm line spacing print is approximately 83% porous based on the design, not including inherent material porosity.

2.3. Analysis of degradation byproducts and changes in mechanical properties of Hyperelastic Bone 3D-prints

Degradation byproducts of 3D-printed Hyperelastic Bone were analyzed using a standardized 'cross design' print (Fig. 2). Prints were washed twice in 70% ethanol for 30 min and then twice in cell grade water for 30 min per the manufacturer's instructions before submerging individual mesh structures in 5 mL of Phosphate Buffered Saline (PBS) in individual glass vials. Sample were then either maintained at 37°C in an incubator (standard degradation; to simulate degradation during *in vitro* cell culture or *in vivo*), or in a 90°C oven (Isotemp Vacuum Oven Model 282A, Fisher Scientific, Massachusetts, USA) to facilitate accelerated degradation [40].

pH. The pH of 3D-print conditioned PBS samples from the 90°C degradation study was measured using a FiveEasy Standard pH meter (Mettler Toledo, Ohio, USA) for n = 8 samples (PBS as a control). This condition was used as an accelerated degradation method to examine changes in pH due to total degradation of the polymer mesh. This allowed us to examine the effect of maximum release of ions and polymer degradation byproducts to determine if these would have an appreciable effect on the pH and cell viability.

Lactic and glycolic acid release. Over the course of a 28-day accelerated release experiment ('cross design' prints in 5 mL PBS at 90°C), the PBS incubation solution was centrifuged at regular intervals to isolate the liquid supernatant for analysis of lactic and glycolic acid concentrations. 5 mL of PBS, along with any particles separated during centrifugation, were added to each sample vial until the next isolation point. Colorimetric determination of lactic acid concentration followed procedures in literature [41]. Briefly, a standard curve was created using a solution of 1% L-(+)-Lactic Acid (Sigma Aldrich, Missouri, USA) and half-dilutions. PBS and iron (III) chloride (Sigma Aldrich) were used as controls. 50 μl of sample was mixed with 2 mL of 0.2% iron (III) chloride, and absorbance was measured at a wavelength of 390 nm on spectrophotometer (Tecan, Switzerland). Colorimetric determination of glycolic acid release followed procedures in literature [42]. A 1 mg/mL solution of glycolic acid (Sigma Aldrich) was used to create half-dilutions to generate a standard curve. 500 μL of sample was evaporated to dryness at 125°C in a vacuum oven at atmospheric pressure. β-Naphthol (Sigma Aldrich) in 92% sulfuric acid was added to vials containing evaporated sample and boiled for 20 min. After boiling, 80% sulfuric acid was added to samples for 10 min before measuring absorbance at a wavelength of 480 nm on a spectrophotometer (Tecan). A sample size of n = 8 was used for both lactic acid and glycolic acid release measurements.

Calcium and phosphate release. Calcium and Phosphate release from 3D-printed Hyperelastic Bone and mineralized collagen scaffolds were quantified through a 28 days standard release experiment (culture in 5 mL of PBS at 37°C). 1 mL PBS aliquots were removed from suspension, then combined with 2 mL of Trace Metal Grade concentrated HNO_3 (Thermo Fisher Scientific 67-70%) for a 30-minute pre-digestion step. The tubes were then capped and placed into a rotating carousel inside MARS 6 (CEM Microwave Technology Ltd., North Carolina, USA) microwave digester (40 minutes). The final digested solution was diluted to a volume of 50 mL in DI water, then analyzed via inductively coupled plasma-mass spectrometer (ICP-OES, Optima 8300, PerkinElmer, USA; elemental analysis in axial mode; Supp. Tables 1 and 2). Eight samples of each group were used per time point.

Mechanical analysis. Mechanical testing was performed on Hyperelastic Bone 3D-prints after 0, 7, and 28 days in PBS at 37°C (PBS was changed every 3 days). Prints were aerated in the incubator overnight and then dried at room temperature overnight before testing. Compression testing was performed with an Instron 5943 mechanical tester (Instron, Massachusetts, USA) using a 100 N load cell at a rate of 1 mm/min. Seven samples at each timepoint were tested and stress-strain curves were analyzed using a custom Matlab program to determine Young's modulus, ultimate stress, and ultimate strain.

2.4. Fabrication of mineralized collagen scaffolds and reinforced composites

Mineralized collagen scaffolds were fabricated via lyophilization from a liquid suspension as previously described [17,18,22]; while composites were fabricated via lyophilization as previously described [32,33,43]. Briefly, 1.9 w/v% type I collagen from bovine Achilles tendon (Sigma Aldrich) was blended together with a 40 wt% mineral suspension of phosphoric acid (Fisher Scientific) and calcium hydroxide (Sigma Aldrich), 0.84 v% chondroitin-6-sulfate sodium salt from shark cartilage (Sigma Aldrich), and additional calcium nitrate tetrahydrate (Sigma Aldrich) using a rotor-stator in a jacketed cooling vessel until smooth [17,18,31,32]. Mineralized collagen scaffolds for *in vitro* and mechanical testing were fabricated by pipetting the suspension into aluminum pans and lyophilizing using a Genesis freeze-dryer (VirTis, New York, USA). Scaffolds were added to the freeze-dryer shelf at 20°C and the temperature was dropped at a rate of 1°C/min to -10°C in order to form ice crystals. Samples were held at -10°C for 2 hours and then ice crystals were sublimated by decreasing the pressure and temperature to create a porous scaffold. After sublimation, solid scaffolds were brought back to room temperature and atmospheric pressure before storing in a desiccator prior to use. Composites (MC-HB or MC-Fluffy) were formed by adding the 3D-printed reinforcement, either Hyperelastic Bone or Fluffy-PLG, into the collagen suspension prior to lyophilization (Fig. 2, Supp. Fig. 4). Prior to incorporation into the mineralized collagen suspension, 3D-prints were washed per supplier instructions: Hyperelastic Bone 3D-prints in 70% ethanol then cell grade water; Fluffy-PLG prints in cell grade water to remove salts, then 70% ethanol, then in cell grade water again [34,39]. Lyophilization conditions to create composites used the same temperature and pressure profiles as scaffolds. Scaffolds and composites for *in vitro* testing were biopsy-punched out of the resulting sheet with a 6 mm diameter biopsy punch, while scaffolds and composites for mechanical testing used a 10 mm diameter biopsy punch.

2.5. Scanning electron microscopy of collagen scaffolds and reinforced composites

Scanning electron microscopy (SEM) was used to visualize collagen infiltration into the 3D-printed structures. Dry collagen scaffolds and reinforced composites (MC-HB, MC-Fluffy) were cut to expose the interior before sputter coating with Au/Pd (Denton Desk II TSC, New Jersey, USA). After sputter-coating, samples were imaged using an FEI Quanta FEG 450 ESEM (FEI, Hillsboro, OR). Both composites reinforced with cross design and mesh design 3D-prints were imaged for collagen infiltration into 3D-prints (Fig. 2, Supp. Fig. 2).

2.6. Compression and shape-fitting testing of collagen scaffolds and reinforced composites

Mechanical performance of collagen reinforced with a standardized 120° mesh morphology 3D-print was evaluated [35]. Scaffolds and reinforced composites formed from either Hyperelastic Bone or Fluffy-PLG were tested under mechanical compression to determine elastic modulus as well as using a standardized push-out test. Reinforced composites and scaffolds measured approximately 10 mm in diameter by 6 mm in height, and both mechanical tests used an Instron 5943 mechanical tester (Instron) with a 100 N load cell. Mechanical compression was performed at a rate of 1 mm/min and the linear portion of stress-strain curves was analyzed using a custom Matlab program to determine Young's Modulus [32,33]. Push out testing was performed at a rate of 2 mm/min following previously described methods [33,44]. Briefly, samples were compressed and fit into an 8.5 mm diameter hole in a Teflon plate and samples were pushed through the mold to measure maximum load achieved to move the samples. Eight samples were used for each test in order to determine stiffness and shape-fitting ability.

2.7. Cell culture and biomaterial preparation

Bone marrow derived human mesenchymal stem cells (BM-hMSCs) (24yr old B female, Lonza, Switzerland) were used at passage 4 – 6 and cultured with complete hMSC media containing low glucose Dulbecco's Modified Eagle Medium and glutamine (School of Chemical Sciences Cell Media Facility, University of Illinois), Fetal Bovine Serum (Gemini Bio Products, California, USA), and antibiotic-antimycotic solution (Thermo Fisher Scientific, Massachusetts, USA). Cell contamination was tested with a MycoAlert™ Mycoplasma Detection Kit (Lonza) and cells tested negative for mycoplasma.

Scaffolds and reinforced composites were sterilized via ethylene oxide treatment with an AN74i Anprolene gas sterilizer (Andersen Sterilizers Inc., North Carolina, USA) for *in vitro* testing. Prior to adding cells to scaffolds and reinforced composites, these followed a standard hydration procedure for mineralized collagen scaffolds previously reported [33,45]. Briefly, samples were hydrated in 70% ethanol, washed in PBS, crosslinked with 1-Ethyl-3-(3-dimethylaminopropyl) carbodiimide and N-Hydroxysuccinimide, followed by washing in PBS, and finally soaking in hMSC complete media for 2 days.

2.8. Influence of Hyperelastic Bone degradation byproducts on cell activity

Cytotoxic effects of Hyperelastic Bone degradation byproducts were determined via a previously defined elution assay [46]. Briefly, Hyperelastic Bone structures were printed into standard 'cross-designs' (Fig. 2) then placed in PBS either in a 37°C incubator or in a 90°C vacuum oven (accelerated degradation) for 28 days to create degradation byproduct conditioned media. Cell cytotoxicity was determined using for 10,000 MSCs in individual wells of a 96-well plate. Briefly, hMSCs were first cultured in complete hMSC media for 24 hrs. After 24 hrs, media was removed and replaced for 24 hours with PBS containing eluted degradation factors at full strength (100%) or conditioned PBS diluted with hMSC media (50% sample, 25% sample, and 12.5% sample). Non-conditioned PBS was used as a control. After 24 hours, metabolic health of hMSCs was examined via an alamarBlue™ (Thermo Fisher Scientific) assay, measuring the fluorescence of resorufin (540 nm excitation, 580 nm emission) using a F200 spectrophotometer (Tecan). Metabolic activity was compared to a standard curve of known cell numbers. There were 8 samples of each group tested with PBS used as a control.

2.9. Cell activity within scaffolds and reinforced composites

Scaffolds and reinforced composites were added to 24-well plates and seeded via a standard static seeding assay (5,000 cells/μL per side; 100,000 cells/scaffold) using previously defined procedures [33,45]. After allowing cell attachment, hMSC complete media was added to wells and plates containing cell-seeded scaffolds and then were added to a 37°C incubator. The metabolic activity of cell-seeded biomaterials was examined via an alamarBlue™ (Thermo Fisher Scientific) assay at days 1, 4, 7, 14, and 28. Briefly, scaffolds and composites were washed in PBS, followed by a 1.5 hr soak in alamarBlue™ and complete hMSC cell media on a shaker in a 37°C incubator [33,45]. A standard curve of known cell number was used to calculate fold change of metabolic activity over the initial cell seeding density (a fold change of 1 represented the metabolic activity of 100,000 cells). Six samples were used to determine metabolic activity, and these were used for the entirety of the study (non-destructive assay).

Expression levels of cell secreted Osteoprotegerin and Vascular Endothelial Growth Factor (VEGF) was examined via ELISA (R&D Systems, Minnesota, USA). Briefly, media was collected and replaced from cell-seeded samples every 3 days until day 28 to determine cumulative protein expression. ELISAs were performed to using 25 μL of sample and 75 μL reagent diluent and compared against a known standard curve to quantify expression level. Six samples were used throughout the study (non-destructive).

Analysis of gene expression profiles was performed at days 1, 4, 7, 14, and 28 of culture. Specimens were washed in PBS, frozen at -80°C, pulverized on dry ice with disposable pestles (Thermo Fisher Scientific), then treated with an RNeasy Plant Mini Kit (Qiagen, California, USA) [47]. Concentrations of isolated RNA were measured using a Nanodrop Lite (Thermo Fisher Scientific). Reverse transcription of RNA to cDNA was performed following directions and supplies from a QuantiNova Reverse Transcription kit (Qiagen) and a S100 thermal cycler (Bio-Rad, Hercules, California). After reverse transcription, PCR was performed on cDNA to quantify gene expression. 10 ng of cDNA was used in each well and Taqman primers were purchased from Thermo Fisher Scientific (*RUNX2, COL1A2, Osterix, FGFR2, IGF2*) with *GAPDH* serving as a housekeeping control (Supp. Table 3). Plate preparation was performed using a Gilson Pipetmax liquid handling machine (Gilson, Wisconsin, USA) and plates were read using a QuantstudioTM 7 Flex Real-Time PCR System (Thermo Fisher Scientific). Data was analyzed using the delta-delta CT method to generate box plots for a fold change of gene expression (with a fold change of 1 representing the gene expression of 100,000 hMSCs before seeding on scaffolds and composites). Five samples were used at each timepoint.

2.10. Analysis of mineral formation in scaffolds and reinforced composites

Inductively Coupled Plasma (ICP) Optical Emission spectrometry was performed to assess mineral formation at the end of *in vitro* culture (day 28). MC, MC-HB, and MC-Fluffy samples were washed in PBS, fixed with formalin (Formal-Fix, Thermo Fisher Scientific) for 24 hrs at 4°C, washed again in PBS, then dried on a Kimwipe before storing at -80°C until use. Before performing ICP, samples were lyophilized at the same conditions used to fabricate the original scaffolds. Samples were weighed then dissolved using concentrated nitric acid, Trace Metal Grade concentrated HNO_3 (Thermo Fischer Scientific 67-70%), followed by automated sequential microwave digestion in a CEM Mars 6 microwave digester. The acidic solution was diluted to a volume of 50 mL using DI water, so as to make the final concentration of the acid <5%. The ICP-OES was calibrated with a series of matrix matched standards before introducing the unknown samples. Digestion and ICP-OES analysis parameters are listed in Supp. Tables 4 and 5. Nine samples were used for each group and these were normalized to the calcium and phosphorous content of respective dry scaffolds and composites without cells in order to get a fold change and new calcium and phosphorous deposition.

2.11. Statistical methods

Statistics followed procedures outlined by Ott and Longnecker [48]. Quantity of samples used was based off previous experiments using similar sample groups and a 95% confidence interval for all tests [33,45]. For all data, normality was evaluated and if data was not normal a Grubb's outlier test was performed and normality was re-assessed. Analysis of more than two groups used an ANOVA, and depending on whether assumptions of normality (Shapiro-Wilk) and equal variance (Levene's Test) of residuals was met, a specific ANOVA was used as outlined in Supp. Table 6. For data involving two groups, either a paired *T*-test or a two-sample *T*-test was used. Normality (Shapiro-Wilk) and two sample *T*-test for variance were completed using OriginPro software (OriginLab, Massachusetts, USA) before analysis. For non-normal data a paired sample Wilcoxon Signed Rank test was used or a two-sample Kolmogorov-Smirnov test was used. For samples with normal data and unequal variance, a two sample *T*-test with a Welch correction was used as outline in Supp. Table 7. For powers lower than 0.8, data was deemed inconclusive. Data is expressed as average ± standard deviation unless otherwise noted.

3. Results

3.1. Degradation byproducts of Hyperelastic Bone does not negatively affect cell viability

Hyperelastic Bone 3D-printed as a 'cross design' completely degraded over the course of a 28 day-accelerated degradation study (PBS; 90°C). Aliquots taken from the Hyperelastic Bone degradation experiments were first analyzed to define changes in pH as well as glycolic acid and lactic acid elution; changes in pH were also compared to a PBS standard (pH 7.4) as well as mineralized collagen scaffolds exposed to accelerated degradation conditions (PBS; 90°C). Overall, both mineralized collagen scaffolds and Hyperelastic Bone 3D-prints drove a drop in solution pH during early stages of degradation; scaffolds showed a sharper decrease in pH while the Hyperelastic Bone showed a temporally extended drop in pH. However, acidic byproducts were only detectable during the first week of degradation (Supp. Fig. 1A). Analysis of lactic and glycolic acid content in the media suggested the majority released lactic and glycolic acid occurred rapidly as well, with a total of 12.7 mg lactic acid and 307.5 μg of glycolic acid released (Supp. Fig. 1B, C). Finally, we investigated whether the degradation byproducts from the Hyperelastic Bone structures drove a measurable change in metabolic activity of hMSCs. The total eluted byproducts from Hyperelastic bone structures in PBS were collected from both standard (37°C) and accelerated (90°C) degradation protocols over 28 days and compared to PBS. hMSCs were cultured in a mixture of conventional cell culture media and PBS (PBS; 37°C degradation byproducts; 90°C degradation byproducts) at discrete ratios: 12.5% PBS, 25% PBS, 50% PBS, 100% PBS. While hMSC metabolic activity reduced with increasing amounts of PBS (vs. cell culture media), there was no significant trend suggesting a decrease in hMSC activity as a function of Hyperelastic Bone degradation byproducts (Supp. Fig. 1D).

Table 1
Youngs Modulus, ultimate stress, and ultimate strain of Hyperelastic Bone 3D-printed cross designs in PBS at 37°C for 7 and 28 days compared to prints not soaked. * denotes that day 28 prints had irregular stress-strain curves and multiple prints snapped before compression testing. Day 0 Young's Moduli and was significantly ($p < 0.05$) different from Day 28 Young's Moduli. Day 0 Ultimate Stress and Ultimate Strain were significantly ($p < 0.05$) greater than the day 7 and day 28 groups. Data expressed as mean ± standard deviation (n=7).

	Average Young's Modulus (MPa)	Average ultimate stress (MPa)	Average ultimate strain (mm/mm)
Day 0	4.8 ± 1.3	0.8 ± 0.3	0.27 ± 0.03
Day 7	3.1 ± 1.4	0.3 ± 0.2	0.18 ± 0.04
Day 28	1.3 ± 1.0 *	0.09 ± 0.03	0.13 ± 0.04

Table 2
Calcium and Phosphorous release from mineralized collagen scaffolds and Hyperelastic Bone 3D-prints at 37°C in PBS after 28 days. * indicates the calcium release in mineralized collagen scaffolds is significantly ($p < 0.05$) greater than the calcium release in Hyperelastic Bone 3D-prints. Data expressed as mean ± standard deviation (n=8).

Sample	Calcium released (ppm)	Phosphorous released (ppm)
Mineralized collagen	33 ± 9 *	43 ± 11
Hyperelastic Bone	2.6 ± 0.7	25 ± 16

3.2. 3D-printed Hyperelastic Bone 3D-prints lose stiffness over time and release less calcium than mineralized collagen scaffolds

We subsequently quantified degradation-induced changes in compressive properties and release of calcium and phosphorous ions from Hyperelastic Bone 3D-printed as a cross design over the course of a 28-day standard degradation experiment (37°C, PBS). While there were non-significant decreases in Young's modulus over the initial 7 days, significant degradation of the constructs over the full 28-day experiment were marked by significant decreases in Young's modulus as well as average ultimate stress and strain (Table 1).

Further, the structures were difficult to handle after 28 days of exposure, with multiple breaking prior to mechanical testing. Significant elution of both calcium and phosphorous was observed for Hyperelastic Bone structures. Interestingly, while significant calcium ($p < 0.05$) and phosphorous was released from the Hyperelastic Bone structures, overall release was less, significantly in the case of calcium, than that released from the native mineralized collagen scaffold in the same conditions (Table 2). However, this release suggests the embedded Hyperelastic Bone component may supplement the mineral ions released from the mineralized collagen scaffold phase to aid osteogenesis.

3.3. Integration of 3D-printed structures and lyophilized scaffold to form a composite

Reinforced collagen composites were formed using 3D-printed structures generated in either a conventional 'Cross Design' for *in vitro* trials or using a standardized 120º 'Mesh Print' (Dimension Inx) for mechanical analysis. SEM analysis of both cross design and mesh design 3D-print composites (MC-HB, MC-Fluffy) showed close integration of the mineralized collagen microstructure with the Hyperelastic Bone or Fluffy-PLG printed structure (Fig. 2C, Supp. Figs. 2 and 3).

3.4. Hyperelastic Bone composites show improved mechanical performance

Mechanical compression and push-out tests were performed on scaffolds and composites formed from a symmetrical 120º mesh morphology. MC-HB composites displayed significantly ($p < 0.05$) greater stiffness than MC-Fluffy composites or the native mineralized collagen scaffolds (Fig. 3A), while inclusion of a Fluffy-PLG 3D-print afforded no increase in modulus relative to the mineralized collagen scaffold on its own. MC-HB composites also displayed increased push-out force than MC-Fluffy composite or the scaffold (Fig. 3B). Altering the mesh spacing of MC-Fluffy composites had no effect on stiffness or shape-fitting ability of the reinforced composite (Supp. Table 8).

3.5. Reinforced composites support hMSC metabolic activity and promote increased osteogenic activity

Both the native mineralized collagen scaffold as well as composites formed from either Fluffy-PLG or Hyperelastic Bone 3D-prints supported significant increases in the metabolic activity of seeded hMSCs over 28 days *in vitro* experiment (Fig. 4A). Interestingly, MC-HB and MC-Fluffy composites showed significantly ($p < 0.05$) greater metabolic activity relative to the mineralized collagen scaffold alone for days 4 – 14. However, by day 28 all groups (MC, MC-HB, MC-Fluffy) showed approximately 3-fold increases in metabolic activity versus the start of the experiment, with no significant differences between groups.

We quantified release profiles for VEGF and OPG from the MSC-seeded scaffold or composites (Fig. 4C). While steady increase in VEGF released into the media was observed for all constructs, there was no significant difference between release profiles for all groups. However, we observed significantly ($p < 0.05$) increased OPG released from hMSC-seeded MC-HB composites versus both hMSC-seeded MC scaffolds (days 3, 9, 15) or hMSC-seeded MC-Fluffy composites (days 3 and 9). However, by day 28 the effect of the Hyperelastic Bone composite on OPG production was no longer significant.

3.6. Scaffolds and composites promote osteogenic gene expression

We examined temporal expression profiles for a series of genes associated with hMSC osteogenic specification: *RUNX2, Osterix, FGFR2, COL1A2,* and *IGF2* (Fig. 5). Expression profiles between groups were largely similar. However, MC-HB composites promoted significantly ($p < 0.05$) greater expression fold changes for *RUNX2* (day 1), *Osterix* and *FGFR2* (days 1, 14), and reduced expression of *COL1A2* (days 4, 14) compared to mineralized collagen scaffolds. MC-Fluffy composites promoted significantly ($p < 0.05$) greater expression fold changes for *RUNX2* (day 7) and reduced expression of *COL1A2* (day 14) compared to mineralized collagen scaffolds. MC-HB composites also promoted significantly ($p < 0.05$) greater expression of *IGF2* than MC-Fluffy composites and MC scaffolds at day 1.

3.7. Fluffy-PLG reinforced composites formed the greatest amount of new calcium by the end of the study

The mineral content (calcium and phosphorous) of all hMSC-seeded constructs was evaluated at day 28, with results normalized to the values for acellular scaffolds or composites (Fig. 4B). MC-Fluffy composites displayed significantly ($p < 0.05$) greater calcium content than both MC scaffolds and MC-HB composites.

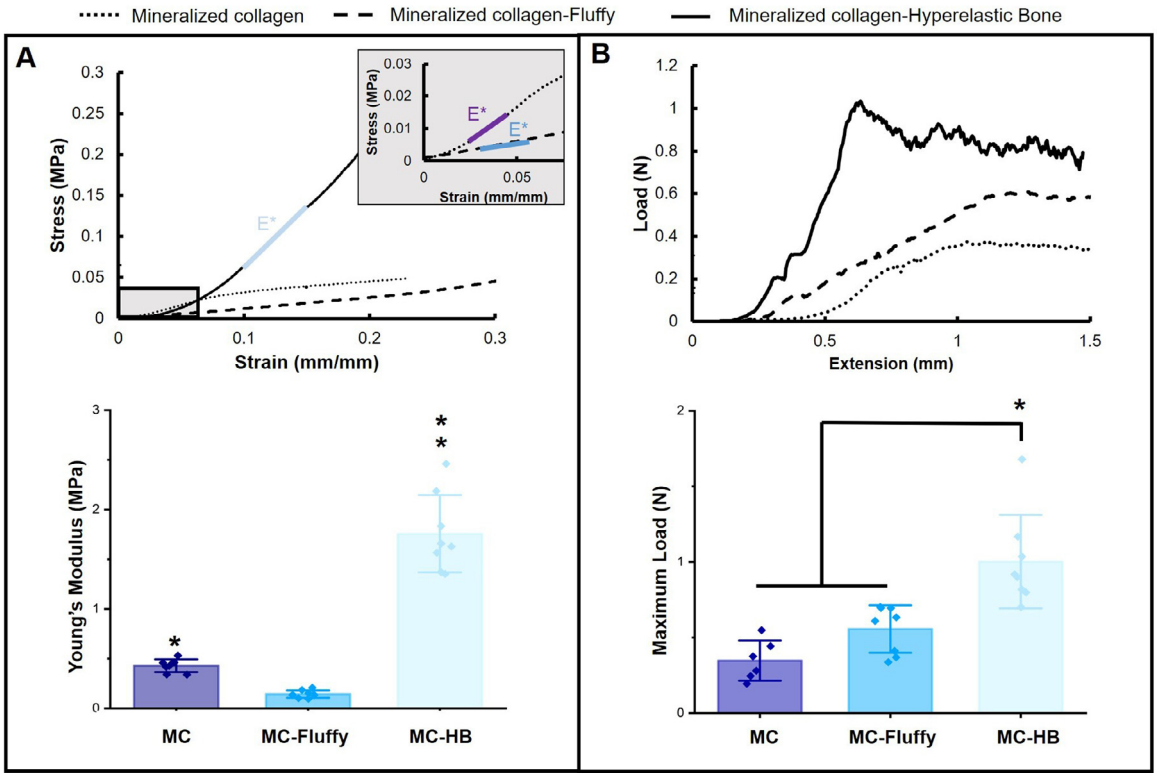

Fig. 3. Mechanical behavior of 3D-printed mesh composites. Compression testing to determine Young's Modulus and shape-fitting testing to determine maximum load during specimen push-out was performed on mineralized collagen, Hyperelastic Bone (MC-Hyperelastic Bone) composites, and Fluffy-PLG (MC-Fluffy) composites. (A) Young's Modulus averages and representative stress-strain curves from compression testing. A grey box represents a closer look at the stress strain curves of mineralized collagen and mineralized collagen-Fluffy. E* represents linear region defining the Young's Modulus with appropriate colors for the representative samples. ** represents the MC-Hyperelastic Bone group is significantly ($p < 0.05$) greater than all other groups. * represents the Mineralized Collagen group is significantly ($p < 0.05$) greater than the MC-Fluffy group. (B) Average maximum load and representative load-extension curves from push-out testing. * represents the MC-Hyperelastic Bone group is significantly ($p < 0.05$) greater than both the mineralized collagen and MC-Fluffy groups. Error bars represent average ± standard deviation (n=8).

Additionally, MC-Fluffy composites also contained significantly ($p < 0.05$) more phosphorous content than MC-HB composites. Although new mineral found in MC and MC-Fluffy samples was higher than MC-HB samples, MC-HB samples had overall much greater amounts of calcium and phosphorous than the other groups (Supp. Table 9).

4. Discussion

Advancing regenerative medicine technologies for CMF bone defects is challenging not only due to the large quantity of bone missing, but their irregular size and shape. There is an increasing need to identify biomaterial technologies to improve integration with the surrounding defect margins to aid cell recruitment and vascular ingrowth. Recent effort has begun to exploit shape-fitting technologies such as porous polymers that can reshape with changes in temperature [29,30]. Mineralized collagen scaffolds developed by our group as well as others have been shown to promote osteogenic processes and bone remodeling [19,21,22,49–52]. However, the porous nature of these scaffolds that is important to aid cell activity results in poor bulk mechanical properties; further, these scaffolds lack inherent design features to promote conformal fitting with the defect margins [31]. Here, we examined inclusion of mechanical and biological reinforcement to a mineralized collagen scaffold via inclusion of 3D-printed structures formed using one of two variations of 3D-printed biomaterials, Fluffy-PLG and Hyperelastic Bone (90wt% CaP). We report compositional, mechanical, and biological performance of these scaffold composites, focusing on the direct role of the 3D-printed structures on mechanical properties but also the potential active role the reinforcing structure could have on an osteogenic response via the effect of degradation byproducts on cell activity.

As both Hyperelastic Bone and Fluffy-PLG contain the same PLG chemistry, and roughly equivalent amounts of PLG polymer per unit volume [34,35,39], we first investigated the degradation byproducts of Hyperelastic Bone to determine if there would be any impact on the metabolic activity of our osteogenic mineralized collagen scaffolds. Over the course of an accelerated 28-day degradation experiment, we observed significant elution of lactic and glycolic acid, as well as short term decrease in pH, though not significantly different than the change in solution pH observed for mineralized collagen scaffolds in the same conditions. More importantly, we observed no negative effect of the elution byproducts, across a range of dilutions, on hMSC metabolic activity. These effects were consistent regardless of the use of an accelerate (90°C) or convention (37°C) degradation conditions. These findings are largely consistent with previous studies using printed structures formed from Hyperelastic Bone 3D-prints that showed significant new bone formation *in vivo* [35,39]. As a result, we did not expect Hyperelastic Bone or Fluffy-PLG 3D-prints to negatively impact osteogenesis and cell viability of mineralized collagen scaffolds. It is interesting to note that we also observed significant release of calcium and phosphorous content from the Hyperelastic Bone structures, though not as much calcium release as from the native mineralized collagen scaffold, which may be due to the more stable nature of the mineral component in Hyperelastic Bone versus that in the mineralized collagen scaffold.

Successful clinical use of a craniofacial bone regeneration scaffold requires the biomaterial to be surgically practical, notably readily customized to fit complex 3D defects and strong enough

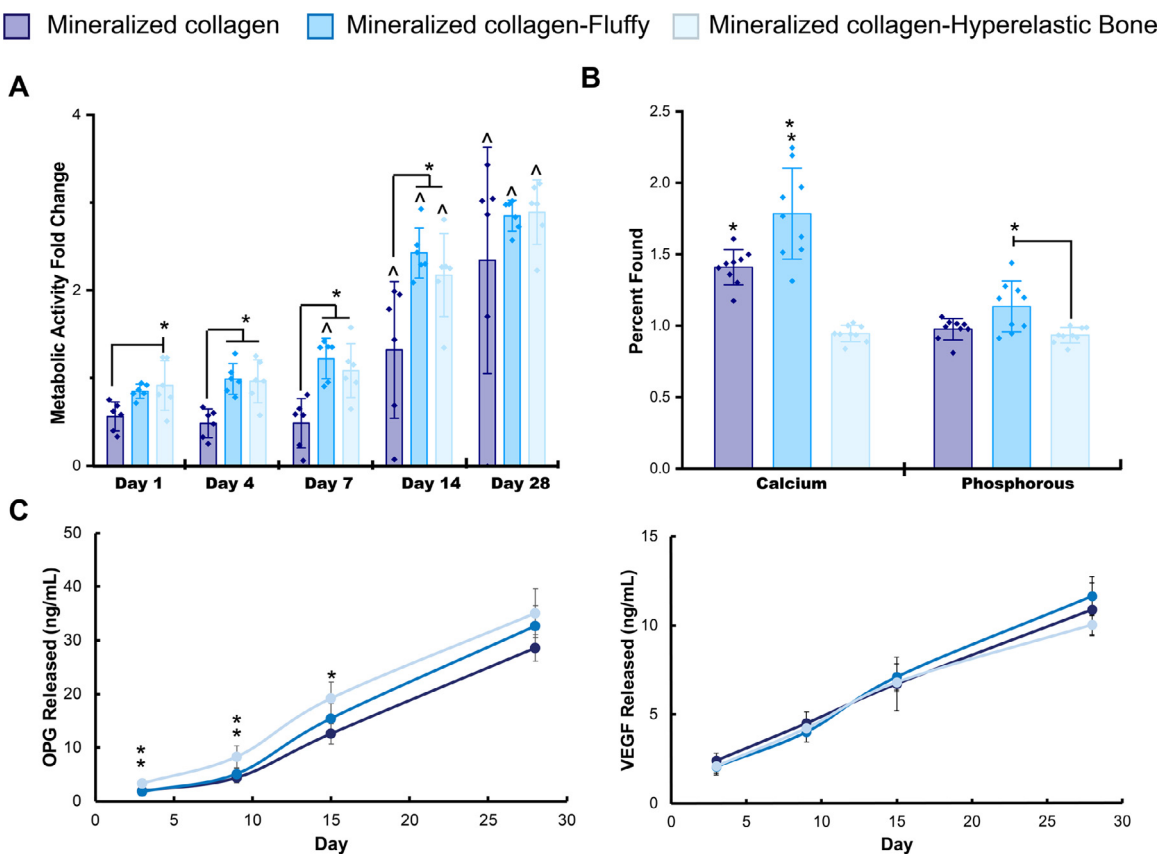

Fig. 4. Metabolic activity, mineral formation, and protein expression of hMSCs seeded on mineralized collagen scaffolds (MC), Fluffy-PLG reinforced composites (MC-Fluffy), and Hyperelastic Bone reinforced composites (MC-HB). (A) The metabolic activity of 100,000 hMSCs is denoted by an activity of 1, with the *y*-axis representing a fold change in activity over this cell seeding density. * indicates one group is significantly ($p < 0.05$) greater than another group. ^ indicates one group is significantly ($p < 0.05$) greater than the same group compared to day 1. Data expressed as average ± standard deviation (n=6). (B) Percent found of Calcium (Ca) and Phosphorous (P) was determined by ICP analysis of groups seeded with cells after 28 days and normalized to the respective day 0 unseeded groups. Asterix indicate significance and all groups have significantly ($p < 0.05$) different calcium content. The MC-Fluffy group has significantly ($p < 0.05$) more phosphorous than the MC-HB group. Data expressed as average ± standard deviation (n=9). (C) Protein expression in scaffolds and composites was analyzed with an ELISA for OPG and VEGF released from pooled media over 28 days. ** indicates the MC-HB group was significantly ($p < 0.05$) greater than the other two groups at day 3 and 9. * indicates the MC-HB group was significantly ($p < 0.05$) greater than the MC group at day 15. There were no significant ($p < 0.05$) differences in VEGF released between all tested groups. Data expressed as average ± standard deviation (n=6).

to withstand physiological loading [9,27]. To address this challenge, we have developed an innovative composite approach, embedding a mechanically-robust polymer (e.g., PCL, PLA) 3D-printed reinforcement with millimeter-scale porosity into the mineralized collagen scaffold [31,33]. The resultant collagen-3D-print composite displays the osteogenic activity of the scaffold, the strength of the 3D-print, and promotes regenerative healing in a porcine bone defect [18,33]. However, poor conformal contact significantly inhibits cell recruitment, angiogenesis, regenerative healing and greatly increases the risk of graft resorption [28]. Common surgical interventions such as resorbable protective plates do not improve microscale conformal contact [53]. We showed selectively removing fibers from a PLA 3D-print creates variants with compressive strength in the longitudinal axis, but serial compression-expansion capacity in the radial [33]. These 3D-prints can be radially compressed and inserted into cylindrical defects, springing back to achieve close conformal contact. As a result, here we examined the mechanical performance of a new class of composite formed from the mineralized collagen scaffold and Fluffy-PLG or Hyperelastic Bone 3D-prints.

Hyperelastic Bone provided the greatest reinforcement to mineralized collagen scaffolds, most likely due to the reinforcements dominating the compressive mechanics similar to previous work with poly(lactic acid) composites [33]. MC-HB composites also displayed the highest loads achieved during a push-out test; however, the MC-HB composites demonstrated a more brittle nature, likely due to the form factor and not material. We expect that reducing the spacing between layers could reduce the brittleness and avoid many stress-concentrating regions created with wider spacing. While MC-Fluffy composites were significantly more flexible, they displayed no additional push-out strength compared to the mineralized scaffold itself. We also found resulting mechanical properties to be largely insensitive to changes in the mesh spacing (2 mm vs. 3 mm) over the range tested for the Fluffy-PLG prints, most likely due to their soft and flexible nature with the mineralized collagen scaffold phase dominating the mechanical performance of the composite. We predict that increasing the mesh spacing of Hyperelastic Bone 3D-prints within mineralized collagen scaffolds will have an appreciable effect due to its stiffer nature and the relationship between elastic modulus and material density of open-cell foams such as meshes [54]. Although MC-HB composites showed significantly improved mechanical performance, they did not achieve a moduli close to cancellous or cortical bone (0.1-2 GPa, 15-20 GPa [55]). While the need for mechanical properties of implant to match those of a target tissue may be relevant for inert materials which never remodel such as permanent joint replacements, design needs are very different for regenerative biomaterials that rely on cell mechanotransduction and remodeling. Indeed, it is essential to consider the multiscale properties of porous biomaterials. Porosity is essential for cell in-

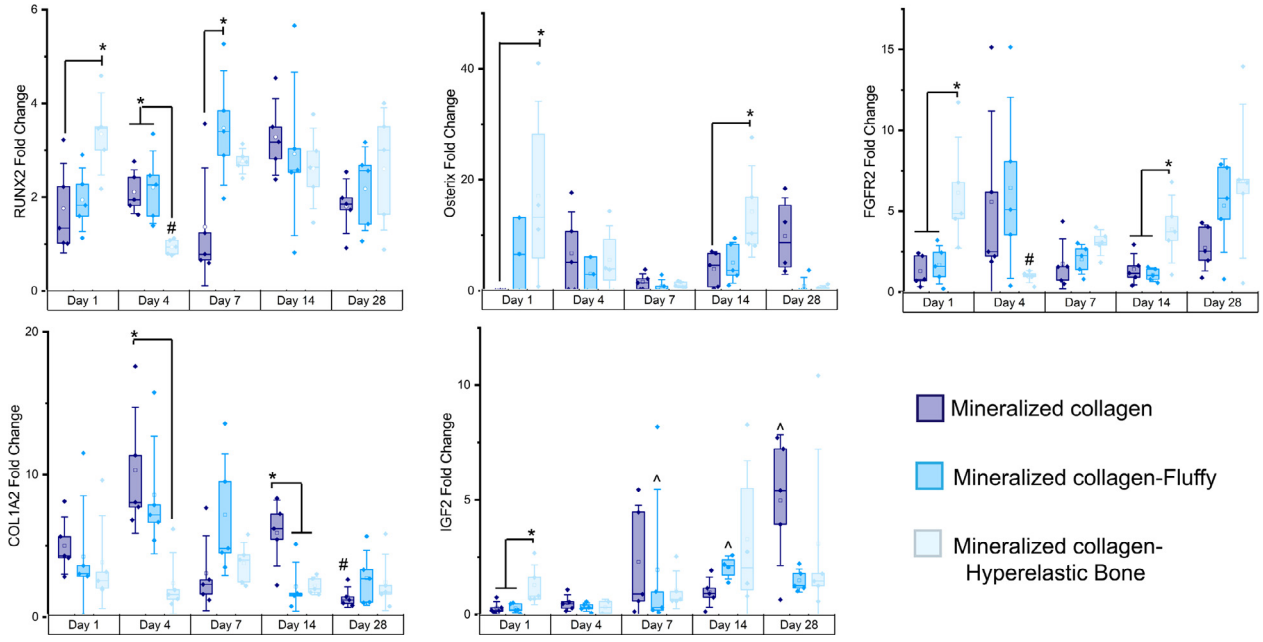

Fig. 5. Osteogenic gene expression of mineralized collagen, Fluffy-PLG composites (MC-Fluffy), and Hyperelastic Bone (MC-Hyperelastic Bone) composites. Gene expression was determined by running RT-PCR on reverse transcribed RNA isolated from scaffolds and composites seeded with 100,000 hMSCs at days 1-28. Fold change of gene expression was normalized to 100,000 cells before seeding on scaffolds and composites, with a value of 1 (grey bar) representing the expression of 100,000 hMSCs. Values underneath this grey bar indicate downregulated genes. * indicates group(s) significant ($p < 0.05$) to another group on same day. # indicates a group on one day is significantly ($p < 0.05$) less than the same group on day 1. ^ indicates a group on one day is significantly ($p < 0.05$) greater than the same group on day 1. Error bars represent average ± standard deviation (n=5). *RUNX2* induces differentiation of mesenchymal stem cells to the osteogenic lineage; *Osterix* has roles in bone formation and osteoblast differentiation; *FGFR2* can stimulate proliferation of osteogenic cells; *COL1A2* is a marker for type I collagen, a main organic component of bone; *IGF2* stimulated osteoblast differentiation and bone deposition.

growth, biotransport, and cell-mediated remodeling. Yet the mechanical performance of a porous material scales as the relative density (density of the porous material divided by the solid material from which it is fabricated) squared compared to the mechanical properties of the solid material that forms the individual pores and with which cells interact [54,56]. Thus, a porous scaffold with cell-scale properties tuned to enhance MSC proliferation, remodeling, and matrix biosynthesis may present initial macroscale mechanical properties a factor of 1000 (or more) lower. The design of the mineralized scaffolds and polymer reinforcement is therefore tuned to improve surgical practicality and cell activity. The mineralized collagen scaffold used in this study has previously been shown to regenerate rabbit cranial defects without growth factor and cell supplementation, achieving directed healing >60% of the density and 50-80% the stiffness of native cranial bone within 3 months after implantation [23]. Hyperelastic Bone has been used *in vivo* in a mouse subcutaneous implant model, a rat posterolateral spinal fusion model, and in a large, non-human primate calvarial defect case study, which demonstrated material biocompatibility, new bone growth, integration with surrounding tissue, and vascularization [36]. Both Hyperelastic Bone and Fluffy-PLG 3D-prints have also been tested in rat calvarial defects compared to autologous bone and empty controls, with Hyperelastic Bone displaying increased new bone formation, specifically 73.8% effective over autologous bone after 8 weeks, and overall greater new bone formation compared to Fluffy-PLG and the empty control group [39]. With these results, we expect that the combination of two materials previously successfully tested separately *in vivo* would be able to promote greater bone regeneration together, and significant future efforts will be needed to identify the appropriate mesh structure to aid strength and conformal fitting capacity. Future efforts will concentrate on alterations to the polymer composition and mineral content to further boost endogenous OPG secretion to accelerate regenerative healing. An exciting opportunity are meshes based on Voronoi foam (random pore) architectures which exhibit well defined mechanical performance characteristics [57]. Under load, the fibers that define the pores of these materials bend elastically during the first ~10% of applied strain, then buckle plastically [57], suggesting implementing these designs with the 3D-Paints may be useful for conformal fitting capabilities.

This work showed exciting osteogenic potential of hMSC-seeded MC-HB and MC-Fluffy composites, maintained in culture in the absence of conventional osteogenic supplements (exogenous BMP2, osteogenic media). We have previously shown that the mineralized collagen scaffolds promotes endogenous activation of BMPR pathways and that inclusion of exogenous BMP2 does not improve the quality of bone regeneration in a critical sized calvarial defect model [22,25,26,58]. Although both the scaffold and polymer component of the composite could be used as a biomolecule delivery substrate, the ability to identify composites that increase bone regeneration without the use of such supplements would avoid significant challenges associated with exogenous factor inclusion (ectopic bone formation, cost, regulatory hurdles). Both composites promoted a higher metabolic activity compared to native mineralized collagen scaffolds in early timepoints of the study (days 1-14); while by day 28 there were no differences between groups, all groups demonstrated significantly (~3-fold) increased metabolic activity compared to the start of the experiment. We also quantified gene expression profiles for a series of osteogenic-linked genes as a function of biomaterial environment. *RUNX2* is a major transcription factor for bone and guides the differentiation of hMSCs to osteoblasts [59]; we saw some evidence of increases in *RUNX2* expression at some early time points in reinforced composites. Downstream of *RUNX2, Osterix* regulates mature osteoblast differentiation and is thus connected to bone formation [60]. MC-HB composites upregulated *Osterix* at day 1 and 14, possibly indicating greater mature osteoblast differentiation in these scaffolds, how-

ever, all groups were upregulated at day 28. In addition to this, MC-HB composites upregulated Fibroblast Growth Factor Receptor-2 (*FGFR2*) at day 1 and 14, which is important due to FGF being a key regulator of bone development and FGF-2 coated scaffolds being shown to stimulate osteogenesis *in vivo* [61]. *COL1A2* is a gene expression marker for type I collagen, the major collagen of bone [62]. While greater in MC scaffolds at days 4 and 14, all groups were upregulated throughout the study. Overall, we observed signatures of biomaterial induced increases in osteogenic signaling, though a MC-HB composite may have the greatest promise to accelerate early osteogenic activity. These findings are largely consistent with previous studies from our group showing the base mineralized scaffold itself is sufficient to promote hMSC osteogenic activity in the absence of osteogenic stimuli [18,63,64]. At minimum, we show inclusion of Fluffy-PLG or Hyperelastic Bone reinforcing structures into the scaffold does not reduce this response.

We also examined endogenous production of two proteins (OPG, VEGF) by hMSCs within the scaffolds and composites. OPG is a soluble glycoprotein and endogenous inhibitor of osteoclastogenesis and osteoclast activity [25,65]. We have previously shown that MSC-osteoprogenitors in the mineralized collagen scaffold endogenously produce osteoprotegerin sufficient to inhibit osteoclast activity without negatively impacting MSC-osteogenesis [26]. Excitingly, we observed significant OPG production in all variants, though MC-HB composites promoted significantly increased OPG secretion over the first two weeks of culture. Calcium ion signaling has previously been suggested as a powerful signal to improve secretion of OPG by osteoblasts [66]. Our findings are consistent with this observation, suggesting increased OPG secretion by hMSCs in MC-HB composites may be due to increased release of Calcium and Phosphate ions during degradation (vs. MC scaffolds or MC-Fluffy composites). This indicates that inclusion of Hyperelastic Bone 3D-prints could not only regenerate bone through increased stiffness, which has been linked with greater mechanotransduction-induced bone formation in mineralized collagen scaffolds [67], but also provide additional inorganic ions to safely elevate OPG levels without the need of gene therapy or growth factors [26]. The timing of increased OPG production during significant Hyperelastic Bone degradation further suggests that the Hyperelastic Bone reinforcement structure may play an active role in promoting an osteogenic response in addition to passive mechanical reinforcement. We also explored VEGF production, as VEGF is a potential regulator of angiogenesis, and can also contribute to recruitment and activity of osteoblasts [68]. Exogenous addition of VEGF can also improve bone formation [61]. While we observed significant increases in VEGF production over the 28-day experiment, the effect was insensitive to the inclusion of Fluffy-PLG or Hyperelastic Bone reinforcement structure.

Analysis of mineral content of the scaffold and composites after *in vitro* culture suggest significant new mineral formation in all constructs, though the greatest new absolute mineral formation was observed in MC-Fluffy composites. MC-HB composites had the least amount of new mineral formed compared to MC scaffolds and MC-Fluffy composites. However, the MC-HB composites had the greatest average amount of Calcium and Phosphorous present at day 28 before normalizing to unseeded controls (approx. 30% Ca and 15% P, 11% Ca and 5% P, 14% Ca and 7% P for MC-HB, MC-Fluffy, and MC, respectively), indicating that there is still a great amount of mineral present to induce osteogenesis. To further understand the low mineral formation at the end of the study in MC-HB composites, we plan to investigate the localization of calcium and phosphorous within the composite to determine if mineral is forming within the scaffold.

Together, our results demonstrate hMSC viability, gene expression, and protein expression that support the use of Hyperelastic Bone and Fluffy-PLG reinforced mineralized collagen composites for craniofacial bone repair applications. Of particular note, was the observation that MC-HB composites demonstrated increased MSC-osteoprogenitor secreted OPG and added stiffness. Although PLGA is biocompatible, use of this material without any additional factors make for poor osteoconductivity, which has been compensated by the addition of other materials to improve its outcome *in vitro* and *in vivo*. Ongoing efforts will more fully compare hMSC osteogenesis *in vitro* as well as *in vivo* bone regeneration for these disparate composites to determine if our composite improves mineral formation similar to other PLGA formulations *in vivo*. Future efforts will also examine changes in the topology of the 3D-printed structure in order to add shape-fitting through structural means, similar to our recently published work with poly(lactic acid) composites [33]. This includes expanding the use of the 3D-print as a bioactive stimulus to increase endogenous OPG production as a means to transiently inhibit osteoclast activity and accelerate craniofacial bone repair.

5. Conclusions

We examined inclusion of reinforcing 3D-prints generated from two distinct 3D-paints (Hyperelastic Bone; Fluffy-PLG) in a mineralized collagen scaffold for craniofacial bone repair applications. Composites formed from Hyperelastic Bone or Fluffy-PLG structures were shown to offer passive and potentially active advantages to aid osteogenic activity. Notably, inclusion of a Hyperelastic Bone 3D-printed mesh significantly increased composite modulus and push-out force, though the brittle nature of the structure limited the conformal fitting capacity. Degradation byproducts of Hyperelastic Bone did not significantly reduce hMSC activity. Interesting, all composites and the native mineralized collagen scaffold supported significant osteogenic activity in the form of hMSC metabolic activity increases, shifts in osteogenic gene expression, and synthesis of new mineral. Further, while the scaffold and composites all promoted increased endogenous production and secretion of OPG and VEGF, Hyperelastic Bone reinforced composites showed significantly increased early secretion of OPG, suggesting these composites may increase hMSC osteogenesis and locally inhibit osteoclast activity to accelerate bone regeneration by mineral ion release and increased stiffness without the addition of growth factors or gene therapy.

Data availability

The raw and processed data required to reproduce these findings are available to download from Dewey, Marley (2020), “Data Repository: Inclusion of a polylactide-co-glycolide co-polymer mesh enhances osteogenesis in mineralized collagen scaffolds”, Mendeley Data, V1, doi: 10.17632/tfx7dt4kyt.1.

Disclosure

The authors Ramille N. Shah and Adam E. Jakus are co-founders and hold financial interests in Dimension Inx, LLC, which may be considered a potential competing interest.

Declaration of Competing Interest

The authors declare that they have no known competing financial interests or personal relationships that could have appeared to influence the work reported in this paper.

Acknowledgment

This work was supported by the Office of the Assistant Secretary of Defense for Health Affairs Broad Agency Announcement for

Extramural Medical Research through the Award No. W81XWH-16-1-0566. Research reported in this publication was also supported by the National Institute of Dental and Craniofacial Research of the National Institutes of Health under Award Number R21 DE026582. We are also grateful for funds provided by the NSF Graduate Research Fellowship DGE-1144245 (MJD) to perform this research. The interpretations and conclusions presented are those of the authors and are not necessarily endorsed by the Department of Defense, NIH, or NSF.

The authors would like to acknowledge the University of Illinois Roy J. Carver Biotechnology Center, the School of Chemical Science Microanalysis Lab, the Carl R. Woese Insitute for Genomic Biology, the Chemical and Biomolecular Engineering Department, and the Beckman Institute for Advanced Science and Technology, all located at the University of Illinois at Urbana-Champaign. The authors would also like to thank members of the Harley Lab who assisted in statistical advice and Matlab programs, Aidan, Samantha, and Aleczandria.

Supplementary materials

Supplementary material associated with this article can be found, in the online version, at doi:10.1016/j.actbio.2020.11.028.

References

[1] T.A. Lew, J.A. Walker, J.C. Wenke, L.H. Blackbourne, R.G. Hale, Characterization of craniomaxillofacial battle injuries sustained by United States service members in the current conflicts of Iraq and Afghanistan, J. Oral Maxillofac. Surg. 68 (1) (2010) 3–7.
[2] A.H. Chao, P. Yu, R.J. Skoracki, F. Demonte, M.M. Hanasono, Microsurgical reconstruction of composite scalp and calvarial defects in patients with cancer: a 10-year experience, Head Neck 34 (12) (2012) 1759–1764.
[3] E.C. Kruijt Spanjer, G.K.P. Bittermann, I.E.M. van Hooijdonk, A.J.W.P. Rosenberg, D. Gawlitta, Taking the endochondral route to craniomaxillofacial bone regeneration: a logical approach? J. Cranio-Maxillofac. Surg. 45 (2017) 1099–1106.
[4] A. Norozy, M.H.K. Motamedi, A. Ebrahimi, H. Khoshmohabat, Maxillofacial fracture patterns in military casualties, J. Oral Maxillofac. Surg. 78 (4) (2020) 611.e1–611.e6.
[5] B.D. Owens, J.F. Kragh Jr., J.C. Wenke, J. Macaitis, C.E. Wade, J.B. Holcomb, Combat wounds in operation Iraqi freedom and operation enduring freedom, J. Trauma 64 (2) (2008) 295–299.
[6] P.R. Brown Baer, J.C. Wenke, S.J. Thomas, C.R. Hale, Investigation of severe craniomaxillofacial battle injuries sustained by U.S. service members: a case series, Craniomaxillofac. Trauma Reconstr. 5 (4) (2012) 243–252.
[7] H. Fodstad, J.A. Love, J. Ekstedt, H. Fridén, B. Liliequist, Effect of cranioplasty on cerebrospinal fluid hydrodynamics in patients with the syndrome of the trephined, Acta Neurochirurgica 70 (1–2) (1984) 21–30.
[8] M. Elsalanty, D. Genecov, Bone grafts in craniofacial surgery, Craniomaxillofac. Trauma Reconstr. 2 (2009) 125–134.
[9] M.H. Smith, C.L. Flanagan, J.M. Kemppainen, J.A. Sack, H. Chung, S. Das, S.J. Hollister, S.E. Feinberg, Computed tomography-based tissue-engineered scaffolds in craniomaxillofacial surgery, Int. J. Med. Robot. 3 (3) (2007) 207–216.
[10] A. Depeyre, S. Touzet-Roumazeille, L. Lauwers, G. Raoul, J. Ferri, Retrospective evaluation of 211 patients with maxillofacial reconstruction using parietal bone graft for implants insertion, J. Cranio-Maxillofac. Surg. 44 (2016) 1162–1169.
[11] J.M. Piitulainen, T. Kauko, K.M.J. Aitasalo, V. Vuorinen, P.K. Vallittu, J.P. Posti, Outcomes of cranioplasty with synthetic materials and autologous bone grafts, World Neurosurg. 83 (5) (2015) 708–714.
[12] S. Ghanaati, M. Barbeck, P. Booms, J. Lorenz, C.J. Kirkpatrick, R.A. Sader, Potential lack of "standardized" processing techniques for production of allogeneic and xenogeneic bone blocks for application in humans, Acta Biomater. 10 (2014) 3557–3562.
[13] J.C. Lee, G.M. Kleiber, A.T. Pelletier, R.R. Reid, L.J. Gottlieb, Autologous immediate cranioplasty with vascularized bone in high-risk composite cranial defects, Plast. Reconstr. Surg. 132 (4) (2013) 967–975.
[14] A.J. Fong, B.T. Lemelman, S. Lam, G.M. Kleiber, R.R. Reid, L.J. Gottlieb, Reconstructive approach to hostile cranioplasty: a review of the University of Chicago experience, J. Plast. Reconstr. Aesthet. Surg. 68 (8) (2015) 1036–1043.
[15] R. Dimitriou, G.C. Babis, Biomaterial osseointegration enhancement with biophysical stimulation, J. Musculoskel. Neuronal Interact. 7 (2007) 253–265.
[16] S.J. Hollister, C.Y. Lin, E. Saito, C.Y. Lin, R.D. Schek, J.M. Taboas, J.M. Williams, B. Partee, C.L. Flanagan, A. Diggs, E.N. Wilke, G.H.V. Lenthe, R. Muller, T. Wirtz, S. Das, S.E. Feinberg, P.H. Krebsbach, Engineering craniofacial scaffolds, Orthod. Craniofacial Res. 8 (2005) 162–173.
[17] B.A. Harley, A.K. Lynn, Z. Wissner-Gross, W. Bonfield, I.V. Yannas, L.J. Gibson, Design of a multiphase osteochondral scaffold. II. Fabrication of a mineralized collagen-glycosaminoglycan scaffold, J. Biomed. Mater. Res.–Part A 92 (2010) 1066–1077.
[18] D.W. Weisgerber, S.R. Caliari, B.A.C. Harley, Mineralized collagen scaffolds induce hMSC osteogenesis and matrix remodeling, Biomater. Sci. 3 (2015) 533–542.
[19] G. Cunniffe, G. Dickson, S. Partap, K. Stanton, F.J. O'Brien, Development and characterisation of a collagen nano-hydroxyapatite composite scaffold for bone tissue engineering, J. Mater. Sci. Mater. Med. 21 (2010) 2293–2298.
[20] J.P. Gleeson, T. Weber, T. Levingstone, A.A. Al-Munajjed, F.J. O'Brien, J. Hammer, N.A. Plunkett, C. Jungreuthmayer, Development of a biomimetic collagen-hydroxyapatite scaffold for bone tissue engineering using a SBF immersion technique, J. Biomed. Mater. Res. Part B 90B (2009) 584–591.
[21] F.G. Lyons, J.P. Gleeson, S. Partap, K. Coghlan, F.J. O'Brien, Novel microhydroxyapatite particles in a collagen scaffold: a bioactive bone void filler? Clin. Orthop. Relat. Res. 472 (2014) 1318–1328.
[22] X. Ren, D.W. Weisgerber, D. Bischoff, M.S. Lewis, R.R. Reid, T.C. He, D.T. Yamaguchi, T.A. Miller, B.A.C. Harley, J.C. Lee, Nanoparticulate mineralized collagen scaffolds and BMP-9 induce a long-term bone cartilage construct in human mesenchymal stem cells, Adv. Healthc. Mater. 5 (2016) 1821–1830.
[23] X. Ren, V. Tu, D. Bischoff, D. Weisgerber, M. Lewis, D. Yamaguchi, T. Miller, B. Harley, J. Lee, Nanoparticulate mineralized collagen scaffolds induce in vivo bone regeneration independent of progenitor cell loading or exogenous growth factor stimulation, Biomaterials 89 (2016) 67–78.
[24] C. Lo Sicco, D. Reverberi, C. Balbi, V. Ulivi, E. Principi, L. Pascucci, P. Becherini, M.C. Bosco, L. Varesio, C. Franzin, M. Pozzobon, R. Cancedda, R. Tasso, Mesenchymal stem cell-derived extracellular vesicles as mediators of anti-inflammatory effects: endorsement of macrophage polarization, Stem Cells Transl. Med. 6 (3) (2017) 1018–1028.
[25] X. Ren, Q. Zhou, D. Foulad, M.J. Dewey, D. Bischoff, T.A. Miller, D.T. Yamaguchi, B.A.C. Harley, J.C. Lee, Nanoparticulate mineralized collagen glycosaminoglycan materials directly and indirectly inhibit osteoclastogenesis and osteoclast activation, J. Tissue Eng. Regener. Med. 13 (5) (2019) 823–834.
[26] X. Ren, Q. Zhou, D. Foulad, A.S. Tiffany, M.J. Dewey, D. Bischoff, T.A. Miller, R.R. Reid, T.-c. He, D.T. Yamaguchi, B.A.C. Harley, J.C. Lee, Osteoprotegerin reduces osteoclast resorption activity without affecting osteogenesis on nanoparticulate mineralized collagen scaffolds, Sci. Adv. 5 (2019) 1–12.
[27] S.J. Hollister, W.L. Murphy, Scaffold translation: barriers between concept and clinic, Tissue Eng. Part B Rev. 17 (6) (2011) 459–474.
[28] B.T. Smith, J. Shum, M. Wong, A.G. Mikos, S. Young, L.E. Bertassoni, P.G. Coelho, Bone tissue engineering challenges in oral & maxillofacial surgery, in: Engineering Mineralized and Load Bearing Tissues, Springer International Publishing, Cham, 2015, pp. 57–78.
[29] L.N. Nail, D. Zhang, J.L. Reinhard, M.A. Grunlan, Fabrication of a bioactive, PCL-based "self-fitting" shape memory polymer scaffold, J. Vis. Exp. 104 (2015) e52981.
[30] R. Xie, J. Hu, O. Hoffmann, Y. Zhang, F. Ng, T. Qin, X. Guo, Self-fitting shape memory polymer foam inducing bone regeneration: a rabbit femoral defect study, Biochimica et Biophysica Acta (BBA) - General Subjects 1862 (4) (2018) 936–945.
[31] D.W. Weisgerber, K. Erning, C. Flanagan, S.J. Hollister, B.A.C. Harley, Evaluation of multi-scale mineralized collagen-polycaprolactone composites for bone tissue engineering, J. Mech. Behav. Biomed. Mater. 61 (2016) 318–327.
[32] D. Weisgerber, D. Milner, H. Lopez-Lake, M. Rubessa, S. Lotti, K. Polkoff, R. Hortensius, C. Flanagan, S. Hollister, M. Wheeler, B. Harley, A mineralized collagen-polycaprolactone composite promotes healing of a porcine mandibular ramus defect, Tissue Eng. Part A (2017) 1–12 0.
[33] M.J. Dewey, E.M. Johnson, D.W. Weisgerber, M.B. Wheeler, B.A.C. Harley, Shape-fitting collagen-PLA composite promotes osteogenic differentiation of porcine adipose stem cells, J. Mech. Behav. Biomed. Mater. 95 (2019) 21–33.
[34] A.E. Jakus, N.R. Geisendorfer, P.L. Lewis, R.N. Shah, 3D-printing porosity: a new approach to creating elevated porosity materials and structures, Acta Biomater. 72 (2018) 94–109.
[35] R. Alluri, A. Jakus, S. Bougioukli, W. Pannell, O. Sugiyama, A. Tang, R. Shah, J.R. Lieberman, 3D printed hyperelastic " bone " scaffolds and regional gene therapy: a novel approach to bone healing, J. Biomed. Mater. Res. Part A 106A (2018) 1104–1110.
[36] A.E. Jakus, A.L. Rutz, S.W. Jordan, A. Kannan, S.M. Mitchell, C. Yun, K.D. Koube, S.C. Yoo, H.E. Whiteley, C.-P. Richter, R.D. Galiano, W.K. Hsu, S.R. Stock, E.L. Hsu, R.N. Shah, Hyperelastic "bone": a highly versatile, growth factor–free, osteoregenerative, scalable, and surgically friendly biomaterial, Sci. Transl. Med. 8 (358) (2016) 358ra127.
[37] X. Liu, A.E. Jakus, M. Kural, H. Qian, A. Engler, M. Ghaedi, R. Shah, D.M. Steinbacher, L.E. Niklason, Vascularization of natural and synthetic bone scaffolds, Cell Transp. 27 (8) (2018) 1269–1280.
[38] J.A. Driscoll, R. Lubbe, A.E. Jakus, K. Chang, M. Haleem, C. Yun, G. Singh, A.D. Schneider, K.M. Katchko, C. Soriano, M. Newton, T. Maerz, X. Li, K. Baker, W.K. Hsu, R.N. Shah, S.R. Stock, E.L. Hsu, 3D-printed ceramic-demineralized bone matrix Hyperelastic Bone composite scaffolds for spinal fusion, Tissue Eng. Part A 26 (3-4) (2020) 157–166.
[39] Y.-H. Huang, A.E. Jakus, S.W. Jordan, Z. Dumanian, K. Parker, L. Zhao, P.K. Patel, R.N. Shah, Three-dimensionally printed Hyperelastic Bone scaffolds accelerate bone regeneration in critical-size calvarial bone defects, Plastic & Reconstructive Surgery 143 (5) (2019) 1397–1407.
[40] A.S. F1635-04a, in: Standard Test Method for in vitro Degradation Testing of Hydrolytically Degradable Polymer Resins and Fabricated Forms for Surgical Implants, ASTM International, West Conshohocken, PA, 2018, pp. 1–5.

[41] L.N. Borshchevskaya, T.L. Gordeeva, A.N. Kalinina, S.P. Sineokii, Spectrophotometric determination of lactic acid, Journal of Analytical Chemistry 71 (2016) 755–758.
[42] J. Viccaro, E. Ambye, Colorimetric determination of glycolic acid with B-naphthol, Microchem. J. 17 (1972) 710–718.
[43] D.W. Weisgerber, K. Erning, C.L. Flanagan, S.J. Hollister, B.A.C. Harley, Evaluation of multi-scale mineralized collagen-polycaprolactone composites for bone tissue engineering, J. Mech. Behav. Biomed. Mater. 61 (2016) 318–327.
[44] H.J. Conrad, W.-J. Seong, J.S. Hodges, S. Grami, S.C. Jeong, Comparison of push-in versus pull-out tests on bone-implant interfaces of rabbit tibia dental implant healing model, Clin. Implant Dent. Relat. Res. 15 (2011) 460–469.
[45] A.S. Tiffany, D.L. Gray, T.J. Woods, K. Subedi, B.A.C. Harley, The inclusion of zinc into mineralized collagen scaffolds for craniofacial bone repair applications, Acta Biomater. 93 (2019) 86–96.
[46] ISO 10993-5, Part 5: Tests for in vitro Cytotoxicity, Biological Evaluation of Medical Devices, in: Biological evaluation of medical devices, 3rd, International Organization for Standardization, Switzerland, 2009, pp. 1–34.
[47] T.F. Scientific, Isolation of total RNA from difficult tissues. https://www.thermofisher.com/us/en/home/references/ambion-tech-support/rna-isolation/tech-notes/isolation-of-total-rna-from-difficult-tissues.html. (Accessed March 30 2020).
[48] R.L. Ott, M.T. Longnecker, An Introduction to Statistical Methods and Data Analysis, seventh ed., Cengage Learning, 2016.
[49] A. Al-Munajjed, J. Gleeson, F. O'Brien, Development of a collagen calcium-phosphate scaffold as a novel bone graft substitute, Stud. Health Technol. Inform. 133 (2008) 11–20.
[50] D. Florent, T. Levingstone, W. Schneeweiss, M. de Swartw, H. Jahns, J. Gleeson, F. O'Brien, Enhanced bone healing using collagen–hydroxyapatite scaffold implantation in the treatment of a large multiloculated mandibular aneurysmal bone cyst in a thoroughbred filly, J. Tissue Eng. Regener. Med. 9 (2015) 1193–1199.
[51] B. Hoyer, A. Bernhardt, S. Heinemann, I. Stachel, M. Meyer, M. Gelinsky, Biomimetically mineralized salmon collagen scaffolds for application in bone tissue engineering, Biomacromolecules 13 (2012) 1059–1066.
[52] F.J. O'Brien, E. Thompson, S.A. Cryan, A. López-Noriega, E. Quinlan, H.M. Kelly, Development of collagen–hydroxyapatite scaffolds incorporating PLGA and alginate microparticles for the controlled delivery of rhBMP-2 for bone tissue engineering, J. Control. Release 198 (2014) 71–79.
[53] J.H. Phillips, B.A. Rahn, Fixation effects on membranous and endochondral onlay bone graft revascularization and bone deposition, Plast. Reconstr. Surg. 85 (6) (1990) 891–897.
[54] M. L.A. Gibson, B. Harley, Cellular Materials in Nature and Medicine, first ed. Cambridge University Press, 2010.
[55] S. Bose, M. Roy, A. Bandyopadhyay, Recent advances in bone tissue engineering scaffolds, Trends Biotechnol. 30 (2012) 546–554.
[56] B.A. Harley, J.H. Leung, E.C.C.M. Silva, L.J. Gibson, Mechanical characterization of collagen-glycosaminoglycan scaffolds, Acta Biomater. 3 (2007) 463–474.
[57] L.J. Gibson, M.F. Ashby, B.A. Harley, Cellular Materials in Nature and Medicine, Cambridge University Press, Cambridge, U.K., 2010.
[58] X. Ren, D. Bischoff, D.W. Weisgerber, M.S. Lewis, V. Tu, D.T. Yamaguchi, T.A. Miller, B.A.C. Harley, J.C. Lee, Osteogenesis on nanoparticulate mineralized collagen scaffolds via autogenous activation of the canonical BMP receptor signaling pathway, Biomaterials 50 (2015) 107–114.
[59] L.D. Carbonare, G. Innamorati, M.T. Valenti, Transcription factor Runx2 and its application to bone tissue engineering, Stem Cell Rev. Rep. 8 (2012) 891–897.
[60] B. Yao, J. Wang, S. Qu, Y. Liu, Y. Jin, J. Lu, Q. Bao, L. Li, H. Yuan, C. Ma, Upregulated Osterix promotes invasion and bone metastasis and predicts for a poor prognosis in breast cancer, Cell Death Dis. 10 (1) (2019) 28.
[61] Y.-R. Yun, J.H. Jang, E. Jeon, W. Kang, S. Lee, J.-E. Won, H.W. Kim, I. Wall, Administration of growth factors for bone regeneration, Regener. Med. 7 (3) (2012) 369–385.
[62] U. Khetarpal, C. Morton, COL1A2 and COL2A1 expression in temporal bone of lethal osteogenesis imperfecta, Arch. Otolaryngol. Head Neck Surg. 119 (1993) 1305–1314.
[63] S.R. Caliari, B.A.C. Harley, Structural and biochemical modification of a collagen scaffold to selectively enhance MSC tenogenic, chondrogenic, and osteogenic differentiation, Adv. Healthc. Mater. 3 (7) (2014) 1086–1096.
[64] J.M. Banks, L.C. Mozdzen, B.A.C. Harley, R.C. Bailey, The combined effects of matrix stiffness and growth factor immobilization on the bioactivity and differentiation capabilities of adipose-derived stem cells, Biomaterials 35 (32) (2014) 8951–8959.
[65] T. Standal, C. Seidel, Ø. Hjertner, T. Plesner, R.D. Sanderson, A. Waage, M. Borset, A. Sundan, Osteoprotegerin is bound, internalized, and degraded by multiple myeloma cells, Blood 100 (2002) 3002–3007.
[66] J.J. Bergh, Y. Xu, M.C. Farach-Carson, Osteoprotegerin expression and secretion are regulated by calcium influx through the L-type voltage-sensitive calcium channel, Endocrinology 145 (1) (2004) 426–436.
[67] Q. Zhou, S. Lyu, A. Bertrand, A. Hu, C. Chan, X. Ren, M. Dewey, A. Tiffany, B. Harley, J. Lee, Stiffness of nanoparticulate mineralized collagen scaffolds triggers osteogenesis via mechanotransduction and canonical Wnt signaling, BioRxiv (2020).
[68] K. Hu, B.R. Olsen, The roles of vascular endothelial growth factor in bone repair and regeneration, Bone 91 (2016) 30–38.

RSC Advances

REVIEW

Cite this: *RSC Adv.*, 2021, **11**, 17809

Biomaterial design strategies to address obstacles in craniomaxillofacial bone repair

Marley J. Dewey[a] and Brendan A. C. Harley *[abc]

Biomaterial design to repair craniomaxillofacial defects has largely focused on promoting bone regeneration, while there are many additional factors that influence this process. The bone microenvironment is complex, with various mechanical property differences between cortical and cancellous bone, a unique porous architecture, and multiple cell types that must maintain homeostasis. This complex environment includes a vascular architecture to deliver cells and nutrients, osteoblasts which form new bone, osteoclasts which resorb excess bone, and upon injury, inflammatory cells and bacteria which can lead to failure to repair. To create biomaterials able to regenerate these large missing portions of bone on par with autograft materials, design of these materials must include methods to overcome multiple obstacles to effective, efficient bone regeneration. These obstacles include infection and biofilm formation on the biomaterial surface, fibrous tissue formation resulting from ill-fitting implants or persistent inflammation, non-bone tissue formation such as cartilage from improper biomaterial signals to cells, and voids in bone infill or lengthy implant degradation times. Novel biomaterial designs may provide approaches to effectively induce osteogenesis and new bone formation, include design motifs that facilitate surgical handling, intraoperative modification and promote conformal fitting within complex defect geometries, induce a pro-healing immune response, and prevent bacterial infection. In this review, we discuss the bone injury microenvironment and methods of biomaterial design to overcome these obstacles, which if unaddressed, may result in failure of the implant to regenerate host bone.

Received 31st March 2021
Accepted 10th May 2021

DOI: 10.1039/d1ra02557k

rsc.li/rsc-advances

[a]*Dept of Materials Science and Engineering, University of Illinois at Urbana-Champaign, Urbana, IL 61801, USA*
[b]*Carl R. Woese Institute for Genomic Biology, University of Illinois at Urbana-Champaign, Urbana, IL 61801, USA*
[c]*Dept of Chemical and Biomolecular Engineering, University of Illinois at Urbana-Champaign, 110 Roger Adams Laboratory, 600 S. Mathews Ave, Urbana, IL 61801, USA. E-mail: bharley@illinois.edu; Fax: +1-217-333-5052; Tel: +1-217-244-7112*

Marley Dewey is a recent graduate from the Harley Lab at the University of Illinois Urbana-Champaign. She received her B.S. in Chemical Engineering from the University of Maine (2016) and her PhD in Materials Science and Engineering from the University of Illinois Urbana-Champaign (2021). Her research in the Harley Lab involves regeneration of craniomaxillofacial bone defects by modification of mineralized collagen scaffolds. She investigates their potential to inhibit bacterial surface attachment, modulate the immune response to repair, promote multiple cell types to synergistically repair bone, and incorporate 3D-printed structures into the collagen scaffolds to create composite materials with improved mechanics.

Brendan Harley is the Robert W. Schaefer Professor in the Dept. of Chemical and Biomolecular Engineering at the University of Illinois Urbana-Champaign. He received a B.S. in Engineering Sciences from Harvard University (2000), a Sc.D. in Mechanical Engineering from MIT (2006), and performed postdoctoral studies at the Joint Program for Transfusion Medicine at Children's Hospital Boston (2006–2008). His research group develops biomaterial platforms to instruct endogenous cell activities in the context of musculoskeletal and craniofacial tissue regeneration, hematopoietic stem cell biomanufacturing, as well as to investigate endometrial pathologies and invasive brain cancer.

Craniomaxillofacial bone defects

Craniomaxillofacial (CMF) bone defects often involve large defects in the bones that make up the skull or jaw, and can arise from trauma associated with high-energy impacts, congenital defects, and cancer.[1,2] Congenital defects, such as cleft lip and palate, have a frequency of 1 in 700 live births, and oral cancer and dentures can lead to bone resection or resorption by the body.[2] The occurrence of these defects in times of war has increased in recent years, with 29% of injuries sustained in Iraq and Afghanistan classified as CMF defects.[3] Due to the critical size of missing bone in these defects, host bone is unable to naturally bridge the gap in missing tissue and regenerate fully, and thus surgical intervention is required for successful healing. Multiple factors lead to additional challenges in healing of these defects, such as their irregular size and shape, multiple cell types involved, and the likelihood of chronic inflammation and infection, which will be discussed in more detail later in this chapter.

The bone microenvironment

Bone is a complex structure composed of multiple cell types and having various mechanical properties. Of note, bones of the skull and jaw have different mechanics and structure than long bones and the spinal column.

Bone is comprised of organic and inorganic materials, with type I collagen fibers and glycosaminoglycans making up the organic material, and hydroxyapatite mineral crystals as the inorganic. Bone is also anisotropic in nature, with mechanical properties varying in the direction of load application.[4] There exist two different types of bone, cortical and cancellous bone, which have similar compositions but different structural properties. Cortical bone is the stronger of the two and surrounds the softer cancellous bone. Cortical bone generally has a Young's Modulus between 15–20 GPa and approximately 10% porosity, while cancellous bone has a 10-fold weaker Young's Modulus between 0.1–2 GPa and a high porosity of 50–90%.[5,6] For skull bones in particular, stiffnesses can range from 0.36–6 GPa, and variability can be attributed to differences in thickness of the skull at various regions.[7] Thicknesses ranging from 3–15 mm have been observed in the occipital region, with an average of 8 mm thickness in the occipital region and 4 mm in the temporal.[8] Additionally, the surrounding soft tissue of the periosteum has an impact on these mechanics and is rarely investigated together with the bone.[9] Based on a small study of human skull bones the volume ratio of cancellous bone to the entire bone volume ranged from 0.7–0.8,[9] and although the cancellous portion of bone is much weaker, the open-porous nature allows quick invasion of blood vessels and nutrient transport.[5] Without this vascular formation bone will become necrotic, leading to resorption and bone loss.[5,10]

Aside from mechanics, the bone microenvironment is composed of multiple cell types, all which act together to maintain healthy bone homeostasis. These include cells important for new bone formation, vascular formation, and bone resorption. Cells involved in bone formation and maintenance include mesenchymal stem cells, osteoblasts, and osteocytes (Fig. 1).

Mesenchymal stem cells (MSCs) are a cell type which can self-replicate and differentiate into many different cell types such as bone, cartilage, muscle, fat, and tendon, and are known to migrate to sites of injury to aid in repair.[11,12] Differentiation of these stem cells along the bone lineage can result in osteoblasts, which are required to form new bone by secretion of bone matrix proteins.[5] When osteoblasts mature they are incorporated into the bone matrix and become osteocytes, which remain within the matrix and have been associated with bone turnover and adaption.[13] Endothelial cells and pericytes are important for vasculature formation to deliver nutrients and other cell types throughout bone. Pericytes originate from MSCs and line the outside of blood vessels, and endothelial cells form tubes which make up these vessels.[14] Angiogenesis has been associated with osteogenesis, and construction of highly vascular networks within bone leads to its successful maintenance.[15] Finally, osteoclasts are responsible for bone resorption. Osteoblasts and osteoclasts work together to maintain bone homeostasis, maintaining normal bone density, porosity, and strength. Without osteoclasts ectopic or excess bone could occur and without osteoblasts bones may become brittle and thin.[16,17] These various cell types work together synergistically to maintain healthy bone in our body, and without one cell type or its functions our bone and our bodies would not be able to function normally.

The bone injury microenvironment

Bone is a complex microenvironment and healing these defects is particularly challenging due to the multiple cell types and various mechanical properties. CMF defects introduce an additional challenge due to the large volume of bone missing and the body's inability to heal this on its own.

In general, bones heal *via* a process known as endochondral ossification or intramembranous ossification. These two processes have similar healing outcomes; however, endochondral ossification involves a cartilage intermediate associated mostly with long bone healing, while intramembranous ossification does not involve cartilage formation and is associated with the flat bones of the skull and jaw.[2,18,19] Many methods to regenerate bone focus on the direct method of bone formation, intramembranous ossification, where mesenchymal stem cells directly differentiate to osteoblasts. Conversely, endochondral ossification is a seemingly side-step away from bone repair by first creating a cartilage intermediate and mesenchymal stem cells differentiating into chondrocytes. This may not be a drawback however, as cartilage intermediates and chondrocytes formed are avascular and do not need as many nutrients as osteoblasts, and are more likely to survive the process or bone regeneration.[2,20] Further, it has even been suggested that using an endochondral approach to repair CMF defects by promoting a cartilage intermediate, along with neural crest-derived stem cells (from hair follicles, oral mucosa, dental pulp, among others), could prove a more promising approach to CMF defect repair.[2] An understanding of a materials method of

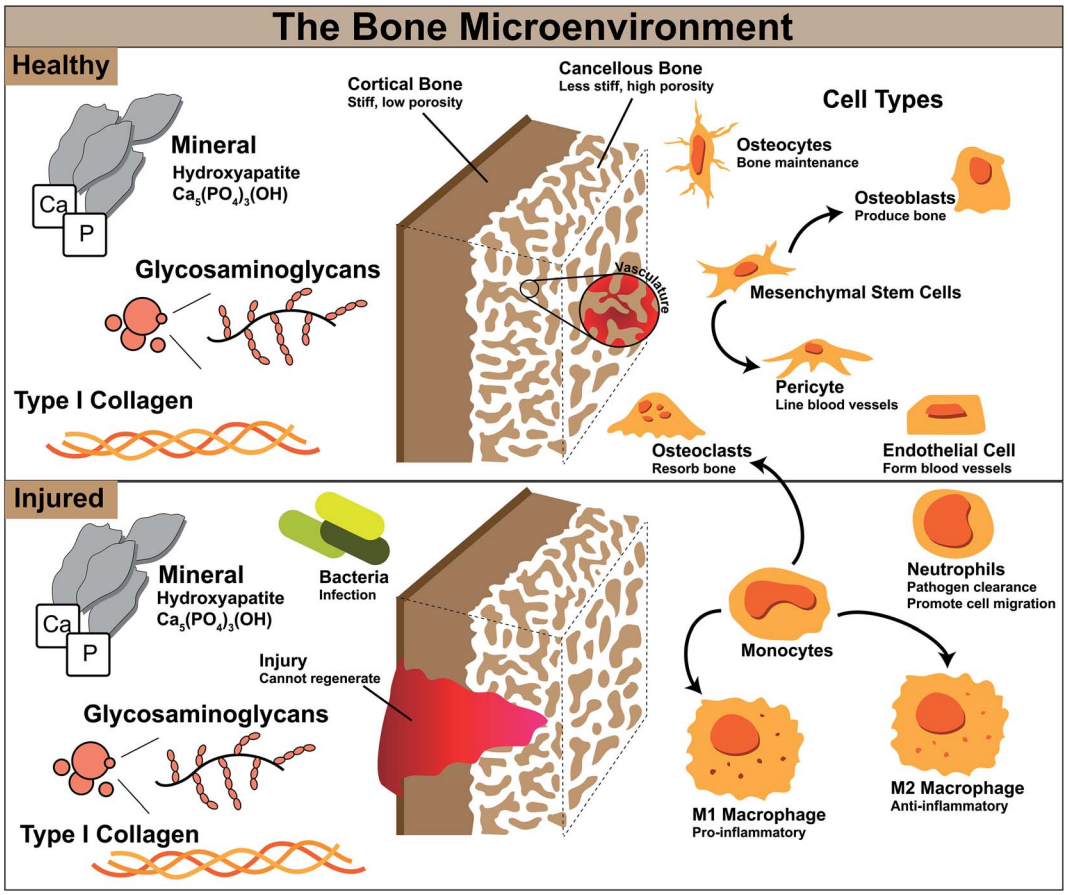

Fig. 1 Cell types involved in bone homeostasis and during injury and their functions.

regenerating CMF defects, by intramembranous or endochondral ossification, could be useful for developing modifications to the material to enhance osteogenesis.

At the onset of injury, there are other cell types involved in repair beyond those in normal bone homeostasis represented in Fig. 1. Bone healing occurs in stages; for segmental defects such as CMF defects, this process can take several months to complete. To heal these defects, substantial bone or a bone-mimicking biomaterial needs to be added to the wound site to bridge the gap in missing bone and regenerate this space. In the first stage after surgical implantation of additional bone or biomaterial to the defect, a hematoma is formed and inflammation begins, transporting with it various immune cells and mesenchymal stem cells (Fig. 2). During this stage, bacteria can be easily introduced within the implanted material if not sterilized properly, or from surrounding patient skin and contamination of surgical tools. Neutrophils are the first immune system cell to migrate to the site of tissue damage and release antimicrobials to kill pathogens, as well as release cytokines to recruit other immune cell types and promote angiogenesis.[21] Failure to regenerate bone can occur if pathogens cannot be cleared by neutrophils and can result in a bacterial biofilm which can be difficult to eliminate by the body and by antibiotics. This can result in persistent inflammatory stimuli as the body works to clear it, and often abscess formation, ultimately leading to chronic infection and the need for a subsequent surgery to remove infected tissue and restart the bone regeneration process.[22]

Monocytes travel to the wound site from the bone marrow and can differentiate into osteoclasts to stimulate bone resorption or M0, unpolarized, macrophages, which can later differentiate into various phenotypes based on environmental cytokines and proteins.[16] Macrophages activate in response damaged tissue signals, and during a healthy immune response, undifferentiated macrophages migrate to the wound site and polarize to the M1, or "pro-inflammatory," phenotype in the early stages (1–7 days).[23–25] The M1 phenotype is activated by interferon gamma (IFNγ), lipopolysaccharide (LPS), or tumor necrosis factor alpha (TNFα).[23] M1 macrophages function to produce inducible nitric oxide synthase (iNOS), reactive oxygen species, and inflammatory cytokines,[23] and are responsible for assisting in early blood vessel formation by VEGF production and removal of debris. After a few days and continuing for weeks, M1 macrophages shift in phenotype to M2 macrophages, also classified as "pro-healing" or "anti-inflammatory," which can be induced by IL-4, IL-10, and IL-13 cytokines.[23] M2 macrophages function to remodel the tissue, deposit new extracellular matrix, and secrete PDGF-BB to assist in late-stage blood vessel development.[24,25] The M1 to M2 transition can occur over the course of weeks, and is important in avoiding

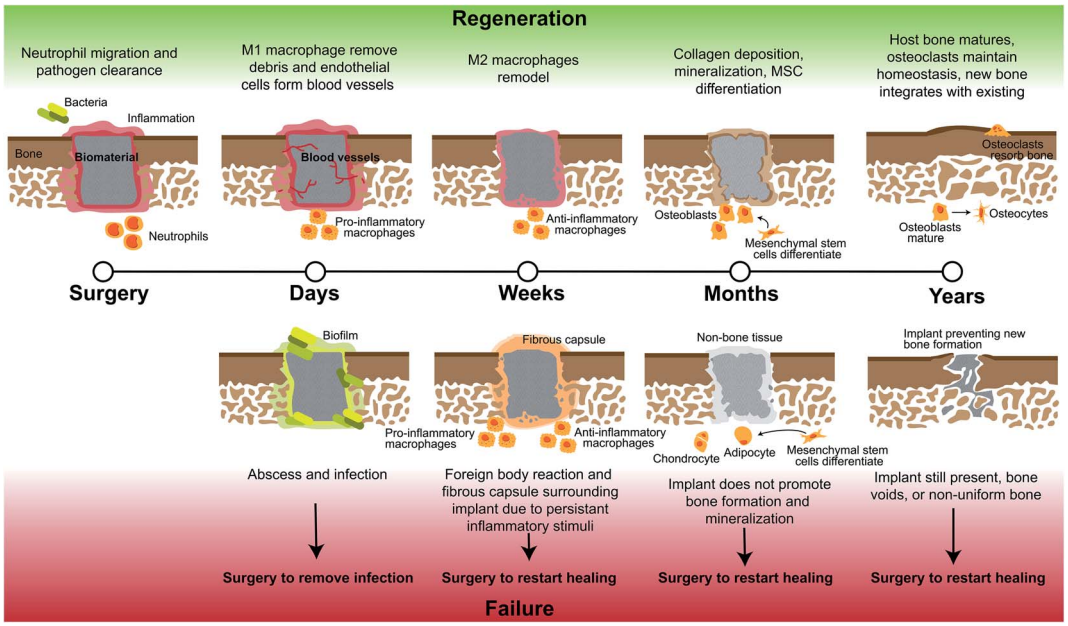

Fig. 2 Stages of craniomaxillofacial bone defect regeneration with biomaterial implants and the possible routes of failure. Full regeneration of these defects can occur over the course of years and from the early to late stages of regeneration there are multiple instances of regeneration failure and when any of these failures occur, the biomaterial most likely will need to be removed and regeneration restarted with a new surgery and material.

persistent or chronic inflammation, which likely occurs in untreated CMF defects where M1 macrophages will persist, and can lead to a foreign body reaction and ultimate need for a secondary surgery.[26,27] If these macrophages or neutrophils are still present after months, this can be classified as persistent inflammation and limited bone healing will occur, as they will continue to produce inflammatory cytokines; without neutrophil apoptosis, tissue damage can occur through continued release of factors meant for pathogen clearance.[21] Additionally, in the case of implanted materials, a foreign body reaction will occur and if the body continues to react to the implant with inflammatory stimuli this can lead to macrophage fusion and surrounding the implant with fibrous tissue and inhibiting bone formation. After inflammation recedes during normal wound repair, mesenchymal stem cells differentiate and mature, and deposit matrix to form bone.[28,29] Finally, secondary bone formation occurs by osteoclast-mediated bone resorption in order to create the anisotropic nature of bone and maintain healthy amounts of bone within the body.[28]

Current standards for repairing bone defects

The gold standard for repairing most CMF defects is *via* the use of bone grafts, and includes both allogenic and autologous sources of bone.

Autografts

Autografts use bone from a secondary site in the patient's own body to replace bone missing in the primary CMF wound site, creating the need for a minimum of two surgeries to attain the bone graft. The most common bone used is the iliac crest, and typically has success rates ranging from 70% to 95%.[30] Removing bone from another area of the patient's body leads to drawbacks such as pain, vascular and nerve injury, bone fracture, and high chance of bone morbidity.[1] Additionally, the large amount of bone necessary for CMF defect repair can limit the amount of bone usable in a patient's own body, and differences in patient health and age can lead to variable healing outcomes.[31] Overall, autografts have the highest success rate in the clinic, attributed to osteogenic and other cell retention in the graft and a desired acute immune response to a material familiar to the body.[1]

Allografts

Allografts use bone commonly from a deceased donor, with cellular materials removed and bone pre-processed into demineralized bone matrix as blocks or particles before implantation.[1] Pathogenic agents and genetic material must be removed prior to implantation to minimize disease transmission and a persistent inflammatory response, which includes heavy processing of the allograft. However, during this cleaning process, osteogenesis of the graft can be impacted as the extracellular matrix (ECM) and collagen can be removed, and this leads to variabilities in healing due to commercial supplier cleaning process differences.[32,33] Drawbacks to allografts include high rates of infection even after sterilization due to foreign substances still remaining after processing, and a more vigorous approach to remove these leads to the bone being less osteogenic.[34] The rate of success of allografts is lower than autografts, but avoids the limitations of a second invasive surgery and limited availability of autografts.[35]

The disadvantages associated with the use of autografts and allografts promote the research and development of tissue engineered biomaterials. Biomaterial approaches allow for patient-tailorable options as well as these typically being easier to modify, enabling changes in mechanics, bioactivity, and drug-loading to improve regeneration.

Biomaterials to repair orthopedic defects

Biomaterials are implants that can be discretely designed to optimize mechanics and biological signals to one day offer the same or better healing than autograft and allograft methods. The greatest advantage of biomaterials is their tailorable nature, allowing for researchers to change multiple properties and add various materials to optimize bone growth. Currently, autograft materials are still the gold standard for CMF defect repair due to highest successful outcomes, but the significant limitations of autografts promotes the discovery and creation of new biomaterials without these limitations.[36–38]

Biomaterials are fabricated from either polymers, metals, or ceramics, and often combinations of multiple material types. These are summarized in Table 1.

Metals

Metals have been classically used in CMF defect repair for permanent solutions to fill missing tissue. Metal implants generally can conduct heat, create difficulties with monitoring health *via* imaging systems, and their stiffness can cause stress-shielding.[34] Additionally, most metals have a risk of corrosion and metal ion release, as well as mismatched mechanics compared to bone, which can lead to surrounding bone atrophy.[39–41] Generally, metals are limited for use in permanent fixation for high loading applications, such as long bone fractures, as opposed to CMF defects. The non-degradable nature of metals also limits their use in pediatric patients due to facial deformities arising from restriction of the growing and developing skull and migration of the metal screws and plates during this process.[42] The most commonly used metal in CMF defects are stainless steel and titanium-based alloys.[43] Titanium is one of the strongest biomaterials used in bone repair, however, for non-load bearing CMF defects such as the skull, this high strength is unnecessary. Additionally, this material is a permanent fixture and has poor osseointegration. Recent developments in the surface modifications of titanium implants have demonstrated osteoinduction *in vitro* and *in vivo* by nanopatterning the surface of these 3D materials.[44] Magnesium-based metal implants have strikingly different properties from titanium, as this metal will rapidly resorb by the body and has osteogenic effects similar to degradable biomaterials.[43] Magnesium offers structural support (*i.e.* high mechanical stiffness), but rapidly corrodes in the body which can result in hyper-magnesia and voids in bone formation, and has no method of preventing implant infection and subsequent biofilm formation.[43,45] Recent developments in magnesium alloys have combined this material with calcium and zinc to release these ions to the surroundings to enhance angiogenesis and osteogenesis, as well as combining with graphene to impart antimicrobial properties.[45,46] Zinc has also been investigated in bone repair due to its biocompatible and antimicrobial properties.[47] However, pure zinc has low mechanical properties and as it degrades releases large amounts of zinc ions to the surroundings, which are detrimental to cells.[47] Recently, zinc alloys have been investigated, and altering the design of this material to include porosity has improved cell attachment and hydroxyapatite coatings have been added to further improve biocompatibility.[47] The use of metals could prove a very promising approach if surface modifications and controlled release of metal ions are further investigated and to provide an osteogenic effect.

Ceramics

Ceramic or hydroxyapatite-based materials are the alternative of choice after autografts and allografts in the clinic.[48] Although these are the preferred biomaterial for bone repair due to their biocompatibility and high mechanical properties, these materials are generally brittle and can have lengthy resorption times.[49] Bioglass is the most commonly used ceramic for bone repair, containing calcium and phosphorous among other elements, but overall this material is generally less successful than autografts.[36,37,50] To improve the mechanical properties of 45S5 bioglass, metal oxides have been doped into this material, as well as nanosilicates such as magnesium silicate, which has demonstrated improved osteogenic differentiation.[51] Specifically, 3D bioglass scaffolds with this nanoclay were able to promote osteogenic differentiation of adipose-derived stem cells and cranial bone formation.[52] Tricalcium phosphates and calcium phosphate cements have similar drawbacks and advantages as bioglass, with slow resorption, brittle properties, and a biocompatible nature.[53] These can also be injectable, and like bioglass, have been doped with similar metals such as zinc and magnesium, and more recently been doped with manganese to improve osteogenesis due to its positive influence and involvement in bone formation.[53] A more recent and promising ceramic material are mesoporous silicate nanoparticles, which have demonstrated high mechanical properties, osteogenic behavior, and have been used as drug carriers due to their porous nature.[54] Most often these nanoparticles are combined with other materials to elute growth factors, but recently Kanniyappan *et al.* investigated the impact of various concentrations of pure mesoporous silicate nanoparticles on osteogenesis.[55] Of note, high concentrations of these nanoparticles demonstrated settling and reduced viability of cells, however, at concentrations of 1 mg mL^{-1} these were osteogenic and promoted angiogenesis.[55] Ceramic materials could prove very promising in combination with metals or other materials to impart improved strength and osteogenesis.

Polymers

Polymers used for tissue regeneration should be biodegradable and biocompatible, with special consideration of degradation byproducts for cytotoxic effects. Polymers offer advantages in large scale reproducibility and unique control over mechanical properties, degradation, and structure by manipulating polymer chains.[56] Drawbacks to these include poor mechanical

Table 1 Benefits and drawbacks of materials used for bone repair

Material	Sub-class	Benefits	Drawbacks	Novel developments
Metals	Stainless steel, titanium	High load bearing	• Permanent fixture • Stress-shielding • Risk of infection • Secondary surgery to remove implant • Limited osseointegration	• Surface coatings • Nanopatterned surfaces
	Magnesium	• High load bearing • Biodegradable	• Rapid dissolution of metal • Implant failure • Risk of infection	Addition of other metal ions
	Zinc	• Biocompatbile • Antibacterial	• Low mechanical properties • Releases large zinc ions harmful to cells	• Porous structures • Calcium phosphate coatings
Ceramics	Bioglass	• Bioactive • Osteoconductive • Integration with host bone • Antibacterial	• Brittle • Low fracture toughness • Poor osteoinductivity	Metal doping
	Calcium phosphates	• Osteoinductive • Resorbable • Injectable as a cement, shapeable	• Brittle • Slow resorption • Limited mechanical strength • Risk of infection	• Metal doping • Addition to polymers as coatings
	Silica nanomaterials	• Low cytotoxicity • High porosity • High mechanical strength • Biocompatible • Tunable pore size • Drug delivery vehicles • Osteogenic • Promotes vasculature	• Crystallinity impacts biocompatibility • Aggregation of nanoparticles • High concentrations can lead to particle setting and cytotoxic effects • Concentration limits • Risk of infection	• Surface modifications • Combination with polymers
Polymers	Polylactic acid (PLA)	• Biocompatible • Biodegradable • Easily 3D-printed into specific shapes and porosities • Shorter degradation time than PCL (6 + months) • High mechanical properties	• Acidic degradation products may cause inflammation • Risk of infection	• Coat with calcium phosphate • Blend with multiple polymers
	Polycaprolactone (PCL)	• Flexible • Hydrophobic • Biodegradable • Biocompatible • Easily 3D-printed into specific shapes and porosities • Shape-memory fabrication	• Low mechanical stiffness • Long degradation times • Acidic degradation products • High transition temperature for shape actuation • Risk of infection	• Blend with multiple polymers • Use different polymer conformations (star)
	Collagen	• Tunable pore size • Biocompatible • Sequester growth factors easily	• Low mechanical properties • Disease transmission risk • Need mineral to induce osteogenesis • Risk of infection	• Reinforce with stronger materials • Collagen derived from marine sources • Add calcium phosphate
	Chitosan	• Antibacterial • Anti-inflammatory	• Poor mechanical properties • Low cell attachment • Poor osteoconductivity • Need mineral to induce osteogenesis	• Reinforce with stronger materials • Modify fabrication (granular hydrogels)

properties compared to bone and the possibility of host rejection and fibrous tissue formation due to released byproducts. Two of the most commonly used polymers are FDA approved polycaprolactone (PCL) and poly(lactic acid) (PLA), which can degrade in the body *via* hydrolysis, but their degradation byproducts are acidic, and in high enough quantities may damage cells.[39,57,58] Both polymers are biodegradable and biocompatible, but PLA offers high mechanical strength and shorter degradation times, while PCL offers flexibility and hydrophobicity.[59] Due to these disadvantages, PLA and PCL have been combined to create polymer blends to leverage the best qualities of both polymers to optimize degradation time and improve mechanical properties and flexibility of the resulting material.[59] To improve the osteogenic response of PLA alone, hydroxyapatite coatings have been used to alleviate acidic byproduct release and increase bioactivity.[60] PCL has also been investigated as a shape-memory polymer to improve fit of the implant with host bone defects, however, a high transition temperature was needed for shape actuation.[61] Recent developments by the Grunlan Lab have further modified the PCL polymer with star architectures in order to lower this transition temperature and increase expansion pressure to fit against host bone.[62] These types of polymers offer biocompatibility and easy structure modification by 3D-printing technologies and polymer composition allowing for a large realm of possibilities to tailor these materials for bone repair.

Other polymers derived from animals and insects, such as collagen and chitosan, have been used extensively to heal both hard and soft tissues. Collagen is the main organic constituent of bone and thus using collagen materials has found great success in bone and wound regeneration. Porous type I collagen scaffolds combined with glycosaminoglycans have been successfully used to repair tendon and skin, and the addition of calcium phosphate to these has resulted in bone repair.[63–71] A benefit to using collagen scaffolds are their tunable pore size and orientation, their ability as high growth factor-retention sponges, and ease of incorporating additional materials during fabrication such as adding zinc particles.[63,66,67,72–76] A drawback to these materials are their extremely mechanically weak nature, which are far from matching the mechanical properties of bone, and most collagen used in biomaterial applications is animal derived and there are concerns of disease transmission, specifically, bovine spongiform encephalopathy (BSE) and transmissible spongiform encephalopathy (TSE).[77] To overcome these limitations, 3D-printed polymers have been incorporated into mineralized collagen scaffolds to create composite materials with moduli similar to the 3D-print material used, and salmon-derived collagen has been investigated as an alternative to bovine collagen to avoid religious concerns and disease transmission.[78–80] Hydrogels have also been investigated as methods to repair bone due to their injectable nature and ability to release drugs to the surroundings. Hydrogel materials such as chitosan or alginate typically have low cell infiltration and vessel formation throughout due to slow degradation.[81] Chitosan offers antibacterial and anti-inflammatory properties but hydrogels made of this have similarly weak mechanics to collagen and low cell attachment and osteoconductivity.[82] Additional mineral can be added to chitosan hydrogels, similar to collagen scaffolds, to induce osteogenic responses, and furthermore, creation of granular hydrogels can enhance porosity and cell infiltration.[81,82] Promising new approaches to improving hydrogels include incorporation of synthetic polymers and extracellular-derived matrices which include glycosaminoglycans and proteins beneficial for tissue repair. Recently, a pig-bone ECM was combined with polyethylene glycol diacrylate to lengthen degradation of the hydrogel and promote osteogenic proliferation.[83] Natural polymer-based materials are biocompatible and with the addition of calcium phosphate mineral, can readily promote osteogenesis, and have a promising future when combined with other materials to increase mechanics and stability of these structures.

Composites

Metals, ceramics, and polymers all have their associated benefits and drawbacks for repairing bone defects, and thus recent biomaterial developments have focused on composite materials. This refers to the combination of two or more distinct materials to leverage the benefits of both materials, in the hopes of overcoming the separate material drawbacks. Many of the recent improvements made to metals, ceramics, and polymers have involved a combination of two or more of these materials together. Another example includes combination of ceramic microspheres in a chitosan matrix. Ceramic microsphere granules have been used to reduce the invasiveness of calcium phosphate ceramics but the porosity of these is very low due to the ability of these to aggregate.[84] To create a more cohesive and porous material, chitosan and polyethylene glycol were combined with these ceramic microspheres to create a better injectable and mechanically stable implant.[84] For example, while chitosan alone is anti-inflammatory it has low mechanical stiffness and calcium–phosphate ceramics are brittle with low porosity, its combination with chitosan can yield a composite with benefits of both to create a more stable material able to regenerate greater host bone with minor inflammation. Many novel materials developed currently, include hydroxyapatite coatings[47,60] and metal or ceramics particles[45,46,53–55,75] incorporated into polymeric base materials to increase mechanical stability and osteogenesis.[79,82,85,86,89] Other unique promising approaches include bone-mimicking structural elements as well as composition, such as the use of Voronoi open-cell architectures to replicate the porosity and mechanical structure of cortical and cancellous bone,[87] and 3D-printing haversian canals to better transport multiple cells and nutrients throughout the entire implant.[88] Composites represent a new way to use existing materials to improve mechanics and biological performance, as well as avoid many of the drawbacks of these materials. Composite materials are likely to be most successful in the clinic in the future, and new developments using these materials will combine metals, ceramics, and polymers.

Strategies to address the challenges of repairing craniomaxillofacial defects

The low success rates of biomaterial solutions to repair CMF defects can be attributed the challenges associated with generalized wound healing and challenges that are specific to

these types of defects. By addressing each of the challenges of CMF defects by biomaterial design and composition, this can improve the outcome of healing in the clinic, but failure to address even one factor may result in catastrophic failure of the implant. General properties of a biomaterial to address the challenges of CMF defect repair are outlined in Fig. 3.

Biomaterial mechanics

The first step to the biomaterial implantation and bone regeneration process begins with the surgical handling and physical placement of the implant. As simple as this may sound, CMF defects are often irregular in size and shape, especially in the case of birth defects and battlefield injuries. To overcome this obstacle, many researchers have focused on using 3D-printing to create unique and patient-specific implants by scanning the skull with MRI or CT and converting the missing space from the scan into a 3D-print.[90] While this makes for enough material to fit the defect space, additional consideration of the surgical handling of the implant is important. Ultimately, if a surgeon has difficulty handling the implant or placing it into the defect space, this will have downstream clinical use and application issues. This can be a problem with extremely stiff implants, which not only must be fabricated extremely precisely to fit within the defect, but also impart unfavorable mechanics to the tissue. Generally, stiffness has been attributed to increases in bone regeneration and many researchers have strived to create implants that can compare to the mechanical properties of bone. However, CMF defects represent an interesting challenge as they are non-load bearing and may not require implants that exactly match their natural properties.

The Young's modulus of cortical and cancellous bone ranges from 15–20 GPa and 0.1–2 GPa, respectively for longer bones, and the compressive modulus of sections of bone from the skull containing both of these regions is on the order of 0.36–5.6 GPa depending on direction of load.[6,7] This high mechanical strength, even for cancellous bone, can be difficult to achieve with materials such as polymers, especially as these materials are needed to be porous to allow for cell penetration. Metals and ceramics may more easily approach these mechanics, but it is possible that such a high stiffness is not necessarily needed for bone repair as increases in moduli from 0.34 kPa to 3.9 kPa in crosslinked and non-crosslinked mineralized collagen scaffolds was enough to induce an increase in osteogenic differentiation.[91] A factor of possible

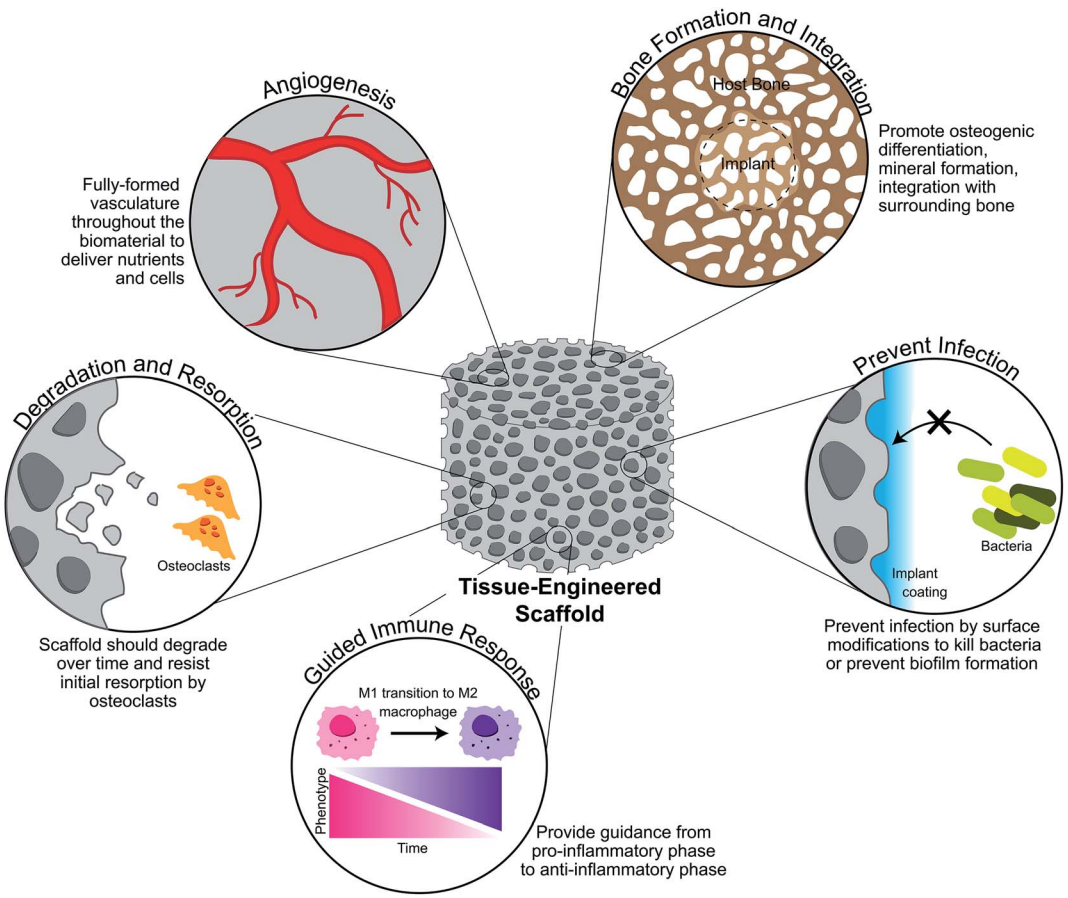

Fig. 3 Ideal properties of a tissue-engineered scaffold for craniomaxillofacial defect repair. A scaffold should promote new and organized vasculature throughout the defect space in order to delivery nutrients and cells to the newly forming bone. It should also be designed to produce new bone and integrate well with the surrounding bone, doing so by degrading over time and resisting initial resorption by osteoclasts. Finally, a scaffold should prevent infection as chances of this are high in CMF defects, while also guiding the immune response to repair rather than persistent inflammation.

greater concern is the fit of the implant to the defect space. If an implant is too stiff, most commonly in metal materials, stress-shielding at the bone and metal contact can cause greater bone loss.[92] Even will softer materials, if an implant is not mechanically stable and limited in motion, this can cause further damage. Outside the range of 28–150 μm of motion possible between the implant and host bone space can be defined as micromotion, which is undesirable.[92] Micromotion can lead to fibrous tissue formation and growth surrounding the implant, ultimately limiting bone regeneration.[92] To overcome this problem, many groups have focused on 'shape-fitting' implants, created from polymers which can be shaped into the defect space by a surgeon and based on temperature changes can set within the defect space.[61,93] These types of materials avoid the issue of micromotion due to hardening within the defect space, but thermo-responsive properties may be limited to synthetic polymers and may not be applicable to metal and ceramic materials. An alternative method to apply shape-fitting properties outside of material composition is through structural modification, which may be applicable to a wider variety of material types. An example of this is using a design able to be conformally contracted by the user, and such a design has been implemented with PLA and used to create tight contact in cylindrical defects smaller than the design itself.[79] Other labs and companies such as Dimension Inx (Chicago, IL, USA) have focused on the fabrication of biomaterials from sheets or ones that are not pre-cut to the patient's defect shape, allowing for the surgeon to cut and shape the biomaterial to their liking and fast processing of these materials by avoiding timely patient-tailoring of shape.[94,95]

In creating an implant that can be formed or manipulated by the surgeon, one can limit the possibility of micromotion that can occur through stiff materials. This not only improves handling, which is desired for clinical applications, but can improve healing as well. Future biomaterial developments for CMF defects in particular should focus on the mechanics of implants, not from the standpoint of matching the stiffness of bone, but to avoid any defect motion and creating materials that can be easily added to the defect space. By doing so, this first obstacle in repair and implantation can be overcome.

Bacterial infection

Bacteria are everywhere and the consequences of their presence in surgical implantation of biomaterials can be devastating. Sterilization of tools, surfaces, skin, and the implant itself are common first precautions to avoid their contamination of the wound, with antibiotics being administered during and after surgery to eliminate any bacteria that may have still been able to enter the wound. Even more concerning, these bacteria that enter the wound site may be antibiotic-resistant, such as the most common bacteria present in bone infections, *Staphylococcus aureus*, and its antibiotic-resistant strain, Methicillin-resistant *Staphylococcus aureus* (MRSA).[96] Additionally, the chance of infection increases to as high as 50% with type III open wound surgeries or fixations, such as CMF defects, making these likely to become infected even with sterilization of equipment and antibiotic treatments.[97,98] Treatment of infections is further complicated by the inability of many antibiotics to penetrate inflamed tissue, and if bacteria are left untreated, this can then cause chronic inflammation and implant failure.[22,99] In particular, *Staphylococcus aureus* (*S. aureus*) acts to inhibit bone formation by invading osteoblasts and osteocytes and becoming internalized within these cells, protecting it from antibiotics and immune system clearance.[97] Once inside osteoblasts, it can inhibit their ability to differentiate and cause apoptosis, which downstream prevents mineral deposition and new bone formation.[97] Through this impact on osteoblasts, *S. aureus* favors osteoclastogenesis and bone resorption, due to an imbalance of osteoclasts and osteoblasts and thus leading to even less bone formation occurring.[97] Other bacteria, such as *Pseudomonas aeruginosa*, will aggregate and form biofilms around an implant, protecting itself from the immune response and antibiotics by the formation of a resistant and protective film.[100] Overall, if unable to be cleared by the body's own immune response and antibiotics, bacteria can infiltrate the implanted material and create abscesses and completely inhibit bone formation, leading to another surgery to remove this infected material and clean the wound site.[97]

To prevent bacterial infection current research has progressed towards developing antibiotic-free methods to eliminate the growing number of antibiotic-resistant bacteria. This can be explored through modifying the topography or composition of biomaterials. The topography of biomaterials can be modified by altering the micron- or nano-scale surface features during fabrication. To illicit bactericidal effects, nano-scale topographies are able to disrupt the bacterial membrane, while micron-scale features can be too large in some cases to have this same effect.[101] Beyond scale, the pattern of the topography can affect the way bacteria adhere to a surface as well. Lines, pillars, hexagons and other patterns can inhibit biofilm formation, while pillars and needle-like patterns can kill bacteria on contact while keeping cells alive.[101] Pillars and rod-like patterns disrupt bacterial membranes due to their small size and closer-spaced pillars can damage membranes better due to shear forces.[102] Fabrication of nanostructured surfaces may be easiest to achieve with polymer and lithography approaches, thus, for materials that may have more difficulties with precise surface modifications, chemical and biological compositional changes may be preferred.

Additives or coatings on biomaterials offer alternatives to antibiotics for reducing bacterial adhesion or promoting bacterial death, and include antimicrobial peptides and enzymes, hydrophobic coatings, nanoparticles, natural materials, among other solutions.[103] Antimicrobial peptides (AMPs) have shown effectiveness against Gram-negative and Gram-positive bacteria as well as viruses, due to their overall positive charge and hydrophobic residues, which disrupt the negatively charged bacterial cell wall.[103,104] Novel developments in this field have included titanium implants containing titania nanotubes for on-demand delivery of AMPs in stimuli-responsive "boxes" which open to release AMPs under bacterial infection due to a drop in pH.[105] This also includes other materials, such as collagen and chitosan scaffolds, loaded with polymeric microspheres containing

peptides to eliminate bacterial growth through sustained release of these peptides.[106,107] Enzymes can operate by interfering with bacterial adhesion or killing bacteria by hydrolysis of the cell wall and lysis of the bacteria.[103] Mesoporous silica nanoparticles have been used as drug delivery vehicles and have been used to deliver levofloxacin, a drug which converts bacterial enzymes into bacteria-toxic enzymes, in response to heightened acid phosphatase levels which occur in bone infection and resorption.[108] One common enzyme used to eliminate *S. aureus* in particular is lysostaphin, a specific anti-staphylococcal enzyme, which has been loaded into hydrogels for eradication of *S. aureus* infection and while regenerating bone.[109,110] Altering the hydrophobicity of a material can prevent adhesion of bacteria and thus prevent accumulation and biofilm formation, but increasing hydrophobicity also prevents host cell attachment and infiltration of the implant to promote tissue regeneration.[103] This method has been used by coating titanium implants with positively charged, hydrophobic silane molecules, which prevented bacterial attachment while demonstrating no cytotoxic impact on human dermal fibroblasts.[111] Others have also developed thin PLA films containing magnesium particles to control the rate of degradation of this metal, and these films displayed hydrophobicity and resulting bacteriostatic behavior.[112] One of the most common antimicrobial additives are metal particles, and specifically silver nanoparticles, which have been used in the food industry. Alternatively to silver, other metals such as gold, aluminum, copper, iron, magnesium, zinc, bismuth, cerium, and titanium have been also used as nanoparticles to combat bacterial infections.[113] Zinc and silver nanoparticles in various ratios have been added to titanium implants for release of these factors over a minimum of 28 days to eliminate adherent and planktonic MRSA.[114] Finally, natural additives have been explored recently as coatings or added compositions to biomaterials, such as honeys, chitosan and animal-derived products, algae and other plant by-products.[115] Chitosan has been most recently used in combination with antibiotics as a material for controlled release of these to the surroundings, as pure chitosan implants have demonstrated little resistance to bacteria compared to antibiotic controls.[116] However, loading these chitosan sponges with antibiotics can increase clearance of *S. aureus* more so than antibiotic application alone.[117] Honey in particular has been of recent focus due to its low pH and hydrogen peroxide content attributing to its antibacterial properties, and has been incorporated into hydrogels and on the surface of materials as honey-needles to kill bacteria.[118–120]

Infection can occur during implantation of a biomaterial and remain unknown after surgery until it is too late, and the removal of the infected biomaterial is necessary. Additionally, antibiotics do not afford the security of infection prevention they once did, therefore design of implants for CMF defects must include antibacterial properties due to the high chance of infection. Whether incorporation of this be as a topographical or compositional design, there are many avenues to choose from to create antibacterial biomaterials.

Immune response

Another challenge to healing CMF defects is directing the immune response to repair. When a biomaterial is implanted into the body, the body can see this as a foreign substance and recruit macrophages to break it down or wall it off from the rest of the body. This foreign body reaction, if persistent, can result in a fibrous wall surrounding the implant and fibrous tissue blocking bone formation from occurring, thus resulting in implant failure. To avoid this, a large body of research has focused on the response of macrophages to implants. As stated previously, M1 and M2 macrophages transition to heal the wound successfully, but persistence of these and their stimuli can lead to fibrous tissue formation and chronic inflammation, and ultimate failure of healing. By designing materials to interact with the immune response to guide in repair and transition eventually out of an inflammatory reaction, we can create more successful healing outcomes.

There are various properties of a biomaterial that can affect the way macrophages and other immune cells react to its implantation. A few of these that have shown significant effect are the pore size and shape, degradation byproducts, and shape and topography of the implant. Previous work by Sussman *et al.* has demonstrated that a pore size of 34 μm can influence macrophages towards a pro-inflammatory phenotype, with 63% of macrophages expressing M1 markers and 81% reduction in M2 markers.[121] This pore size also led to an increase in myofibroblasts, most likely due to an increase in M1 response, but non-porous materials had thicker fibrotic capsule resulting from a foreign body reaction and less vascularization.[121] Studies by Madden *et al.* implanted porous materials for cardiac regeneration and demonstrated that pore sizes above 45 μm in diameter resulted in organized fibrotic tissue, and they discovered a pore size from 30–40 μm promoted a M2-like response, reducing fibrosis and increasing angiogenesis.[122] Not only does the pore size affect macrophage polarization, but shape of pores also impacts this, as work by McWhorter *et al.* demonstrated that micropatterning a surface to cause macrophage elongation shifts the phenotype towards M2 and enhances M2 cytokine effects.[123] Careful consideration must be made on choosing a biomaterial for bone regeneration in the case of degradation byproducts, as many of these can by cytotoxic in high quantities. Generally, particles from wear of implants and degradation by hydrolysis can cause production of pro-inflammatory cytokines, with an example of this are poly(lactic-acid)-based biomaterials, which have been shown to cause an inflammatory response.[124,125] This inflammatory response can be attributed to large releases of the degradation byproducts, specifically acidic lactic acid, and small PLA particles (<2 μm) can induce a foreign body response, by persistence of M1 macrophages, and bone resorption.[126] Additionally, the large-scale size and shape of the implanted material can illicit an inflammatory response. Thicker materials have been shown to illicit a greater foreign body response and fibrotic tissue, and a greater surface area as well as sharp and angular shapes are more likely to induce a foreign body response and M1 phenotype.[127,128] Alternatively, growth factors and other molecules can

be added to the surface of materials to facilitate the M1 to M2 transition to prevent chronic inflammation. Some examples of this include coatings that release IL-4 from polypropylene meshes to promote M2 responses,[129] early release of IFNγ and then later release of strontium ions to force an early M1 and later M2 phenotype transition in glass composite scaffolds,[130] and scaffolds containing bioactive anti-inflammatory nanocapsules which block M1 inflammatory cytokines while promoting M2 phenotypes to improve bone repair.[131] Overall, more care must be taken in the surface and whole design of implants, as pore size, shape, degradation and released products, and material thickness can all influence the response of macrophages and if not designed correctly, can elicit a foreign body response and fibrotic capsule surrounding the implant.

Balancing multiple cell types and interactions

After the immune response dwindles, formation of bone can begin with collagen and mineral deposition. However, there are multiple cell types involved in bone regeneration outside of the immune response, and their interactions must be balanced and promoted in a way that allows them to use the implant for repair. Such cells involved in the regeneration process and bone homeostasis are mesenchymal stem cells, osteoblasts, osteocytes, osteoclasts, pericytes, and endothelial cells. By designing an implant to promote these cells to create healthy bone tissue, one can have a more successful outcome.

Many researchers have studied the effect of osteoblasts on biomaterials for bone, and metals, ceramics, and polymer materials have all demonstrated their ability to work well with osteoblasts.[132] Without osteoblasts, new bone formation could not occur, but research should also focus on the precursor to these cells: mesenchymal stem cells. MSCs migrate the wound site and depending on the biomaterial characteristics this can determine the fate of these cells, as they can differentiate into many other lineages besides bone. Additionally, osteoblasts should eventually mature to osteocytes and maintain healthy bone once regenerated. Osteoclasts function to maintain homeostasis in fully-formed bone, but careful consideration must be made to not promote the actions of these cell types early on and cause unwanted resorption of the implant. Finally, endothelial cells and pericytes form vasculature throughout the material to deliver nutrients and continue to supply cells to the wound. Promoting angiogenesis and bone formation while limiting bone resorption can be directed by material composition, stiffness, and pore structure and size.

The composition and structure of biomaterial implants should be as closely related to the natural composition of bone as possible, including a combination of type I collagen and hydroxyapatite mineral.[133] The mineral and glycosaminoglycan content within a material alone can have dramatic effects on multiple cell fates. Studies using mineralized collagen scaffolds compared to non-mineralized collagen variants have demonstrated significantly more bone formed in rabbit calvarial defects using mineralized scaffolds.[134] Not only does mineral within a biomaterial act to facilitate further mineral deposition by osteoblasts, but also limits bone resorption, as calcium ion signaling may improve secretion of OPG by mesenchymal stem cells and limit osteoclastogenesis.[133,135] This has been further demonstrated by the ability of mineralized collagen scaffolds to promote greater OPG release by MSCs and less osteoclast resorptive activity than non-mineralized collagen counterparts.[136,137] Additionally, glycosaminoglycans are important constituents of healthy bone and specifically glycosaminoglycans chondroitin-6-sulfate and heparin sulfate have been shown to promote mineral formation in mineralized collagen scaffolds.[138] Glycosaminoglycans have dramatic effects on other cells and processes such as angiogenesis and inflammation. Studies using chondroitin sulfate have demonstrated an inhibitory effect of this glycosaminoglycan on monocyte migration *in vitro* and thus a potential anti-angiogenic effect *in vivo*.[139,140] Additionally, chondroitin sulfate and heparin sulfate have been known to have anti-inflammatory effects, and heparin sulfate has also been shown to demonstrate enhanced osteoclastogenesis.[141–144]

The stiffness and porosity of a substrate can also act to shift mesenchymal stem cell fate and it is well observed that a stiffer material will influence MSCs towards differentiation into osteoblasts.[145] Stiffness not only affects mesenchymal stem cell differentiation, but also angiogenesis, with stiffer materials exhibiting greater angiogenesis *in vivo*, with this attributed to endothelial cells spreading more on stiffer substrates.[146] Electrospinning has been used to study the effect of MSC differentiation due to fiber alignment, and stem cells seeded on aligned substrates promoted osteogenic gene expression over randomly oriented structures.[147] This has also held true for anisotropic pores in mineralized collagen scaffolds, where alignment caused an increase in osteogenic gene expression and mineralization.[138] This alignment may also have beneficial effects in directing vessel network formation through channel-like materials and providing guidance for angiogenesis.[148] Pore size and shape can effect multiple cell types, and thus there is some speculation on the best pore size for enhancing osteogenesis due to multiple cell interactions. It is generally thought that for MSC infiltration and differentiation into osteoblasts pores should range from 50–200 μm in diameter. However, some materials on the order of 1 mm pore diameters have demonstrate bone regeneration, but pores smaller than 50 μm fail to produce mineral.[145] Additionally, pore sizes on the larger scale are typically better for blood vessel formation, but pore sizes greater than 400 μm have demonstrated no improvement in this.[149] One must also consider pore spacing, as blood vessels in normal bone are no more than 300 μm apart to continue to deliver nutrients.[149]

Additional materials outside of those naturally found in bone can be added to biomaterials to enhance multiple cell types, such as metal particles. As stated previously, metal particles can be beneficial as antimicrobial additives, and some metal particles have even demonstrated improving bone formation. Incorporation of zinc nanoparticles on mineralized collagen scaffolds induced greater MSC osteogenesis and mineral formation, and magnesium ions have demonstrated the ability to induce MSCs to osteoblasts.[75,150] A variety of nanoparticles including gold and silver have been shown to

Table 2 Biomaterial modification strategies to address the challenges of CMF defect repair

Challenge	Ideal properties	Methods to address	Ref.
Mechanics			
Surgical handling	Easy for surgeons to add to defect	• 3D-printing exact defect shape • Shapeable by surgeon (*i.e.* putty) • Trimmable material (*i.e.* sheet)	61, 90, 93–95
Stiffness	Should not be stiffer than bone to avoid stress-shielding and not too soft to avoid material collapse	• Avoid stiff metal materials • Create composite structures to increase stiffness of soft materials • Cross-linking to add stiffness	78 and 91
Micromotion	Limit to 28–150 μm of motion or else fibrosis will occur	• Design implant with shape-fitting properties	61, 79 and 93
Bacterial infection			
Infection	Killing bacteria or preventing bacterial adhesion to implant surface without antibiotics	• Nano-scale surface topography kills bacteria (*i.e.* pillars or unique patterns) • Compositional changes can kill bacteria or prevent attachment: • Antimicrobial peptides and enzymes • Hydrophobic coatings • Metal nanoparticles • Natural materials (*i.e.* honey, chitosan)	101–104, 113 and 115
Immune response			
Macrophage phenotype	M1 to M2 transition over weeks	• Porous material facilitates healing, >30 μm pore size to promote M2 • Patterned surfaces or anisotropic pores promote macrophage elongation and M2 phenotype	121 and 123
Foreign body response (FBR)	Avoid material causing FBR	• Degradation byproducts should not be cytotoxic or in high quantities • Particles sizes <2 μm can cause FBR and bone resorption • Avoid thick, hard to degrade materials • Avoid designing materials with points or sharp edges	124–128
Balancing multiple cell types			
Mesenchymal stem cells, osteoblasts, and osteocytes	Osteogenesis and differentiation to the bone lineage	• Metal particles such as zinc and magnesium can induce osteogenesis • Pore sizes > 50 μm can induce osteogenesis • Aligned fibers and pores promote bone formation over random orientations • Increasing stiffness increases osteogenesis • Mineral (Ca, P) promotes MSC differentiation and osteogenesis • Glycosaminoglycans (*i.e.* Chondroitin-6-sulfate, heparin sulfate) induce osteogenesis	75, 134, 138, 145 and 150
Osteoclasts	Limit early resorptive activity of implant	• Calcium enhances OPG production to block osteoclastogenesis	133 and 136
Pericytes and endothelial cells	Promote angiogenesis and fully formed and functional vasculature	• Stiffer materials encourage angiogenesis and endothelial cell spreading • Aligned or channel-like pores can guide vessel formation • Larger pores are better at promoting angiogenesis	146, 148 and 149
Regenerative healing			
Host bone regeneration	New bone should form throughout the material without voids	• Micro-scale porosity enhances bone formation throughout implants • Metals do not allow for new bone formation	157 and 158
Material degradation	Material degradation should match host bone regeneration	• Thinner materials allow for quicker degradation • Ideally a material should degrade within 3–6 months for CMF defect repair • Polymer chemistry can be modified to hasten degradation by pH changes, temperature, and hydrolysis • Mechanical stimuli can help to balance degradation and regeneration	6, 155 and 156

enhance angiogenesis, possibly through the modulation of reactive oxygen species.[151–153] When testing the ability of biomaterials to regenerate bone, one can make changes in multiple properties, but the behavior of cells important for bone formation, bone resorption, vascularization, and the immune response need to be studied in order to more accurately predict the outcomes *in vivo* or in clinical trials, as osteoblasts are not the only cell type that instruct healthy bone formation.

Regenerative healing

The final design criteria of a bone regenerative biomaterial is the full regeneration of the defect space. This design decision is based on the material properties, mainly the degradation and resorption of the implant. One main criteria for a regenerative material is that the host bone regenerate in the defect space, so ultimately this leaves out the use of metals, as these are permanent implants and may integrate with surrounding host bone, but will never be replaced by bone. This is not to say that metal nanoparticles cannot be used to achieve bone regeneration, but metal as a high-volume replacement of the missing tissue will not cause regeneration due to the body's inability to break down this material. Beyond metals, careful care must be exercised when choosing ceramics or polymers as the biomaterial main constituent, especially as polymer degradation times can be easily manipulated.

Ideally, if an implant has not been hindered by the many challenges of early healing then bone regeneration will start to occur within the defect space and within the implant. For full regeneration this means that the degradation of the material must match the rate of new bone formation. If these are not balanced then the material to support bone regeneration may degrade before it can provide essential ingredients for bone repair and leave voids in the defect space, or conversely, the material may remain for too long and inhibit host bone formation. This can be avoided by choosing a material with a degradation time that matches new bone formation and even the thickness of the material. The thicker a polymer or other material leads to a lengthier time for cells and hydrolysis to degrade this material. Typically, it is thought that craniomaxillofacial defects with implants will regenerate bone within 3–6 months after biomaterial implantation if healing occurs healthily.[6] Polymers can be specifically designed to degrade slower or more quickly by altering the chemistry and composition, as PCL polymers typically can take over 2 years to degrade, PLA can take over 6 months, and PLGA can take less than 6 months.[57,154] To overcome this, chemical changes can be made to the polymer to change its response to temperature, hydrolysis, pH, and other factors, which may help it to degrade faster during bone regeneration.[155] Factors outside of materials chemistry have been demonstrated to help in degradation and bone formation, specifically mechanical stimuli has been shown to synchronize degradation and bone formation in calcium sulfate cements for long bone repair.[156] However, the application of mechanical stimuli to craniofacial bones may be more difficult as they are not usually under load-bearing conditions.

An additional issue with regenerative biomaterials that may lead incomplete bridging of the bone defect space or non-uniform bone formation due to incomplete cell penetration of the implant. This can be controlled once again by scaffold architecture and porosity. Work by the Wagoner Johnson group at the University of Illinois has demonstrated that microporous hydroxyapatite-containing BCP scaffolds had more uniform bone formation than scaffolds without these pores.[157] Additionally, they found micro-porosity effected trabecular thickness and the distance between struts in their 3D-printed scaffolds only effected this thickness at the periphery of the scaffold.[157] This work as well as work by Wu *et al.* have demonstrated that 3D-printing can be used to effectively study and optimize the pore size for bone growth within the center of implants.[158]

Summary of design principles for next-generation implants to improve craniomaxillofacial bone regeneration

There are many challenges associated with CMF defect repair and implants will face multiple obstacles before successful outcomes, outlined in Table 2. Bulk implant mechanical properties can govern surgical handling and ill-fitting implants can lead to a fibrous encapsulation. Increasing the stiffness of implants increases bone formation by osteoblasts as well as endothelial cell spreading which enhances angiogenesis. The porosity and microstructure of implants can be used to inhibit bacterial attachment, as well as promote M1 or M2-like macrophage response and cell penetration throughout the entire implant. However, this porosity can range from very small pores for promoting pro-healing macrophage phenotype, to being large enough to allow for cell penetration throughout the implant by MSCs, endothelial cells, and osteoblasts. Future studies must include the consideration of the impact of multiple cell types on the pore size and structure, as one pore size may be beneficial for osteogenesis but may promote a pro-inflammatory response. Finally, the composition of the implant plays a very important role in its ability to kill bacteria, promote osteogenesis, degrade during bone formation, and elicit a pro-healing immune response. Biomaterial design principles that focus on addressing the challenges at the many stages of healing are likely to have a more successful clinical outcome for CMF defect repair.

Author contributions

Marley Dewey contributed to the conceptualization, visualization, and writing – original draft of this manuscript. Brendan Harley contributed to supervision and writing – review & editing of this manuscript.

Conflicts of interest

There are no conflicts of interest to declare.

Acknowledgements

The authors would like to acknowledge the Carl R. Woese Institute for Genomic Biology, and the Chemical and Biomolecular Engineering Department located at the University of Illinois at Urbana-Champaign. The authors would also like to members of the Harley Lab (UIUC) for the assistance editing this review. Research reported in this publication supported by the National Institute of Dental and Craniofacial Research of the National Institutes of Health under Award Number R21 DE026582 as well as funding provided by the NSF Graduate Research Fellowship DGE-1144245 (MD). The content is solely the responsibility of the authors and does not necessarily represent the official views of the NIH or NSF.

References

1 M. Elsalanty and D. Genecov, Bone Grafts in Craniofacial Surgery, *Craniomaxillofac Trauma Reconstr.*, 2009, **2**, 125–134.
2 E. C. Kruijt Spanjer, B. GKP, I. E. M. van Hooijdonk, A. J. W. P. Rosenberg and D. Gawlitta, Taking the endochondral route to craniomaxillofacial bone regeneration: a logical approach?, *J Craniomaxillofac Surg.*, 2017, **45**, 1099–1106.
3 P. R. Brown Baer, J. C. Wenke, S. J. Thomas and C. R. Hale, Investigation of severe craniomaxillofacial battle injuries sustained by u.s. Service members: a case series, *Craniomaxillofac Trauma Reconstr.*, 2012, **5**(4), 243–252.
4 A. D. P. Bankoff. Biomechanical Characteristics of the Bone. in *Human Musculoskeletal Biomechanics*, ed. T. Goswami, InTech, 2012.
5 B. Quang, L. Id, V. Nurcombe, S. M. Cool, C. A. V. Blitterswijk, J. D. Boer, *et al.*, The Components of Bone and What They Can Teach Us about Regeneration, *Materials*, 2018, **11**, 1–16.
6 S. Bose, M. Roy and A. Bandyopadhyay, Recent advances in bone tissue engineering scaffolds, *Trends Biotechnol.*, 2012, **30**, 546–554.
7 J. H. McElhaney, J. L. Fogle, J. W. Melvin, R. R. Haynes, V. L. Roberts and N. M. Alem, Mechanical properties of cranial bone, *J. Biomech.*, 1970, **3**(5), 495–511.
8 H. A. M. Mahinda and O. P. Murty, Variability in thickness of human skull bones and sternum – an autopsy experience, *J. Forensic Med. Toxicol.*, 2009, **26**(2), 26–31.
9 J. H. C. Lee, B. Ondruschka, L. Falland-Cheung, M. Scholze, N. Hammer, D. C. Tong, *et al.*, An Investigation on the Correlation between the Mechanical Properties of Human Skull Bone, Its Geometry, Microarchitectural Properties, and Water Content, *J. Healthc. Eng.*, 2019, **2019**, 6515797.
10 J. M. Aldrige and J. R. Urbaniak, Avascular necrosis of the femoral head: Role of vascularized bone grafts, *Orthop. Clin. N. Am.*, 2007, **38**, 13–22.
11 S. P. Bruder, N. Jaiswal, N. S. Ricalton, J. D. Mosca, K. H. Kraus and S. Kadiyala, Mesenchymal Stem Cells in Osteobiology and Applied Bone Regeneration, *Clin. Orthop. Relat. Res.*, 1996, **355S**, S247–S56.
12 X. Wang, Y. Wang, W. Gou, Q. Lu, J. Peng and S. Lu, Role of mesenchymal stem cells in bone regeneration and fracture repair: a review, *Int Orthop.*, 2013, **37**(12), 2491–2498.
13 E. M. Aarden, P. J. Nijweide and E. H. Burger, Function of osteocytes in bone, *J. Cell. Biochem.*, 1994, **55**(3), 287–299.
14 G. Bergers and S. Song, The role of pericytes in blood-vessel formation and maintenance, *Neuro-Oncology*, 2005, **7**(4), 452–464.
15 T. Tian, T. Zhang, Y. Lin and X. Cai, Vascularization in Craniofacial Bone Tissue Engineering, *J. Dent. Res.*, 2018, **97**, 969–976.
16 S. L. Teitelbaum, Osteoclasts: What Do they Do and How Do They Do It?, *Am. J. Pathol.*, 2007, **170**(2), 427–435.
17 M. Che, R. D. Bonfil, R. Fridman, X. Deng, Z. Dong, J. C. Trindade Filho, *et al.*, Matrix Metalloproteinase Activity and Osteoclasts in Experimental Prostate Cancer Bone Metastasis Tissue, *Am. J. Pathol.*, 2011, **166**, 1173–1186.
18 C. K. Scott and J. A. Hightower, The matrix of endochondral bone differs from the matrix of intramembranous bone, *Calcif. Tissue Int.*, 1991, **49**, 349–354.
19 E. Thompson, A. Matsiko, E. Farrell, D. J. Kelly and F. O'Brien, Recapitulating endochondral ossification: a promising route to *in vivo* bone regeneration, *J. Tissue Eng. Regener. Med.*, 2015, **9**, 889–902.
20 D. Gawlitta, E. Farrell, J. Malda, L. B. Creemers, J. Alblas and W. J. A. Dhert, Modulating Endochondral Ossification of Multipotent Stromal Cells for Bone Regeneration, *Tissue Eng., Part B*, 2010, **16**(4), 385–395.
21 T. A. Wilgus, S. Roy and J. C. McDaniel, Neutrophils and Wound Repair: Positive Actions and Negative Reactions, *Adv. Wound Care*, 2013, **2**(7), 379–388.
22 M. V. Thomas and D. A. Puleo, Infection, inflammation, and bone regeneration: a paradoxical relationship, *J. Dent. Res.*, 2011, **90**(9), 1052–1061.
23 B. N. Brown, B. D. Ratner, S. B. Goodman, S. Amar and S. F. Badylak, Macrophage polarization: an opportunity for improved outcomes in biomaterials and regenerative medicine, *Biomaterials*, 2012, **33**, 3792–3802.
24 K. L. Spiller, D. O. Freytes and G. Vunjak-Novakovic, Macrophages Modulate Engineered Human Tissues for Enhanced Vascularization and Healing, *Ann. Biomed. Eng.*, 2015, **43**, 616–627.
25 K. L. Spiller, S. Nassiri, C. E. Witherel, R. R. Anfang, J. Ng, K. R. Nakazawa, *et al.*, Sequential delivery of immunomodulatory cytokines to facilitate the M1-to-M2 transition of macrophages and enhance vascularization of bone scaffolds, *Biomaterials*, 2015, **37**, 194–207.
26 Y. K. Kim, E. Y. Chen and W. F. Liu, Biomolecular strategies to modulate the macrophage response to implanted materials, *J. Mater. Chem. B*, 2016, **4**, 1600–1609.
27 E. Gibon, L. Y. Lu, K. Nathan and S. B. Goodman, Inflammation, ageing, and bone regeneration, *J. Orthop. Translat.*, 2017, **10**, 28–35.
28 C. M. Runyan and K. S. Gabrick, Biology of bone formation, fracture healing, and distraction osteogenesis, *Journal of Craniofacial Surgery*, 2017, **28**, 1380–1389.

29 R. A. Hortensius and B. A. C. Harley, Naturally derived biomaterials for addressing inflammation in tissue regeneration, *Exp. Biol. Med.*, 2016, **241**, 1015–1024.

30 M. Pogrel, S. Podlesh, J. Anthony and J. Alexander, A comparison of vascularized and nonvascularized bone grafts for reconstruction of mandibular continuity defects, *J Oral Maxillofac. Surg.*, 1997, **55**, 1200–1206.

31 A. Depeyre, S. Touzet-Roumazeille, L. Lauwers, G. Raoul and J. Ferri, Retrospective evaluation of 211 patients with maxillofacial reconstruction using parietal bone graft for implants insertion, *J Craniomaxillofac Surg.*, 2016, **44**, 1162–1169.

32 S. Ghanaati, M. Barbeck, P. Booms, J. Lorenz, C. J. Kirkpatrick and R. A. Sader, Potential lack of "standardized" processing techniques for production of allogeneic and xenogeneic bone blocks for application in humans, *Acta Biomater.*, 2014, **10**, 3557–3562.

33 H. Bae, L. Zhao, L. Kanim, P. Wong, R. Delamarter and E. Dawson, Intervariability and Intravariability of Bone Morphogenetic Proteins in Commercially Available Demineralized Bone Matrix Products, *Spine*, 2006, **31**, 1299–1306.

34 B. Abuzayed, S. Aydin, S. Aydin, B. Kucukyuruk and G. Sanus, Cranioplasty: review of materials and techniques, *J. Neurosci. Rural. Pract.*, 2011, **2**, 162.

35 K. Nelson, T. Fretwurst, A. Stricker, T. Steinberg, M. Wein and A. Spanou, Comparison of four different allogeneic bone grafts for alveolar ridge reconstruction: a preliminary histologic and biochemical analysis, *Oral Surg. Oral Med. Oral Pathol. Oral Radiol.*, 2014, **118**, 424–431.

36 A. M. Tatara, G. L. Koons, E. Watson, T. C. Piepergerdes and S. R. Shah, Biomaterials-aided mandibular reconstruction using *in vivo* bioreactors, *Proc. Natl. Acad. Sci. U. S. A.*, 2019, **116**, 6954–6963.

37 N. Broggini, D. D. Bosshardt, S. S. Jensen, M. M. Bornstein, C.-c Wang and D. Buser. *Bone healing around nanocrystalline hydroxyapatite, deproteinized bovine bone mineral , biphasic calcium phosphate , and autogenous bone in mandibular bone defects*, 2014, pp. 1478–1487.

38 W. Wang and K. W. K. Yeung, Bone grafts and biomaterials substitutes for bone defect repair: a review, *Bioact. Mater.*, 2017, **2**, 224–247.

39 T. Gredes, F. Kunath, T. Gedrange and C. Kunert-Keil, Bone Regeneration after Treatment with Covering Materials Composed of Flax Fibers and Biodegradable Plastics: A Histological Study in Rats, *BioMed Res. Int.*, 2016, **2016**, 1–8.

40 S. Radzi, G. Cowin and B. Schmutz, Metal artifacts from titanium and steel screws in CT, 1.5T and 3T MR images of the tibial Pilon: a quantitative assessment in 3D, *Quant. Imaging. Med. Surg.*, 2014, **4**, 163–172.

41 T. Terjesen, A. Nordby and V. Arnulf, Bone atrophy after plate fixation: compute tomography of femoral shaft fractures, *Acta Orthop. Scand.*, 1985, **56**, 416–418.

42 T. E. Crist, P. J. Mathew, E. L. Plotsker, A. C. Sevilla and S. R. Thaller, Biomaterials in Craniomaxillofacial Reconstruction: Past, Present, and Future, *J. Craniofac. Surg.*, 2021, **32**(2), 535–540.

43 K. Alvarez and H. Nakajima, Metallic scaffolds for bone regeneration, *Materials*, 2009, **2**, 790–832.

44 A. I. M. Greer, V. Goriainov, J. Kanczler, C. R. M. Black, L.-A. Turner, R. M. D. Meek, *et al.*, Nanopatterned Titanium Implants Accelerate Bone Formation *In Vivo*, *ACS Appl. Mater. Interfaces*, 2020, **12**(30), 33541–33549.

45 N. Safari, N. Golafshan, M. Kharaziha, M. Reza Toroghinejad, L. Utomo, J. Malda, *et al.*, Stable and Antibacterial Magnesium–Graphene Nanocomposite-Based Implants for Bone Repair, *ACS Biomater. Sci. Eng.*, 2020, **6**(11), 6253–6262.

46 H. S. Han, I. Jun, H. K. Seok, K. S. Lee, K. Lee, F. Witte, *et al.*, Biodegradable Magnesium Alloys Promote Angio-Osteogenesis to Enhance Bone Repair, *Adv. Sci.*, 2020, **7**(15), 1–12.

47 Y. Zhuang, Q. Liu, G. Jia, H. Li, G. Yuan and H. Yu, A Biomimetic Zinc Alloy Scaffold Coated with Brushite for Enhanced Cranial Bone Regeneration, *ACS Biomater. Sci. Eng.*, 2021, **7**(3), 893–903.

48 M. Bohner, Physical and chemical aspects of calcium phosphates used in spinal surgery, *Eur. Spine J.*, 2001, **10**, S114–S21.

49 S. Scaglione, R. Quarto and P. Giannoni, Stem cells and tissue scaffolds for bone repair, *Cell. Response Biomater.*, 2008, 291–312.

50 V. Athanasiou, D. Papachristou, A. Panagopoulos, A. Saridis, C. Scopa and P. Megas, Histological comparison of autograft, allograft-DBM, xenograft, and synthetic grafts in a trabecular bone defect: an experimental study in rabbits, *Med. Sci. Monit.*, 2010, **16**, BR24–31.

51 A. Hoppe, N. S. Güldal and A. R. Boccaccini, A review of the biological response to ionic dissolution products from bioactive glasses and glass–ceramics, *Biomaterials*, 2011, **32**(11), 2757–2774.

52 X. Zheng, X. Zhang, Y. Wang, Y. Liu, Y. Pan, Y. Li, *et al.*, Hypoxia-mimicking 3D bioglass-nanoclay scaffolds promote endogenous bone regeneration, *Bioact. Mater.*, 2021, **6**(10), 3485–3495.

53 T. Wu, H. Shi, Y. Liang, T. Lu, Z. Lin and J. Ye, Improving osteogenesis of calcium phosphate bone cement by incorporating with manganese doped β-tricalcium phosphate, *Mater. Sci. Eng., C*, 2020, **109**, 110481.

54 R. Eivazzadeh-Keihan, K. K. Chenab, R. Taheri-Ledari, J. Mosafer, S. M. Hashemi, A. Mokhtarzadeh, *et al.*, Recent advances in the application of mesoporous silica-based nanomaterials for bone tissue engineering, *Mater. Sci. Eng., C*, 2020, **107**, 110267.

55 H. Kanniyappan, M. Venkatesan, J. Panji, M. Ramasamy and V. Muthuvijayan, Evaluating the inherent osteogenic and angiogenic potential of mesoporous silica nanoparticles to augment vascularized bone tissue formation, *Microporous Mesoporous Mater.*, 2021, **311**, 110687.

56 X. Liu and P. Ma, Polymeric Scaffolds for Bone Tissue Engineering, *Ann. Biomed. Eng.*, 2004, **32**, 477–486.

57 K. Athanasiou, G. Niederauer and C. M. Agrawal, Sterilization, toxicity, biocompatibility and clinical applications of polylactic acid/polyglycolic acid copolymers, *Biomaterials*, 1996, **17**, 93–102.

58 K. Athanasiou, C. Agrawal, F. Barber and S. Burkhart, Orthopaedic applications for PLA-PGA biodegradable polymers, *Arthroscopy*, 1998, **14**, 726–737.

59 Q. Yao, J. G. L. Cosme, T. Xu, J. M. Miszuk, P. H. S. Picciani, H. Fong, *et al.*, Three dimensional electrospun PCL/PLA blend nanofibrous scaffolds with significantly improved stem cells osteogenic differentiation and cranial bone formation, *Biomaterials*, 2017, **115**, 115–127.

60 B. Zhang, L. Wang, P. Song, X. Pei, H. Sun, L. Wu, *et al.*, 3D printed bone tissue regenerative PLA/HA scaffolds with comprehensive performance optimizations, *Mater. Des.*, 2021, **201**, 109490.

61 D. Zhang, O. J. George, K. M. Petersen, A. C. Jimenez-Vergara, M. S. Hahn and M. A. Grunlan, A bioactive "self-fitting" shape memory polymer scaffold with potential to treat cranio-maxillo facial bone defects, *Acta Biomater.*, 2014, **10**, 4597–4605.

62 M. R. Pfau, K. G. McKinzey, A. A. Roth, L. M. Graul, D. J. Maitland and M. A. Grunlan, Shape memory polymer (SMP) scaffolds with improved self-fitting properties, *J. Mater. Chem. B*, 2021, **9**, 3826–3837.

63 S. Caliari, W. Grier, D. Weisgerber, Z. Mahmassani, M. Boppart and B. Harley, Collagen scaffolds incorporating coincident gradations of instructive structural and biochemical cues for osteotendinous junction engineering, *Adv. Healthcare Mater.*, 2015, **4**, 831–837.

64 A. Gaspar, L. Moldovan, D. Constantin, A. M. Stanciuc, P. M. Sarbu Boeti and I. C. Efrimescu, Collagen-based scaffolds for skin tissue engineering, *J Med Life.*, 2011, **4**(2), 172–177.

65 A. Getgood, S. Kew, R. Brooks, H. Aberman, T. Simon, A. Lynn, *et al.*, Evaluation of early-stage osteochondral defect repair using a biphasic scaffold based on a collagen–glycosaminoglycan biopolymer in a caprine model, *The Knee*, 2012, **19**, 422–430.

66 S. R. Caliari and B. A. C. Harley, Structural and biochemical modification of a collagen scaffold to selectively enhance MSC tenogenic, chondrogenic, and osteogenic differentiation, *Adv. Healthcare Mater.*, 2014, **3**, 1086–1096.

67 C. M. Murphy and F. J. O'Brien, Understanding the effect of mean pore size on cell activity in collagen-glycosaminoglycan scaffolds, *Cell Adhes. Migr.*, 2010, **4**, 377–381.

68 R. A. Hortensius and B. A. C. Harley, The use of bioinspired alterations in the glycosaminoglycan content of collagen-GAG scaffolds to regulate cell activity, *Biomaterials*, 2013, **34**, 7645–7652.

69 B. P. Kanungo, E. Silva, K. V. Vliet and L. J. Gibson, Characterization of mineralized collagen-glycosaminoglycan scaffolds for bone regeneration, *Acta Biomater.*, 2008, **4**, 490–503.

70 B. A. Harley, A. K. Lynn, Z. Wissner-Gross, W. Bonfield, I. V. Yannas and L. J. Gibson, Design of a multiphase osteochondral scaffold. II. Fabrication of a mineralized collagen–glycosaminoglycan scaffold, *J. Biomed. Mater. Res., Part A*, 2010, **92**, 1066–1077.

71 A. Al-Munajjed, J. Gleeson and F. O'Brien, Development of a collagen calcium-phosphate scaffold as a novel bone graft substitute, *Stud. Health Technol. Inform.*, 2008, **133**, 11–20.

72 F. J. O'Brien, B. A. Harley, I. V. Yannas and L. J. Gibson, The effect of pore size on cell adhesion in collagen-GAG scaffolds, *Biomaterials*, 2005, **26**, 433–441.

73 F. J. O'Brien, B. A. Harley, I. V. Yannas and L. Gibson, Influence of freezing rate on pore structure in freeze-dried collagen-GAG scaffolds, *Biomaterials*, 2004, **25**, 1077–1086.

74 W. K. Grier, H. Sun, R. A. Chang, M. D. Ramsey and B. A. C. Harley, The influence of cyclic tensile strain on multi-compartment collagen-GAG scaffolds for tendon-bone junction repair, *Connect. Tissue Res.*, 2019, **60**, 530–543.

75 A. S. Tiffany, D. L. Gray, T. J. Woods, K. Subedi and B. A. C. Harley, The inclusion of zinc into mineralized collagen scaffolds for craniofacial bone repair applications, *Acta Biomater.*, 2019, **93**, 86–96.

76 A. S. Tiffany, M. J. Dewey and B. A. C. Harley, Sequential sequestrations increase the incorporation and retention of multiple growth factors in mineralized collagen scaffolds, *RSC Adv.*, 2020, **10**(45), 26982–26996.

77 E. Song, S. Yeon Kim, T. Chun, H.-J. Byun and Y. M. Lee, Collagen scaffolds derived from a marine source and their biocompatibility, *Biomaterials*, 2006, **27**(15), 2951–2961.

78 D. W. Weisgerber, K. Erning, C. L. Flanagan, S. J. Hollister and B. A. C. Harley, Evaluation of multi-scale mineralized collagen–polycaprolactone composites for bone tissue engineering, *J. Mech. Behav. Biomed. Mater.*, 2016, **61**, 318–327.

79 M. J. Dewey, E. M. Johnson, D. W. Weisgerber, M. B. Wheeler and B. A. C. Harley, Shape-fitting collagen–PLA composite promotes osteogenic differentiation of porcine adipose stem cells, *J. Mech. Behav. Biomed. Mater.*, 2019, **95**, 21–33.

80 B. Hoyer, A. Bernhardt, S. Heinemann, I. Stachel, M. Meyer and M. Gelinsky, Biomimetically mineralized salmon collagen scaffolds for application in bone tissue engineering, *Biomacromolecules*, 2012, **13**, 1059–1066.

81 T. H. Qazi and J. A. Burdick, Granular hydrogels for endogenous tissue repair, *Biomaterials and Biosystems*, 2021, **1**, 100008.

82 X. Zhang, Y. He, P. Huang, G. Jiang, M. Zhang, F. Yu, *et al.*, A novel mineralized high strength hydrogel for enhancing cell adhesion and promoting skull bone regeneration *in situ*, *Composites, Part B*, 2020, **197**, 108183.

83 F. Obregon-Miano, A. Fathi, C. Rathsam, I. Sandoval, F. Deheghani and A. Spahr, Injectable porcine bone demineralized and digested extracellular matrix—PEGDA

hydrogel blend for bone regeneration, *J. Mater. Sci.: Mater. Med.*, 2020, **31**(2), 21.

84 D. B. Lima, M. A. A. de Souza, G. G. de Lima, E. P. Ferreira Souto, H. M. L. Oliveira, M. V. L. Fook, *et al.*, Injectable bone substitute based on chitosan with polyethylene glycol polymeric solution and biphasic calcium phosphate microspheres, *Carbohydr. Polym.*, 2020, **245**, 116575.

85 M. J. Dewey, A. V. Nosatov, K. Subedi, R. Shah, A. Jakus and B. A. C. Harley, Inclusion of a 3D-printed Hyperelastic Bone mesh improves mechanical and osteogenic performance of a mineralized collagen scaffold, *Acta Biomater.*, 2021, **121**, 224–236.

86 D. Weisgerber, D. Milner, H. Lopez-Lake, M. Rubessa, S. Lotti, K. Polkoff, *et al.*, A mineralized collagen-polycaprolactone composite promotes healing of a porcine mandibular ramus defect, *Tissue Eng., Part A*, 2017, **0**, 1–12.

87 S. Gomez, M. D. Vlad, J. Lopez and E. Fernandez, Design and properties of 3D scaffolds for bone tissue engineering, *Acta Biomater.*, 2016, **42**, 341–350.

88 M. Zhang, R. Lin, X. Wang, J. Xue, C. Deng, C. Feng, *et al.*, 3D printing of Haversian bone–mimicking scaffolds for multicellular delivery in bone regeneration, *Sci. Adv.*, 2020, **6**(12), eaaz6725.

89 J. A. Killion, S. Kehoe, L. M. Geever, D. M. Devine, E. Sheehan, D. Boyd, *et al.*, Hydrogel/bioactive glass composites for bone regeneration applications: Synthesis and characterisation, *Mater. Sci. Eng., C*, 2013, **33**(7), 4203–4212.

90 A. Haleem and M. Javaid, Role of CT and MRI in the design and development of orthopaedic model using additive manufacturing, *J. Clin. Orthop. Trauma.*, 2018, **9**(3), 213–217.

91 Q. Zhou, S. Lyu, A. Bertrand, A. Hu, C. Chan, X. Ren, *et al.*, Stiffness of Nanoparticulate Mineralized Collagen Scaffolds Triggers Osteogenesis *via* Mechanotransduction and Canonical Wnt Signaling, *Macromol Biosci.*, 2021, **21**(3), e2000370.

92 M. J. Cross, G. J. Roger and J. Spycher, Cementless fixation techniques and challenges in joint replacement. in *Joint Replacement Technology*, ed. P. A. Revell, Woodhead Publishing Limited, Cambridge, UK 2 edn, 2014,pp. 186–211.

93 L. N. Nail, D. Zhang, J. L. Reinhard and M. A. Grunlan, Fabrication of a Bioactive, PCL-based "Self-fitting" Shape Memory Polymer Scaffold, *J. Visualized Exp.*, 2015, **104**, e52981.

94 Yu-H. Huang, A. E. Jakus, S. W. Jordan, Z. Dumanian, K. Parker, L. Zhao, *et al.*, Three-Dimensionally Printed Hyperelastic Bone Scaffolds Accelerate Bone Regeneration in Critical-Size Calvarial Bone Defects, *Plast. Reconstr. Surg.*, 2019, 1397–1407.

95 A. E. Jakus, A. L. Rutz, S. W. Jordan, A. Kannan, S. M. Mitchell, C. Yun, *et al.*, Hyperelastic "bone": a highly versatile, growth factor–free, osteoregenerative, scalable, and surgically friendly biomaterial, *Sci. Transl. Med.*, 2016, **8**(358), 358ra127.

96 R. Prabhoo, R. Chaddha, R. Iyer, A. Mehra, J. Ahdal and R. Jain, Overview of methicillin resistant *Staphylococcus aureus* mediated bone and joint infections in India, *Orthop. Rev.*, 2019, **11**(2), 8070.

97 J. Josse, F. Velard and S. Gangloff, *Staphylococcus aureus vs.* Osteoblast: Relationship and Consequences in Osteomyelitis, *Front. Cell. Infect. Microbiol.*, 2015, **5**(85), 1–17.

98 A. Trampuz and W. Zimmerli, Diagnosis and treatment of implant-associated septic arthritis and osteomyelitis, *Curr. Infect. Dis. Rep.*, 2008, **10**, 394–403.

99 F. L. Luthje, S. A. Blirup-Plum, N. S. Moller, P. M. H. Heegaard, H. E. Jensen, K. Kirketerp-Moller, *et al.*, The host response to bacterial bone infection involves a local upregulation of several acute phase proteins, *Immunobiology*, 2020, **225**(3), 1–10.

100 T. Bjarnsholt, The role of bacterial biofilms in chronic infections, *APMIS, Suppl.*, 2013, (136), 1–51.

101 S. W. Lee, K. S. Phillips, H. Gu, M. Kazemzadeh-Narbat and D. Ren, How microbes read the map: Effects of implant topography on bacterial adhesion and biofilm formation, *Biomaterials*, 2021, **268**, 120595.

102 M. N. Dickson, E. I. Liang, L. A. Rodriguez, N. Vollereaux and A. F. Yee, Nanopatterned polymer surfaces with bactericidal properties, *Biointerphases*, 2015, **10**(2), 021010.

103 J. J. Swartjes, P. K. Sharma, T. G. van Kooten, H. C. van der Mei, M. Mahmoudi, H. J. Busscher, *et al.*, Current Developments in Antimicrobial Surface Coatings for Biomedical Applications, *Curr. Med. Chem.*, 2015, **22**(18), 2116–2129.

104 R. E. Hancock and H. G. Sahl, Antimicrobial and host-defense peptides as new anti-infective therapeutic strategies, *Nat. Biotechnol.*, 2006, **24**(12), 1551–1557.

105 J. Chen, X. Shi, Y. Zhu, Y. Chen, M. Gao, H. Gao, *et al.*, On-demand storage and release of antimicrobial peptides using Pandora's box-like nanotubes gated with a bacterial infection-responsive polymer, *Theranostics*, 2020, **10**(1), 109–122.

106 Y. He, Y. Jin, X. Ying, Q. Wu, S. Yao, Y. Li, *et al.*, Development of an antimicrobial peptide-loaded mineralized collagen bone scaffold for infective bone defect repair, *Regener. Biomater.*, 2020, **7**(5), 515–525.

107 Y. Li, R. Na, X. Wang, H. Liu, L. Zhao, X. Sun, *et al.*, Fabrication of Antimicrobial Peptide-Loaded PLGA/Chitosan Composite Microspheres for Long-Acting Bacterial Resistance, *Molecules*, 2017, **22**(10), 1637.

108 L. Polo, N. Gómez-Cerezo, A. García-Fernández, E. Aznar, J. L. Vivancos, D. Arcos, *et al.*, Mesoporous Bioactive Glasses Equipped with Stimuli-Responsive Molecular Gates for Controlled Delivery of Levofloxacin against Bacteria, *Chem.–Eur. J.*, 2018, **24**(71), 18944–18951.

109 C. T. Johnson, M. C. P. Sok, K. E. Martin, P. P. Kalelkar, J. D. Caplin, E. A. Botchwey, *et al.*, Lysostaphin and BMP-2 co-delivery reduces *S. aureus* infection and regenerates critical-sized segmental bone defects, *Sci. Adv.*, 2019, **5**(5), eaaw1228.

110 J. K. Kumar, Lysostaphin: an antistaphylococcal agent, *Appl. Microbiol. Biotechnol.*, 2008, **80**(4), 555–561.

111 J. Shen, P. Gao, S. Han, R. Y. T. Kao, S. Wu, X. Liu, *et al.*, A tailored positively-charged hydrophobic surface reduces the risk of implant associated infections, *Acta Biomater.*, 2020, **114**, 421–430.

112 V. Luque-Agudo, D. Romero-Guzmán, M. Fernández-Grajera, M. L. González-Martín and A. M. Gallardo-Moreno, Aging of Solvent-Casting PLA-Mg Hydrophobic Films: Impact on Bacterial Adhesion and Viability, *Coatings*, 2019, **9**(12), 814.

113 Y. N. Slavin, J. Asnis, U. O. Häfeli and H. Bach, Metal nanoparticles: understanding the mechanisms behind antibacterial activity, *J Nanobiotechnology*, 2017, **15**(1), 65.

114 I. A. J. van Hengel, N. E. Putra, M. W. A. M. Tierolf, M. Minneboo, A. C. Fluit, L. E. Fratila-Apachitei, *et al.*, Biofunctionalization of selective laser melted porous titanium using silver and zinc nanoparticles to prevent infections by antibiotic-resistant bacteria, *Acta Biomater.*, 2020, **107**, 325–337.

115 R. Gyawali and S. A. Ibrahim, Natural products as antimicrobial agents, *Food Control*, 2014, **46**, 412–429.

116 S. I. Kobata, L. E. M. Teixeira, S. O. A. Fernandes, A. A. G. Faraco, P. V. T. Vidigal and I. Dd Araújo, Prevention of bone infection after open fracture using a chitosan with ciprofloxacin implant in animal model, *Acta Cir. Bras.*, 2020, **35**(8), e202000803.

117 L. R. Boles, R. Awais, K. E. Beenken, M. S. Smeltzer, W. O. Haggard and A. J. Jessica, Local Delivery of Amikacin and Vancomycin from Chitosan Sponges Prevent Polymicrobial Implant-Associated Biofilm, *Mil. Med.*, 2018, **183**(1), 459–465.

118 G. H. Frydman, D. Olaleye, D. Annamalai, K. Layne, I. Yang, H. M. A. Kaafarani, *et al.*, Manuka honey microneedles for enhanced wound healing and the prevention and/or treatment of Methicillin-resistant *Staphylococcus aureus* (MRSA) surgical site infection, *Sci. Rep.*, 2020, **10**(13229), 1–11.

119 K. R. Hixon, T. Lu, M. N. Carletta, S. H. McBride-Gagyi, B. E. Janowiak and S. A. Sell, A preliminary *in vitro* evaluation of the bioactive potential of cryogel scaffolds incorporated with Manuka honey for the treatment of chronic bone infections, *J. Biomed. Mater. Res., Part B*, 2018, **106**(5), 1918–1933.

120 R. F. El-Kased, R. I. Amer, D. Attia and M. M. Elmazar, Honey-based hydrogel: *in vitro* and comparative *in vivo* evaluation for burn wound healing, *Sci. Rep.*, 2017, **7**(1), 9692, available from: http://europepmc.org/abstract/MED/28851905, https://doi.org/10.1038/s41598-017-08771-8, https://europepmc.org/articles/PMC5575255, https://europepmc.org/articles/PMC5575255?pdf=render.

121 E. Sussman, M. Halpin, J. Muster, R. Moon and B. Ratner, Porous Implants Modulate Healing and Induce Shifts in Local Macrophage Polarization in the Foreign Body Reaction, *Ann. Biomed. Eng.*, 2014, **42**, 1508–1516.

122 L. R. Madden, D. J. Mortisen, E. M. Sussman, S. K. Dupras, J. A. Fugate and J. L. Cuy, Proangiogenic scaffolds as functional templates for cardiac tissue engineering, *Proc. Natl. Acad. Sci. U. S. A.*, 2010, **107**, 15211–15216.

123 W. F. Liu, T. Wang, P. Nguyen, F. Y. McWhorter and T. Chung, Modulation of macrophage phenotype by cell shape, *Proc. Natl. Acad. Sci. U. S. A.*, 2013, **110**, 17253–17258.

124 K. S. Stankevich, A. Gudima, V. D. Filimonov, H. Klüter, E. M. Mamontova, S. I. Tverdokhlebov, *et al.*, Surface modification of biomaterials based on high-molecular polylactic acid and their effect on inflammatory reactions of primary human monocyte-derived macrophages: perspective for personalized therapy, *Mater. Sci. Eng., C*, 2015, **51**, 117–126.

125 G. Vallés, P. González-Melendi, J. L. González-Carrasco, L. Saldaña, E. Sánchez-Sabaté, L. Munuera, *et al.*, Differential inflammatory macrophage response to rutile and titanium particles, *Biomaterials*, 2006, **27**(30), 5199–5211.

126 J. Suganuma and H. Alexander, Biological response of intramedullary bone to poly-L-lactic acid, *J. Appl. Biomater.*, 1993, **4**(1), 13–27.

127 O. Veiseh, J. C. Doloff, M. Ma, A. J. Vegas, H. H. Tam, A. R. Bader, *et al.*, Size- and shape-dependent foreign body immune response to materials implanted in rodents and non-human primates, *Nat. Mater.*, 2015, **14**(6), 643–651.

128 N. L. Davison, F. Barrère-de Groot and D. W. Grijpma, Degradation of Biomaterials, in *Tissue Engineering*, ed. C. A. V. Blitterswijk and J. D. Boer, Academic Press. United States, 2 edn, 2015. pp. 177–215.

129 D. Hachim, S. T. LoPresti, C. C. Yates and B. N. Brown, Shifts in macrophage phenotype at the biomaterial interface *via* IL-4 eluting coatings are associated with improved implant integration, *Biomaterials*, 2017, **112**, 95–107.

130 M. Luo, F. Zhao, L. Liu, Z. Yang, T. Tian, X. Chen, *et al.*, IFN-γ/SrBG composite scaffolds promote osteogenesis by sequential regulation of macrophages from M1 to M2, *J. Mater. Chem. B*, 2021, **9**(7), 1867–1876.

131 C. Yin, Q. Zhao, W. Li, Z. Zhao, J. Wang, T. Deng, *et al.*, Biomimetic anti-inflammatory nano-capsule serves as a cytokine blocker and M2 polarization inducer for bone tissue repair, *Acta Biomater.*, 2020, **102**, 416–426.

132 A. Amini, C. Laurencin and S. Nukavarapu, Bone Tissue Engineering: Recent Advances and Challenges, *Crit. Rev. Biomed. Eng.*, 2012, **40**(5), 363–408.

133 X. Wu, K. Walsh, B. L. Hoff and G. Camci-Unal, Mineralization of Biomaterials for Bone Tissue Engineering, *Bioengineering*, 2020, **7**(4), 132.

134 X. Ren, V. Tu, D. Bischoff, D. Weisgerber, M. Lewis, D. Yamaguchi, *et al.*, Nanoparticulate mineralized collagen scaffolds induce *in vivo* bone regeneration independent of progenitor cell loading or exogenous growth factor stimulation, *Biomaterials*, 2016, **89**, 67–78.

135 J. J. Bergh, Y. Xu and M. C. Farach-Carson, Osteoprotegerin expression and secretion are regulated by calcium influx through the L-type voltage-sensitive calcium channel, *Endocrinology*, 2004, **145**(1), 426–436.

136 X. Ren, Q. Zhou, D. Foulad, A. S. Tiffany, M. J. Dewey, D. Bischoff, *et al.*, Osteoprotegerin reduces osteoclast resorption activity without affecting osteogenesis on nanoparticulate mineralized collagen scaffolds, *Sci. Adv.*, 2019, **5**, 1–12.

137 X. Ren, Q. Zhou, D. Foulad, M. J. Dewey, D. Bischoff, T. A. Miller, *et al.*, Nanoparticulate mineralized collagen glycosaminoglycan materials directly and indirectly inhibit osteoclastogenesis and osteoclast activation, *J. Tissue Eng. Regener. Med.*, 2019, **13**(5), 823–834.

138 M. J. Dewey, A. V. Nosatov, K. Subedi and B. Harley, Anisotropic mineralized collagen scaffolds accelerate osteogenic response in a glycosaminoglycan-dependent fashion, *RSC Adv.*, 2020, **10**(26), 15629–15641.

139 Y. Liu, H. Yang, K. Otaka, H. Takatsuki and A. Sakanishi, Effects of vascular endothelial growth factor (VEGF) and chondroitin sulfate A on human monocytic THP-1 cell migration, *Colloids Surf., B*, 2005, **43**(3), 216–220.

140 C. Lambert, M. Mathy-Hartert, J.-E. Dubuc, E. Montell, J. Vergés, C. Munaut, *et al.*, Characterization of synovial angiogenesis in osteoarthritis patients and its modulation by chondroitin sulfate, *Arthritis Res. Ther.*, 2012, **14**(2), R58.

141 M. Vallières and P. Souich, Modulation of inflammation by chondroitin sulfate, *Osteoarthritis Cartilage*, 2010, **18**, 18–23.

142 A. G. García, J. Vergés and E. Montell, Immunomodulatory and anti-inflammatory effects of chondroitin sulphate, *J. Cell. Mol. Med.*, 2009, **13**, 1451–1463.

143 A. Irie, M. Takami, H. Kubo, N. Sekino-Suzuki, K. Kasahara and Y. Sanai, Heparin enhances osteoclastic bone resorption by inhibiting osteoprotegerin activity, *Bone*, 2007, **41**(2), 165–174.

144 S. Mousavi, M. Moradi, T. Khorshidahmad and M. Motamedi, Anti-Inflammatory Effects of Heparin and Its Derivatives : A Systematic Review, *Adv. Pharmacol. Sci.*, 2015, **2015**, 1–14.

145 J. K. Leach and J. Whitehead, Materials-Directed Differentiation of Mesenchymal Stem Cells for Tissue Engineering and Regeneration, *ACS Biomater. Sci. Eng.*, 2018, **4**(4), 1115–1127.

146 T. Yeung, P. C. Georges, L. A. Flanagan, B. Marg, M. Ortiz, M. Funaki, *et al.*, Effects of substrate stiffness on cell morphology, cytoskeletal structure, and adhesion, *Cell Motil. Cytoskeleton*, 2005, **60**(1), 24–34.

147 H. Chen, Y. Qian, Y. Xia, G. Chen, Y. Dai, N. Li, *et al.*, Enhanced Osteogenesis of ADSCs by the Synergistic Effect of Aligned Fibers Containing Collagen I, *ACS Appl. Mater. Interfaces*, 2016, **8**(43), 29289–29297.

148 A. Klaumünzer, H. Leemhuis, K. Schmidt-Bleek, S. Schreivogel, A. Woloszyk, G. Korus, *et al.*, A biomaterial with a channel-like pore architecture induces endochondral healing of bone defects, *Nat. Commun.*, 2018, **9**, 4430.

149 A. Marrella, T. Y. Lee, D. H. Lee, S. Karuthedom, D. Syla, A. Chawla, *et al.*, Engineering vascularized and innervated bone biomaterials for improved skeletal tissue regeneration, *Mater. Today*, 2018, **21**(4), 362–376.

150 C. C. Hung, A. Chaya, K. Liu, K. Verdelis and C. Sfeir, The role of magnesium ions in bone regeneration involves the canonical Wnt signaling pathway, *Acta Biomater.*, 2019, **98**, 246–255.

151 A. K. Barui, S. K. Nethi, S. Haque, P. Basuthakur and C. R. Patra, Recent Development of Metal Nanoparticles for Angiogenesis Study and Their Therapeutic Applications, *ACS Appl. Bio Mater.*, 2019, **2**(12), 5492–5511.

152 A. K. González-Palomo, K. Saldaña-Villanueva, J. D. Cortés-García, J. C. Fernández-Macias, K. B. Méndez-Rodríguez and P. Maldonado, Effect of silver nanoparticles (AgNPs) exposure on microRNA expression and global DNA methylation in endothelial cells EA.hy926, *Environ. Toxicol. Pharmacol.*, 2021, **81**, 103543.

153 S. K. Nethi, S. Mukherjee, V. Veeriah, A. K. Barui, S. Chatterjee and C. R. Patra, Bioconjugated gold nanoparticles accelerate the growth of new blood vessels through redox signaling, *Chem. Commun.*, 2014, **50**(92), 14367–14370.

154 M. A. Woodruff and D. W. Hutmacher, The return of a forgotten polymer – polycaprolactone in the 21st century, *Prog. Polym. Sci.*, 2010, **35**, 1217–1256.

155 S. Deshayes and A. M. Kasko, Polymeric biomaterials with engineered degradation, *J. Polym. Sci., Part A: Polym. Chem.*, 2013, **51**(17), 3531–3566.

156 J. Zhang, L. Wang, W. Zhang, M. Zhang and Z.-P. Luo, Synchronization of calcium sulphate cement degradation and new bone formation is improved by external mechanical regulation, *J. Orthop. Res.*, 2015, **33**(5), 685–691.

157 L. E. Rustom, T. Boudou, B. W. Nemke, Y. Lu, D. J. Hoelzle, M. D. Markel, *et al.*, Multiscale Porosity Directs Bone Regeneration in Biphasic Calcium Phosphate Scaffolds, *ACS Biomater. Sci. Eng.*, 2017, **3**(11), 2768–2778.

158 R. Wu, Y. Li, M. Shen, X. Yang, L. Zhang, X. Ke, *et al.*, Bone tissue regeneration: the role of finely tuned pore architecture of bioactive scaffolds before clinical translation, *Bioact. Mater.*, 2021, **6**(5), 1242–1254.

Fernando P.S. Guastaldi
Bhushan Mahadik *Editors*

Bone Tissue Engineering

Bench to Bedside Using 3D Printing

Springer

Editors
Fernando P. S. Guastaldi
Boston, MA, USA

Bhushan Mahadik
College Park, MD, USA

ISBN 978-3-030-92013-5 ISBN 978-3-030-92014-2 (eBook)
https://doi.org/10.1007/978-3-030-92014-2

This Springer imprint is published by the registered company Springer Nature Switzerland AG
The registered company address is: Gewerbestrasse 11, 6330 Cham, Switzerland

Preface

Since the advent of tissue engineering in the 1980s, bone has been a primary target for tissue regeneration. This field has seen some fantastic developments to assist patients in need of bone-related clinical interventions, but we are still far away from regenerating fully functional bone tissue. The hope and promise of tissue engineering to rebuild this complex organ has been mirrored on the rapidly evolving field of 3D printing that allows us to fabricate complex structures in a systematic manner. With this in mind, we are pleased to introduce the first book that offers a comprehensive overview of the state of the art, current challenges, and strategies to reconstruct large bone defects employing 3D printing technology.

This book is intended to be a concise handbook regarding 3D printing for bone tissue engineering, covering different 3D printing technologies that can be applied for bioengineering bone, the aspects of basic bone biology critical for clinical translation, the progress made in the field of regenerative medicine for the reconstruction of large bone defects, and tissue engineering platforms to investigate the bone niche microenvironment. Commercialization, legal and regulatory considerations are also discussed to help translate bone tissue engineered constructs and 3D printing-based products to the marketplace and the clinic. Although significant progress has been achieved over the past 2–3 decades, challenges that still exist and approaches to address them are discussed. This book can be read as a whole entity that provides an overall perspective on 3D printing in bone tissue engineering. Readers can also refer to select chapters that cater to specific topics without needing information from the preceding chapters.

This book is intended for scientists and researchers interested in learning more about the state-of-the-art progress made employing different 3D printing technologies for bone tissue engineering. This includes but is not limited to students (undergraduate, graduate) and postdoctoral researchers, professors who can assign this as a handbook for quick background studies to capture salient features of this field, scientists across academia and industry as a reference guide for their research, clinicians (dentistry and medicine), and professionals in the biomedical engineering, medical devices, tissue engineering, and biomaterial fields.

We wish to thank all the distinguished and expert contributors for their enthusiastic participation in this endeavor. We contacted the authors during the particularly challenging times of the COVID-19 global pandemic in 2020 and were heartened by their support. It was with utmost kindness and grace that they accepted our invitation and agreed to multiple chapter revisions, despite what we can only describe as being in unprecedented times. Finally, we sincerely thank the Springer staff for their support, patience, understanding, and encouragement while we compiled this book over almost 2 years. Their contribution to this academic venture is extremely appreciated.

We understand that the fields of tissue engineering and 3D printing are advancing rapidly with exciting new discoveries made regularly. It will be our sincere goal to keep the contents updated to reflect latest advances in the following editions of this book. We hope that this book serves as a guide and perhaps a source of inspiration to continue pushing scientific boundaries every day.

Boston, MA, USA — Fernando P. S. Guastaldi
College Park, MD, USA — Bhushan Mahadik
October 1, 2021

Contents

Biomaterial Design Principles to Accelerate Bone Tissue Engineering

Marley J. Dewey and Brendan A. C. Harley

1 Bone Injury and Repair

1.1 Types of Injuries

In this chapter we will focus on the methods available to repair bone defects, focusing specifically on those that require surgical intervention to repair. These types of injuries include craniomaxillofacial defects, long bone segmental defects, and spinal fusion. Craniomaxillofacial injuries are classified as defects to the skull or jaw. These can arise from high energy impact trauma, cleft palate birth defects, and oral cancer [1–4]. Similar to craniofacial defects, long bone defects can arise from trauma, tumor resection, and nonunion [5]. Spinal fusions involve surgery to place an implant within the space of vertebrae to eliminate motion. Spinal fusion is used to treat spinal fractures, deformities, and instability [6]. Craniomaxillofacial and other segmental bone defects are particularly challenging due to their irregular size and shape and the amount of missing bone tissue. These types of defects are usually critical in size, in which the section of bone missing is too large for the body to regenerate. Biomaterial implants need to be optimized to repair these defects in

M. J. Dewey
Department of Materials Science and Engineering, University of Illinois at Urbana-Champaign, Urbana, IL, USA

B. A. C. Harley (✉)
Department of Materials Science and Engineering, University of Illinois at Urbana-Champaign, Urbana, IL, USA

Department Chemical and Biomolecular Engineering, University of Illinois at Urbana-Champaign, Urbana, IL, USA

Carl R. Woese Institute for Genomic Biology, University of Illinois at Urbana-Champaign, Urbana, IL, USA
e-mail: bharley@illinois.edu

F. P. S. Guastaldi, B. Mahadik (eds.), *Bone Tissue Engineering*,
https://doi.org/10.1007/978-3-030-92014-2_3

order to promote new bone formation as well as avoid implant inflammation and infection, which is common in large missing portions of bone [7].

1.2 The Healing Cascade

In normal homeostasis, uninjured bone is constantly being remodeled. Bone is resorbed by a resident population of osteoclasts and new bone synthesized by resident osteoblasts in a precise balance [8]. This process is facilitated by mechanosensitive processes that respond to bone deformation and provide the stimuli to alternately produce or resorb more bone and maintain the mechanical support of soft tissues. In order to design materials for bone regeneration, the coupling of osteoclasts and osteoblasts needs to be recognized and kept in balance in order to avoid complete resorption of implants or unnecessary and often painful excess bone formation.

Bones of the body heal via either endochondral ossification or intramembranous ossification. The two methods have similar healing endpoints; however, endochondral ossification involves a cartilage intermediate and is typically the process involved in long bone healing, while intramembranous ossification does not involve cartilage formation and is the process by which the flat bones of the skull and jaw heal [9–11]. Bone healing occurs in stages; for segmental defects this can take several months to complete. Firstly, a hematoma is formed and inflammation occurs, bringing in various immune cells and bone progenitor cells. During a typical immune response, undifferentiated macrophages would migrate to the wound site and polarize to the M1 phenotype in the early stages (1–3 days) [12, 13]. This phenotype is considered "pro-inflammatory" and is responsible for the initial removal of any cellular debris and host defense mechanisms. After 3 days and continuing for weeks, M1 macrophages should shift in phenotype to the "anti-inflammatory" M2 macrophages, which remodel the tissue and deposit matrix [12, 13]. In the case of a biomaterial implant, M1 macrophages are responsible for graft resorption and rejection, while M2 macrophages are accountable for graft acceptance by the body. The M1 to M2 transition over the course of a week is important in avoiding persistent or chronic inflammation, which can lead to a foreign body reaction and ultimate need for a secondary surgery [14, 15]. The way in which mesenchymal stem cells and immune cells differentiate can be partly attributed to the pore size of implant materials. Pore size can determine how vessels form, how cells infiltrate and differentiate, whether inflammation or infection will occur, and how macrophages polarize [16], and suggest exciting opportunities to engineer biomaterial design to not only promote osteogenic activity but also modulate the immune and inflammatory cascade after injury. Ultimately, these macrophages and the topography of an implant can determine the success early-on in the wound healing process. After inflammation, cartilage formation occurs in long bones and vascular growth occurs within the cartilage [17]. Next, chondrocytes die off and cartilage is resorbed in order for mesenchymal stem cells to differentiate into osteoblasts. In intramembranous

ossification this cartilage step is skipped and mesenchymal stem cells differentiate and mature, while blood vessels are formed during the primary bone formation step [17]. Finally, secondary bone formation occurs and bone is remodeled by osteoclasts in order to create the anisotropic nature of bone [17].

2 Current State of the Art in Repair: Bone Grafting

The gold standard to repair many bone defects is through the use of bone grafting. Autografts, allografts, and xenografts fall under this category. Grafting typically uses human or mammalian bone in order to repair a patient's defect. Here, we will discuss the various types of bone grafting used to repair critical-sized bone defects.

2.1 Autografts

Autografts involve using bone from a secondary site in the patient's own body in order to regenerate bone missing in the wound site. Multiple types of bone can be used, such as cancellous, cortical, vascularized bone, and bone marrow [18]. One of the most commonly used grafting sites is the iliac crest, a part of the pelvis. From this, one can take segments of cortical or cancellous bone for a variety of sized defects [18]. For craniofacial and long bone defects, bone can be repaired using iliac crest autografts with 70–95% success rates [19]. For repairing small bone defects, a chin graft or a retromolar graft from the area behind the third molar can be used [18, 20]. Other less commonly used grafts include tibial, rib, scapula, fascia, sternum, pedicled clavicle, and pedicled temporal bone [18, 20]. Unfortunately, defects longer than 6 cm have much lower success rates, and 50% failure rates have been reported for long bone defects [5, 19]. Drawbacks to removing the iliac crest include iliac fractures, pain, vascular and nerve injury, and persistent hematomas [18]. A popular cortical bone graft in craniofacial reconstruction is the calvarial graft, due to its slow resorption rate [18]. However, the thickness of this graft is highly variable and important vessels exist near this area of bone which should avoid being damaged. Removing this bone from a patient can cause deformity at the removal site and fracture of the bone. Although drawbacks limit the use of this graft, typically success rates are high. A study on 211 patients with calvarial grafts found that after 10–11 months there was a 95% chance of implant integration which matched with other findings of high success rates [21]. However, there was a high number of secondary procedures due to bone resorption, which was attributed to the need for a large amount of bone to be used as an autograft, and patient health differences [21].

General advantages of autografts include retention of some osteogenic cells and an immune response that does not persist [18]. Drawbacks to these methods include limited availability of bone and high chance of morbidity of bone at the site where the graft was taken from [18].

2.2 *Allografts*

Allografts use bone typically from a deceased donor, with cellular materials removed before implantation [18]. Repair using allografts involves demineralized bone matrix as particles, blocks, or sheets. This removal involves thorough treatment to eliminate any pathogenic agents and genetic material in order to minimize disease transmission. Removal of these pathogenic agents is necessary; however, in order to promote bone repair the extracellular matrix and collagen should not be removed [22]. A main drawback to using allografts is that the osteogenic properties of these vary from one commercial supplier to another due to the treatment and cleaning process [22, 23]. In general there can be high infection rates even after sterilization due to foreign substances remaining in the graft, but more vigorous removal of graft material ultimately leads to the bone being less likely to promote regeneration [20]. A study investigated four different allogenic bone matrices found that in all of the samples there were cells and cell residues before implantation, which in canine studies has shown to illicit an immune response [24]. Although cleaning of the bone matrix can be difficult, the implant survival rate is more than 95%, and new bone formation at 30% after 6 months [24].

2.3 *Xenografts*

Xenografts use bone from a mammalian source, typically bovine or porcine derived. Similar to allografts, infectious materials and cells must be removed from the bone prior to implantation. One study examined the structure of five different suppliers' allograft and xenograft materials and discovered that three of the five bone substitutes failed to meet criteria the manufacturers had promised [22]. This was due to the grafts either containing cellular content, loss of lamellar bone structure, or no collagen present [22]. Xenografts do not repair as well as autografts, they have a slower integration with host bone than autografts, and disease transmission such as bovine spongiform encephalopathy is a concern [25, 26].

Given some of the disadvantages associated with existing autograft, allograft, or xenograft procedures, biomaterials for regenerative repair of bone have become increasingly popular conceptually. One advantage of biomaterial approaches is the ability to potentially generate shelf-stable implants in order to remove considerations regarding time between graft harvest and use.

3 Implant Design to Optimize Bone Regeneration

In the next sections we will discuss design strategies for biomaterial implants as alternatives to graft materials. We will discuss the properties of an such an implant, specifically what criteria need to be met in order to successfully regenerate bone.

These criteria include selecting biocompatible materials that can promote bone and vessel formation, creating designs that can mimic the mechanical properties of bone and provide mechanical stability, altering the pore size and orientation through fabrication methods, and controlling degradation of the material. We will also discuss the variety of material classes available for implantation and the ways in which these can be modified to fit bone repair applications. These include polymers, both synthetic and natural, metals, and ceramics, focusing on their outcomes *in vitro* and *in vivo* and their specific advantages and disadvantages. We also highlight the method of 3D printing, which can be used to add functionality in shape, porosity, and release of biomolecules and cells. Finally, we will discuss cellular and growth factor additions to scaffold materials in order to improve bone formation.

4 Biomaterial Implants for Bone Regeneration

Biomaterial design criteria have to meet a wide range of benchmarks along with considerations of ease of surgical use and economic feasibility [20]. These criteria include biocompatibility, mechanical properties, pore size and orientation, and degradation and bioresorption. Presently, no biomaterial exists that meets all the following criteria. However, in Fig. 1 we outline a series of design criteria for biomaterial implants to address challenges in bone repair.

4.1 Biocompatibility

A biomaterial used for bone regeneration must be able to recruit cells from the surrounding tissues and provide nutrition and signals to support the vitality of these cells. There are many facets of biocompatibility related to bone repair; an implant

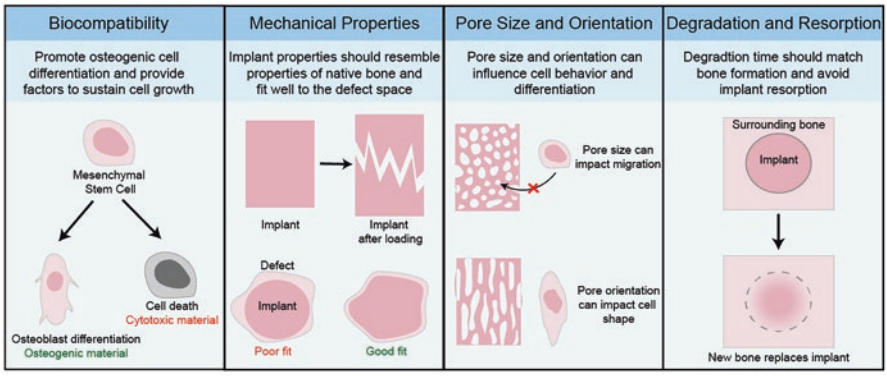

Fig. 1 Biomaterial properties for enhancing bone repair

should promote osteoconduction, osteoinduction, and osteogenesis. Cells should adhere to the biomaterial implant, enhance mineral formation and deposition of new bone, also known as osteoconduction. A variety of signals need to be provided to cells; ones that include osteoinduction, the promotion of differentiation of stem cells to mature bone cells. In addition to this, avoiding signals that may cause persistent inflammation, macrophage fusion, and foreign body response will lead to a more successful outcome. An implant also needs to promote osteogenesis, such that it attracts new cells from the surrounding tissue to the implant site to remodel and form bone [18]. A final important aspect of biocompatibility is the need for the implant to promote the formation of blood vessels. This should occur within a few weeks of biomaterial implantation to support nutrient transport and cell viability and induce osteoconduction, osteoinduction, and osteogenesis [27].

4.2 Mechanical Properties

Ideally, the mechanical properties of an implant would match the properties of the host bone at implant. However, this is extraordinarily difficult to meet, for a number of reasons. Firstly, bone is a multi-scale composite, with cortical and cancellous bone having vastly different mechanical properties. The Young's modulus and compressive strength of cortical and cancellous bone can vary from a Young's Modulus of 0.1–20 GPa (Table 1) [27]. Further, these properties reflect the mechanical properties of fully mature bone tissue with integrated vasculature; conceptually, biomaterials for bone repair may be much better suited having an environment designed for diffusive transport of nutrients and oxygen to facilitate cell penetration, proliferation, and extensive remodeling required to form new bone. An additional challenge with designing modulus-matched biomaterials is that many bone defects, notably craniomaxillofacial defects, are typically irregular in size and shape. This makes for difficulties shaping the implant to fit the defect site, which can affect mechanical stability. In general, the mechanical stability of the implant can also affect the healing outcome, as micromotion can directly inhibit osseointegration, so a mechanically stable implant is desired [28, 29].

4.3 Pore Size and Orientation

Typically, porous implants are used for bone regeneration as they provide a template for rapid cell infiltration and metabolic support via diffusion. The pore size of an implant greatly influences the cell behavior and ultimate success or failure of the surgery. There exists debate about optimal pore size to promote bone regeneration, as multiple cell types are involved in the healing process. *Bose et al.* suggest that pore sizes should be at least 100 μm in diameter for diffusion of nutrients and

oxygen, and pore sizes ranging from 200 to 350 μm are optimal for the in-growth of bone tissue [27, 30]. As for macrophages, a pore size of 34 μm promotes a more pro-inflammatory phenotype [31], yet other sources have suggested that 30–40 μm pores promote a pro-healing phenotype and avoid a foreign body response [32, 33]. Bone is an anisotropic tissue, and thus the pore orientation is increasingly considered as an important design parameter to consider in implant design. Recent work have begun to describe the use of aligned pores to promote bone formation by structural guidance cues to increase blood vessel ingrowth, accelerate cellular migration, and guide osteogenic cell differentiation [34–36].

4.4 Degradation and Bioresorption

In order to fully repair bone, the implant must be able to degrade while still providing signals for the patient's own cells to form new bone. This degradation time should match the time it takes for new bone to be formed in order to replace the implant. Different bones regenerate over different times, which are summarized in Table 1 [27, 37]. If a material degrades too quickly, then there will not be enough material to continue to promote host bone regeneration and mechanically support the implant site [38]. Conversely, if a material degrades too slowly, remaining material will block new bone formation, as seen in Fig. 2. Any degradation to a material leads to a loss of mechanical properties, and if this is controlled correctly, then load transfer from the implant to the host bone will occur [40–42]. Therefore, to create a biomaterial that can successfully regenerate bone, the design must have a controlled material degradation rate.

Table 1 Properties of a biomaterial implant for bone regeneration

Property	Optimal range
Mechanics	
Young's modulus	Cortical: 15–20 GPa; Cancellous: 0.1–2 GPa
Compressive strength	Cortical: 100–200 MPa; Cancellous: 2–20 MPa
Pore size and orientation	
Nutrient diffusion	At least 100 μm in diameter
Bone in-growth	200–350 μm in diameter
Immune cells	30–40 μm in diameter to avoid foreign body reaction
Cell migration	Anisotropic pores promote faster migration
Direction vessel growth	Anisotropic pores promote aligned vessels
Degradation and bioresorption	
Spinal fusion	9 months or more
Craniomaxillofacial	3–6 months
Long bone	5–7 months

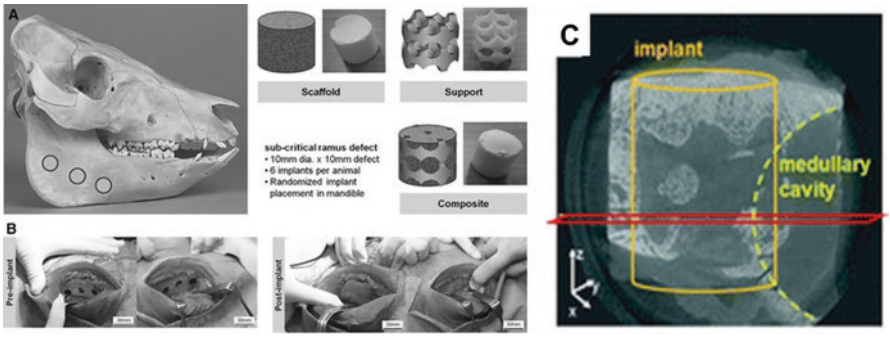

Fig. 2 PCL and mineralized collagen implant in porcine ramus defect model. (**a**) Schematic of subcritical ramus defect locations along with 10 mm diameter, 10 mm thick mineralized collagen (CGCaP) scaffold, PCL support, and mineralized collagen-PCL composite implants. (**b**) Specimen locations were randomized on each side of the mandible and within each porcine animal model. Representative images of the subcritical ramus defect preimplant and postimplant. *CGCaP* collagen-glycosaminoglycan calcium phosphate, *PCL* polycaprolactone. (**c**) Representative μCT data showing partial penetration of the implant into the medullary cavity. Light regions represent bone mineral and dark regions represent no mineral or PCL still present within the implant. (Image adapted from [39])

5 Scaffolds: Mechanical, Chemical, and Biological Properties

Scaffolds are commonly thought of as an initial template that provides a constellation of structural, compositional, and mechanical signals to potentially accelerate the process of bone regeneration. Common scaffold materials include polymers, ceramics and hydroxyapatite materials, metals, and collagen-based implants. Some advantages of scaffolds are their ability to be tailored to specific patients and avoid the cellular material cleaning process that bone-derived graft materials require. When deciding between allograft or xenograft materials versus synthetic or other scaffold materials, sources have found a variety of results, ranging from better to worse healing outcomes [43, 44]. Alternatively, autograft materials have shown favorable healing and mechanics over scaffold materials, but autografts drawbacks outweigh their benefits [45–47]. Scaffolds do not require a secondary surgery as autografts do and do not suffer from a limited supply of material. If materials have the same or very similar healing outcomes, it is then favorable to use scaffolds over grafts due to their advantages over bone-derived materials. Scaffolds can also be patient-tailored, such as 3D printed or cast in the particular size and shape of the defect. In addition to this, patient-derived cells can be added to affect the outcome, and growth factors can be added to target specific cell functions to improve osteogenesis and angiogenesis [48]. A summary of clinically available implant materials and their outcomes *in vitro* and *in vivo* can be found in Table 2.

Table 2 Commercially available bone implant materials and their healing outcomes *in vivo* and *in vitro*

Implant type	Outcome	References
Demineralized bone matrix		
Grafton Putty (Synthes, USA)	Good handling, complete spinal fusion in all animals, promotes new and mature bone formation in critical-sized defects	[49, 50]
DBX® Putty (Synthes, USA)	Good handling, half of animals tested had spinal fusion, promotes mature bone formation in critical-sized defects	[49, 50]
AlloMatrix Injectable Putty (Wright Medical Technology Inc, USA)	Fair handling, no spinal fusion occurred, limited bone formation in critical-sized defects	[49, 50]
Regenafil (Regneration Technologies Inc, USA)	Fair handling, limited bone formation in critical-sized defects	[50]
Dynagraft (Gensci Regeneration Sciences Inc, Canada)	Good handling, limited bone formation in critical-sized defects	[50]
Lubboc® bovine xenograft	Better bone healing than Grafton, Ceraform, and Osteoset, induced activation of host bone cells	[25, 51]
Biocoral® coral xenograft (Biocoral Inc, USA)	Superior healing compared to ceramic and hydroxyapatite materials in alveolar bone defects, bone formation within 2 weeks post-operation	[51, 52]
Metals		
Plasma sprayed titanium	Good osteoblast adhesion, proliferation, and differentiation, better early-stage healing conditions	[53]
Sand-blasted, acid-etched titanium	Similar results to plasma sprayed, but worse early-stage healing, osseointegration in dental implants	[53, 54]
Actipore™ porous NiTi (Biorthex, Canada)	High bone ingrowth stimulation, performs similarly to traditional titanium implants, complete bone bridging after 12 months	[55, 56]
Ceramics and hydroxyapatites		
ZrO_2 ceramic (Ziterion GmbH, Germany)	Osseointegration with surface-modification comparable to titanium for dental implants	[54]
Ceraform® hydroxyapatite substitute (Teknimed, France)	Newly formed bone was restricted to graft area, osteoconductive properties, poor healing compared to Osteoset and Lubboc	[25, 51]
SRS® carbonated apatite bone cement (Norian Coporation, USA)	Extraosseous extrusion of bone cement, remodels into natural bone but occurs slowly in the distal radius repair	[51, 57]
Osteoset® calcium sulfate substitute (Synthes, USA)	Osteoconductive properties, no evidence of osteoinductive activity, superior to Ceraform and similar to demineralized bone substitute	[25, 51]
BonAlive® bioactive glass (Vivoxid, Finland)	Longer time for material to biodegrade, form and remodel bone compared to autografts, cortical bone grew in thickness over time	[51, 58]

(continued)

Table 2 (continued)

Implant type	Outcome	References
Biosilicate®/Bioglass® 45S5	Biosilicate has higher osteogenic activity and higher amounts of fully formed bone compared to bioglass, biosilicate does not have the potential to be cytotoxic/genotoxic that bioglass does	[51, 59]
ProOsteon 500R (Interpore International, USA)	Better option than collagraft for spine and lower extremity applications with need for more mechanical support, slow resorption of material	[60]
Polymers		
Poly(DL-lactide) mesh plate (Synthes, USA)	Fair handling, poor healing response, and scant new bone formation in critical-sized defects, mesh was replaced by fibrous tissue	[50]
Cortoss® Bisphenol-a-glycidyl dimethacrylate resin (Orthovita, USA)	Minimal formation of apatite layer *in vitro*, less leachable toxic monomer than compared to PMMA cements, possibly cytotoxicity	[51, 61]
Collagen scaffolds		
Healos® type I collagen/ hydroxyapatite matrix (DuPuy Spine Inc, USA)	Osteoconductive and osteoinductive, not recommended for interbody cages for spinal fusion, similar healing to autografts in posterolateral fusions	[51, 62]
Collagraft® collagen/ hydroxyapatite/tricalcium phosphate composite (Zimmer and Collagen Corporation, USA)	Greatest ingrowth of bone compared to ProOsteon and demineralized bone xenograft, rapid resorption	[51, 60]

5.1 Synthetic Polymeric Scaffolds

Synthetic polymers are man-made polymers, commonly seen in household items such as plastics, rubbers, and glue. Synthetic polymers for tissue engineering must be biodegradable and biocompatible while avoiding a negative immune reaction and matching biomaterial properties as closely as possible. Much of this can be accomplished through modifying the polymer itself, and careful consideration must be made when examining the degradation byproducts. An advantage to using synthetic polymers are their large scale reproducibility with controlled mechanical properties, degradation, and structure [63].

A wide variety of techniques can be used to create porous scaffold architectures. These include casting and forming based methods such as solvent-casting, particulate leaching, and gas-foaming. Solvent-casting and particulate leaching techniques are simple, involving a water-soluble salt homogenously distributed through the polymer solution. The polymer is cast into shape and the solvent is removed by evaporation or lyophilization, while the salt is leached out by soaking in water to create an open-porous polymer [63]. Gas-foaming removes the need for organic solvents and instead carbon dioxide is used to create a polymer foam. In brief, the solid polymer is exposed to high pressure carbon dioxide, which is then saturated into the polymer, and then gas bubbles expand to create a closed-pore structure [63].

Increasingly, more exotic methods are also being used such as electrospinning, 3D printing, and thermally induced phase separation. Electrospinning can create polymeric fibers on the nanoscale by applying a high voltage and an electric field to a polymer solution on a collector which can be rotated in order to create various alignments of fibers. This method can easily create fine fibers; however, it can be difficult to create small diameter fibers with biocompatible materials, and creating 3D scaffolds and complex pore geometry still remain a challenge [64]. Scaffolds with nanofibers have shown to improve stem cell differentiation toward the osteogenic lineage and can be beneficial to bone repair due to their ability to mimic the type I collagen alignment in bone [64]. In addition, sacrificial nanofibers can be added to poly(caprolactone) fibers in order to align cells, direct the formation of extracellular matrix, increase tensile properties, and control the release of collagenase and growth factors to increase cellularity [65, 66]. 3D printing can be used to fabricate scaffolds with complex architectures; however, small pore sizes are difficult to achieve. Various methods of 3D printing exist, such as laser sintering, photopolymerization printing, and extrusion printing, which will be expanded on in Sect. 6. Thermally induced phase separation can be used to fabricate biodegradable 3D polymers by first dissolving the polymer in a solvent at high temperature and then phase separation occurs by lowering the temperature and final sublimation to create a porous polymer [63]. Ultimately, another advantage to this is the ability to modify the surface of polymers in order to alter cell interactions with the polymer surface.

The most extensively used polymeric material in cranioplasty is poly(methylmethacrylate) (PMMA). This is an easy to shape and lightweight material and does not radiate heat [20]. Polyethylene has also been used due to its porous nature, and if infections occur antibiotics can be used instead of complete removal of the implant [67–69]. Polyethylene glycol (PEG) hydrogels have been investigated for new bone formation due to their ability to slowly release growth factors. However, unlike other polymers, PEG hydrogels added to a mandibular defect saw no difference in new bone formation and did not have an osteogenic effect [70].

Other commonly used polymers in bone tissue engineering are poly(lactic acid) (PLA), poly(lactide-co-glycolide) (PLGA), 3-hydroxybutyric acid (PHB), and poly(caprolactone) (PCL) [39, 71–74]. PLA degradation byproducts are expected to be nontoxic; however, degradation by hydrolysis releases lactic acid and in a zygomatic fracture fixation, PLA caused swelling at the implant site in 60% of patients [75–77]. Some polymers used for bone regeneration, such as lactic acid based polymers, have caused fibrous tissue formation and foreign body responses [78]. Alternatively, PHB scaffolds have been shown to be highly compatible with osteoblasts and can induce ectopic, or abnormal, bone formation [79]. Benefits to using PLA, PCL, and PLGA are their FDA approval for certain use in humans and degradation rates can be tailored by altering the molecular weight and composition. However, drawbacks include poor mechanical properties compared to bone and the possibility of rejection by the body and foreign body responses. Mechanical properties can be tailored based on polymer crystallinity, and growth factor release can be added to these polymer systems, in the future these two factors can possibly eliminate the drawbacks of polymer systems.

5.2 *Natural Polymeric Scaffolds*

Natural polymers, such as collagen scaffolds, have been used extensively as an alternative material to heal bone defects. A common variant of the collagen scaffolds contains type I collagen, glycosaminoglycans such as chondroitin-6-sulfate, and acid [80–84]. These materials are homogenized together to create a liquid suspension and then freeze dried in order to create an open-porous structure that enables cell migration and penetration through the material. Other natural polymers, such as chitosan have also been investigated [51]. Chitosan is also highly biodegradable and biocompatible and can differentiate osteoblasts *in vitro*. However, this material is not osteoconductive and has caused allergic reactions [51]. Typically, collagen scaffolds without any mineral supplements are used to regenerate tendon or skin due to their poor ability to heal bone [51, 85–88]. A benefit to using collagen scaffolds is their tunable pore size and orientation, which can be achieved by using molds with different thermal properties in which scaffolds are lyophilized and altering the freezing rate and temperature [30, 81, 86, 89, 90]. Issues with using naturally derived polymers are that they may contain pathogenic impurities and produce a negative immune response, and it is harder to control the mechanical properties, however, they typically support cell adhesion and proliferation [63].

Variants of collagen materials can be made in order to heal different tissues in the body, such as scaffolds containing calcium phosphate mineral in order to repair bone defects [83, 84, 91–95]. These scaffolds have been shown to be more appropriate for bone repair, due to their biocompatible, biodegradable, and bone formation-inducing behaviors. This has been demonstrated by mineral formation *in vitro* and bone formation *in vivo* without additional osteogenic supplements and inhibiting bone resorption [96–98]. Disadvantages to these scaffolds are their weak mechanical properties, due to their extremely porous nature. However, mechanical properties can be altered by adding additional materials during freeze drying, such as polymer reinforcements like PLA and PCL [99, 100]. These reinforcements can be 3D printed in various architectures, and one design in particular has been used to achieve shape-fitting in order to avoid micromotion upon implantation [99]. Mineralized collagen scaffolds combined with laser-sintered PCL have demonstrated a 6000-fold increase in Young's Modulus compared to scaffolds alone [100], and in a porcine ramus defect model this composite material had greater bone repair than the scaffold or PCL construct alone [74]. Other elements such as allogenic tissues, growth factors, and other minerals can easily be added to these scaffolds by mixing into the suspension step before lyophilization [101–103]. Specifically, the amniotic membrane derived from placentas has been added to collagen and mineralized collagen scaffolds in order to control the wound healing process and avoid inflammation while increasing bone formation [101, 102, 104].

Increasingly, the delivery or endogenous production of growth factors has been investigated in collagen scaffolds. For example, PDGF-BB and IGF-I delivery was shown to influence migration into these scaffolds [87]. Additionally, current research is focused on sequestering and tethering these growth factors to collagen scaffolds

or using micelles as controlled release mechanisms. Other minerals, most notably zinc, have been investigated to improve osteogenesis, and various glycosaminoglycans can be used in order to alter the mineral formation [103, 105]. Additionally, pore sizes and orientations have been investigated in collagen and mineralized collagen scaffolds in order to drive a response to increase viability of tenocytes or increase bone mineral formation [30, 34, 80, 81, 89, 105–107]. Finally, the important interaction of mesenchymal stem cells and osteoclasts has been investigated in these scaffolds, and research has shown that mineralized collagen scaffolds inhibit osteoclastogenesis by releasing osteoprotegerin [97, 98]. These scaffolds have the vast potential to be expanded on in order to achieve the criteria for bone regeneration. Whether it be altering the pore size and orientation, adding other minerals, glycoproteins, or tissue matrices, or adding growth factors and specific cell types, there is much work to be done to advance these mineralized scaffolds.

Commercially available natural polymers, such as the mineralized collagen material Healos®, have found comparable results in some cases to autografts. Healos® soaked in bone marrow aspirate without any exogenous factors demonstrated similar healing to autografts in posterolateral fusions. However, this same material performed poorly for interbody cages in spinal surgeries, due to volume of material and mechanical properties [62]. Thus, improvements still need to be made in order to increase mechanical strength and stability to repair other bone defects.

5.3 Metallic Scaffolds

Metal scaffold use is limited due to their ability to conduct heat, difficulty to shape during implantation, and radio-opacity [20]. Metal screws or plates can interfere with imaging of the defect site and monitoring the patient's health. In addition to this, metals risk corrosion and fatigue over time, the stress shielding effect can cause bone atrophy, and it is difficult to have a metal implant fit well to the implant site without micromotion [75, 108, 109].

Titanium has been the metal of choice for use in large bone defects and like most metals is hard to shape, but resists infection and will be accepted by the body [20]. In order for titanium and its alloys to be successful in bone repair, typically surface modifications are necessary to promote cell attachment and integration. Various methods to do this include mechanical grinding or polishing the surface, physical vapor deposition, acid etching, or chemical vapor deposition [110].

Other metallic materials used include stainless steel 316 L, cobalt based alloys, porous tantalum, and magnesium. Disadvantages include their lack of biocompatibility, wear, and corrosion can release ions and particles that can lead to inflammation. Stainless steel specifically has a very high stiffness, so high in fact that it can lead to bone resorption due to the mismatch in mechanical properties of bone and the implant [111]. Unfortunately, in order to make porous metallic materials to mimic the natural structure of bone, these usually end up too weak to be a viable option [110]. Porous tantalum, however, has a high porosity, a Young's modulus

comparable to bone, and has been shown to be biocompatible in animal models [110]. Magnesium and its alloys are fully bioresorbable, have mechanical properties similar to native bone, do not induce a negative immune response, and promote bone growth [110]. Concerns of using magnesium are the hazards associated with rapid dissolution of the magnesium in the body. An alloy of titanium, nickel-titanium (Nitinol) can be used as a shape-memory material and has demonstrated biocompatibility and mechanical properties similar to bone. Studies have shown that nitinol is more biocompatible than stainless steel [110]; however, release of nickel ions poses a toxicity and allergy concern.

In vivo studies comparing metal implants have shown that porous nitinol had increased osseointegration compared to titanium alloys [112]. Of the metals available, nitinol and resorbable magnesium are the most promising due to low stiffness [111]. In general metals suffer from stress shielding, corrosion, and biofilm formation, all of which contribute to their concerns with clinical use. Overall, the use of metals is mostly desired for permanent implants at sites that need high mechanical loading or as fixation devices.

5.4 Ceramic and Hydroxyapatite Scaffolds

Hydroxyapatite and bioactive ceramics are the most widely used alternative to autografts and allografts in the preclinical and clinical settings [113]. One very common ceramic used in healing of bone defects are bioactive glasses. Bioglass is comprised of sodium, silicone, magnesium, potassium, oxygen, phosphorous, and calcium [114]. As far as healing results, a study examined two different versions of compressed hydroxyapatite scaffolds versus a xenogenic graft in mandibular defects and found no healing differences between the groups at the end of the study [43]. Another study used bioreactors to create bone over time in an autograft and a commercially available bioceramic and found that both were able to create mineral tissue, but autograft materials had more mature bone and mechanical properties more similar to bone [45]. In general, calcium phosphate or hydroxyapatite bone substitutes have less osteogenic potential than autografts [25, 45, 46]. However, hydroxyapatite coatings have different effects than used as a bulk material, and coatings promote cellular contact of osteoblasts [115]. Bioceramics can have various degradation times in the body, an example being hydroxyapatite and tricalcium phosphate (TCP), with hydroxyapatite scaffolds degrading after 2–5 years and TCP degrading within 1 year [113]. This degradation time impacts healing outcomes, as a clinical trial involving hydroxyapatite scaffolds demonstrated that after 15 months the scaffold was still present, and another study claimed the scaffolds were still present even after 7 years [37, 116]. In contrast to this, a β-TCP scaffold deposited new bone after 9 months but complete regeneration of the fibula was only found in 1 out of 14 patients [117].

An alternative to bioactive ceramics is bioinert nanoceramics. These include implants made of titanium, alumina, and zirconia [118]. These ceramics are not

designed to regenerate the host bone due to their inert nature; however, they have high fracture toughness and mechanical strength at the implant site [118]. Titanium implants can be modified with Ca^{2+} ions in order to create titanium oxide, which helps prevent corrosion and absorb proteins to the surface of the material [118]. In addition, other treatments to titanium can be made to modify the surface to promote integration with the host bone, such as etching or sand blasting [118]. Similar to other bioinert ceramics, alumina does not promote osseointegration due to its inert nature, and thus coatings must be added, or the surface topography must be altered to enhance protein adhesion. Zirconia-yttria ceramics are often used as bone fillers due to the ability to prevent biofilms [119]. However, the drawback to these is their inert nature, and these ceramics will still remain in the body instead of host bone.

Bioceramics are thought of to be one of the preferred scaffolds for bone repair due to biocompatibility and high mechanical properties. However, due to the nature of ceramics, these materials can be brittle and only so much of the material can be resorbed by the body [115]. In order to achieve a biomaterial implant it is likely that a composite material will be needed that balances mechanical, chemical, and biological properties. Composite materials have already been discussed as better choices for tissue engineering applications, as no implant material exists today that includes all of the implant criteria [63].

6 3D Printing as a Tool to Improve Bone Formation

3D printing, also known as additive manufacturing, has been used to create materials in our daily lives as well as materials for the medical field. Various methods for creating designs and architectures that would be difficult or impossible using other methods can be accomplished by 3D printing. 3D printing involves a user-created design, which the printer then creates layer-by-layer. This approach overcomes the issue of irregular size and shape defects for bone repair, as the design can be tailored to fit a patient-specific shape. A patient's defect can be scanned using MRI or CT technology to map the defect space, and subsequently this scan can be converted and used on a 3D printer to fill the defect space [120–122]. 3D printing methods can fall into four categories: extrusion, polymerization, laser sintering, and direct writing [123]. The extrusion method takes a solid polymer, extrudes the material through a nozzle by the application of heat and pressure, and allows the print to cool to room temperature to solidify. Fused deposition printing is an example of extrusion-based printing. Polymerization printing uses a bed of resin that is polymerized by lasers, for example, stereolithography [124]. Selective laser sintering involves a bed of polymer powder in which lasers are used to fuse the powder together to create a 3D print. Finally, direct writing uses powder and a regular inkjet printing head with binder, in which the binder is printed onto the loose powder. This method can be used to create interconnected pores; however, intensive optimization of the printing process for a new material is required [122, 123].

An expanding range of materials can be 3D printed, such as the polymers polyethylene, polylactic acid, and polycaprolactone, as well as ceramic materials such as TCP and HA. In addition to these, metals can also be 3D printed; however, this is less common, with an example being bioactive titanium scaffolds fabricated by inkjet 3D printing [125]. In this case, titanium was printed and then fired in order to strengthen the material, and the bioactivity was modified by the deposition of hydroxyapatite on the surface [125]. 3D printing can be used to make these materials very porous; however, a drawback to this is that the mechanical strength is lowered, which limits their use in load-bearing applications. Not only can 3D printing offer a better implant fit, it also can be modified with growth factors and cells. Growth factors and cells for use in 3D printing, also known as bioprinting, will be elaborated on in the following sections, but can be incorporated into polymers such as hydrogels for encapsulating cells and the slow release of biomolecules.

A further opportunity for 3D printing is the addition of these 3D prints to existing materials for bone regeneration. As it can be difficult to create load-bearing 3D prints with very porous structures, an alternative is to use 3D prints as mechanical supports and other biomaterials as the bioactive matrix. This has been demonstrated with mineralized collagen scaffolds and 3D printed polymers. The mineralized collagen acts as the bioactive and osteogenic matrix, and the polymer 3D print acts to give mechanical strength to the whole material in order to better match the mechanical properties of bone [29, 39, 74, 100]. This method provides another way to consider 3D printing; besides using the method to create a scaffold, 3D printing can be used to fabricate pieces of the overall structure. Overall, 3D printing is an extremely useful tool for creating patient-specific implants as it can create complex and porous shapes using a wide variety of materials and methods while also including the option of printing cells and growth factors. More research needs to be performed on optimizing 3D printed materials, as well as investigating combinations of 3D printing with other factors to create composites which can leverage multiple benefits.

7 Stem Cells: Biology and the Application for Tissue Regeneration

7.1 Stem Cells for Bone Repair

Multiple cell types are involved in the bone formation and remodeling process, such as osteocytes, osteoblasts, osteoclasts, and immune cells. Osteocytes maintain the existing bone and are considered mature bone cells. Osteoblasts are responsible for bone growth and can differentiate into osteocytes, while osteoclasts are responsible for bone resorption. Finally, immune cells are important for the healing outcome of the wound, as they clean the area and can lead to fibrous tissue formation or a foreign body reaction if a negative immune response persists [14, 15].

Based on literature, the addition of stem cells to implant materials before implantation has shown more success than implants without stem cells [126, 127]. Overall, the use of autologous or allogenic cells in combination with scaffolds for long bone repair has resulted in positive healing outcomes [5]. The most commonly used stem cells used are embryonic stem cells (ESCs), induced pluripotent stem cells (iPSCs), and adult mesenchymal stem cells (MSCs). ESCs are derived from embryos through *in vitro* fertilization, can proliferate infinitely, and can differentiate into any cell type. iPSCs are somatic cells that have been genetically reprogrammed to express the pluripotent properties similar to ESCs. Finally, MSCs, which are the most commonly used cell type for bone repair, are isolated from the liver, fetal blood, bone marrow, and umbilical cord. All of these cell types are able to differentiate into various bone cells, making them important in the bone repair process.

Typically, cells are cultured to a pre-confluent state and then added to graft materials and cultured for a short period of time before implantation into the defect space. Alternatively, cells can be injected directly into defects, which has shown some promise *in vivo* [128]. Cell death upon transplantation is a drawback; however, MSCs can be contained in spheroids to improve survival, and these have been injected into damaged tissues to promote repair [129, 130]. Interestingly, these have also shown that restricting MSC migration out of these spheroids can enhance the osteogenic potential of these spheroids [130]. In general, adult stem cells have a wide variety of results which can be due to the differences in donors, such as where the cells were sampled, the age of the donor, and life habits [115].

Of the mesenchymal stem cells used, bone marrow stromal cells are favored and can differentiate into almost all mesoderm-derived cell types, including cartilage, bone, hematopoietic stroma, tenocytes, and skeletal muscle cells [115]. However, loss of differentiation properties toward the adipocyte or chondrocyte lineage has been observed after multiple cell passages [131]. Pericytes have also been investigated and are derived from the peripheral blood. These cells are positive for some osteogenic markers and can differentiate along the osteogenic, chondrogenic, and adipogenic lineage [115]. Another commonly used cell line are adipose-derived stem cells, due to their being easy to acquire, abundant, and can differentiate into adipocytes, chondrocytes, osteoblasts, and myocytes. However, this cell line is more biased toward the osteogenic lineage, which can make for biased *in vitro* studies and have demonstrated less favorable outcomes compared to bone marrow stromal cells [132, 133]. In a study by *Follmar et al.*, combining adipose-derived stem cells with allografts in a rabbit model demonstrated a foreign body response; however, these same cells in a porcine model accelerated bone healing [128, 134]. Another alternative is to use cells derived from pregnancies, such as umbilical cord and placental stem cells. Umbilical cord blood multilineage cells take longer to culture and express lower bone antigens, but exposure to osteoblast-conditioned media enhanced their rate of osteogenic differentiation [135, 136]. Placental stem cells have also been shown to have a bone marrow stromal cell-like behavior and possess multilineage differentiation potentials [115].

3D printing offers the unique opportunity to encapsulate cells into printed constructs and even encapsulate various cell types into the same print. These cells can

be cultured and encapsulated into hydrogels, which can then be used in syringe pumps in bioprinters to print layer-by-layer. Mesenchymal stem cells and chondrocytes have been embedded into alginate hydrogels, and this hydrogel exhibited extracellular matrix formation both *in vitro* and *in vivo* [123]. Organ bioprinting, an approach to print fully capable organs, can be accomplished through printing a variety of cells and culturing the resultant scaffold post-printing. Firstly, the organ blueprint must be designed, next, stem cells required for the organ are isolated and differentiated, and then these are encapsulated into hydrogels or other medium to support the life of the cells, and finally, these are printed and placed into a bioreactor or incubator to continue cell growth [137]. Bioprinting enables cells to be printed in distinct areas using various nozzles containing hydrogels with different encapsulated cells. This can make for interesting studies comparing co-cultures in different compartments. Bioprinting with cells offers new complex architectures with a wide variety of cells; however, the material in which the cells are encapsulated within still needs to meet bioactivity requirements while being able to be printed. Cells must remain viable within these materials and further research needs to investigate improving these printers and materials to sustain cell viability.

7.2 Cells Involved in the Wound Healing Cascade

There are a wide variety of cells to consider using in biomaterial implants, and more research needs to be performed on using patient-derived cells in order to accelerate healing as well as the interactions of each cell type on the biomaterial implant. Maintaining the balance between osteoclasts and osteoblasts, creating a controlled environment for M1 to M2 macrophage phenotype transition, and allowing blood vessels to grow and deliver nutrients are all factors that need consideration in biomaterial implant design. The promise of better healing using biomaterial scaffold implants lies in the ability for these to be tailored to meet these requirements. In order to balance osteoclasts and osteoblasts, these cell types could be examined in a co-culture on the implant in order to determine the possible mechanisms and healing that may proceed *in vivo*. This has been performed on collagen-based scaffolds in order to determine that these scaffolds inhibit osteoclastogenesis [97, 98]. Similar studies should be carried out investigating this balance in other biomaterial implants as well. Uncovering the type of M1 to M2 macrophage transition in implants can be investigated by seeding M0 macrophages or monocytes on scaffolds *in vitro*. These transitions have been investigated by *Spiller et al.* [13, 138–141], and this can provide useful information over time about how these cells polarize in response to implant released factors and implant topography and composition. This phenotype transition could be helpful to elucidate whether inflammation may persist or if a foreign body response may occur before an *in vivo* experiment is undertaken. In addition to investigating these specific cells, placental-derived tissues have shown promise in modulating this transition and ultimately the immune response. The amnion and chorion membrane of the placenta have been investigated as an addition

to scaffolds and have shown to dampen the pro-inflammatory immune response while promoting osteogenesis [101, 102, 104, 139, 142, 143]. Finally, angiogenesis is important for delivery of nutrients to the growing bone and inadequate vascularization of bone has been associated with a decrease in bone mass [144]. An interesting opportunity exists to test vessel formation in biomaterial implants for bone regeneration, an example being endothelial vessel formation created in hydrogels by co-culture of umbilical vein endothelial cells and normal lung fibroblasts [145]. This type of study could be expanded using released factors from implant or solely focusing on blood vessel formation in implants for bone regeneration. This may give a better understanding of how blood vessel formation would occur *in vivo.*

Overall there are many variables to consider when using stem cells and more research needs to be examined on the effect of adding these to implants. There exists potential for these cells to accelerate healing, and in combination with 3D printing even greater potential exists to improve bone repair with complex tissue architectures.

8 Growth Factors, Chemical Cues, Differentiating Agents for Bone

8.1 Growth Factors to Enhance Bone Repair

Growth factors are polypeptides and are used in bone regeneration to differentiate bone cells, promote angiogenesis, or promote migration and retention of cells to the implant site. These can act on the autocrine (influences the cell of origin), paracrine (influences nearby cells), or endocrine (influences the nearby microenvironment) systems. Growth factors bind to cell receptors and induce intracellular signal transduction which determines the biological response upon reaching the cell nucleus [146]. Additionally, a single growth factor may bind to different receptors. Growth factors are typically introduced to the body in one of the two methods, as a protein therapy or gene therapy. Protein therapy involves direct recombinant growth factor delivery to the site of interest, whereas gene therapy delivers growth factors to cells by gene encoding [146].

Most common growth factors interacting with the skeletal system are bone morphogenic proteins (BMPs), fibroblast growth factors (FGF), platelet-derived growth factor (PDGF), insulin-like growth factors (IGFs), transforming growth factor-β (TGF-β), and vascular endothelial growth factor (VGEF) to name a few. A summary of growth factors and their impact on bone and cartilage formation can be found in Table 3. Using growth factors to heal critically sized defects has shown to mostly improve the healing process; however, there have been reports that BMPs and TGFβ-3 did not improve healing [5].

Bone morphogenic proteins are typically considered the most promising approach to repair bone due to their osteoinductive nature. BMP-2, -4, -6, -7, and -9

Table 3 Growth factors used in bone repair and their functions

Growth factor	Function	References
BMPs	Promotes osteoprogenitor migration	[146]
	Promotes proliferation and differentiation of chondrocytes and osteoblasts	
	Promotes bone formation	
EGF	Promotes osteoblast proliferation	[147]
	Combined with BMP-2 and -7 can further upregulate proliferation	
FGFs	Promotes chondrocyte maturation (FGF-1)	[146, 148]
	Differentiates osteoblasts	
	Involvement in bone resorption and formation (FGF-2)	
HGF	Promotes osteoblast proliferation	[149, 150]
	Promotes osteoblast migration	
	In some instances it has been found to inhibit BMP-2-induced bone formation	
IGFs	Promotes osteoblast proliferation	[146, 148]
	Promotes bone formation and controls resorption	
	Induces the deposition of type I collagen	
MGF	Repairs tissues	[151, 152]
	Improves osteoblast proliferation	
PDGF	Promotes osteoprogenitor migration and differentiation	[146, 153, 154]
	Promotes wound healing and bone repair	
TGF-β	Stimulates differentiation of mesenchymal stem cells to osteoblasts and chondrocytes	[146, 155, 156]
	Promotes bone formation	
	Recruits osteoblast and osteoclast precursors	
VEGF	Mineralized cartilage	[146]
	Promotes osteoblast proliferation	
	Control angiogenesis	

have shown to have the greatest osteogenic success *in vitro* [157]. However, there have been mixed results with using BMPs. A review found that 11 results supported the use of BMPs, three results found no effect on bone repair, and two demonstrated negative outcomes [158]. This variability can be attributed to the variety of BMPs used and the treatment conditions. To repair fractures, recombinant human BMP-2 (rhBMP-2) is used most frequently, and rhBMP-7 is most commonly used for non-union repairs [158]. Overall, rhBMPs have been shown to accelerate healing of tibial fractures and reduce infection rates [158]. There exist drawbacks to using BMPs, especially rhBMP-2 which has resulted in surgery complications, especially spinal surgeries. The majority of these complications stem from heterotopic ossification, or bone growth in areas of other tissues. Literature finds it difficult to compare the two BMPs, BMP-2 and -7, as most studies lack comparisons between the two which can elucidate differences. Another issue with BMPs and many growth factors is the delivery method. Due to their soluble nature, if these growth factors

are not appropriately carried to the site of interest they can diffuse into nearby tissues and form bone in undesirable locations. In general, large doses of BMPs are required to achieve osteogenic effects, which can be both expensive and increase the risk of heterotopic ossification [158]. Thus, further research into BMP delivery needs to be performed in order to control the release of these factors better.

Fibroblast growth factors have been found to be suitable for regeneration of a wide range of tissues and are key regulators of bone development [148]. In particular, FGF-2, -9, and -18 are involved in bone development and FGF signaling can stimulate proliferation of osteogenic cells and angiogenesis [148]. Recombinant FGF-2 has shown to accelerate bone repair in rabbits, but its anabolic effect is limited to the first 24 h after fracture occurs [159]. In a rabbit model, FGF-2-coated hydroxyapatite scaffolds were shown to greatly enhance the osteoinductive effect compared to uncoated implants [160].

Platelet-derived growth factor is involved in the development of embryos but also plays important roles in bone repair in adults. Systemic application of PDGF has shown to result in increased bone mineral density and compressive properties in rat vertebrae [161], conversely, PDGF inhibited bone regeneration in rat calvarial defects [162]. However, with the appropriate carrier, the opposite was true and bone formation was increased in rat calvarial defects [163].

Insulin-like growth factors can influence both metabolic and growth activity in many cell and tissue types, and of the isoforms IGF-I and IGF-II, IGF-I has been typically only used in skeletal reconstruction [164]. IGF-I is the most abundant growth factor found in the skeletal system and regulates bone development and osteoblasts [165]. IGF-I has also been used to increase bone formation, but this did not have the desired effect in young animals [166]. IGF-I delivered via PLGA microparticles was shown to enhance new bone formation, but there was little therapeutic effect of using IGF-I alone for cartilage and bone repair in osteoarthritic joints [167, 168]. IGF-II is the most abundant growth factor in bone and both IGFs play important roles in stimulating osteoblast differentiation, deposition of bone, and collagen protein expression [169]. Insulin-like growth factors can be differentiated from one other by their functions, as IGF-II can induce proliferation and differentiation of MSCs to osteoblasts, while IGF-I cannot, and functions to maintain and grow bone [169].

Transforming growth factor beta is one of the most common cytokines and influences the development of various tissues [164]. The carrier of TGF-β plays an important role in its activity, as single doses of TGF-β_1 had no effect in rabbit calvarial defects but gelatin capsules enhanced bone formation [170]. Similar to this, TGF-β hydrogels with very rapid or very slow degradation times had no effect on bone formation [171].

Finally, vascular endothelial growth factor not only controls vasculogenesis and angiogenesis, but is involved in recruitment and activity of bone forming cells [148]. VEGF had been shown to enhance blood vessel formation and ossification in murine femur fractures [172]. In addition, VEGFs have been shown to enhance bone formation when combined with other growth factors [148].

An alternative to growth factors is platelet rich plasma (PRP), which is centrifuged autogenous blood that contains high concentrations of cells containing various growth factors such as PDGF, TGF-β, IGF, and VEGF [164]. PRP has been considered a better alternative to the single use of growth factors due to its composition of many growth factors and its cost-effective sourcing [173]. However, there are variabilities in success due to the preparation methods, concentration, and methods of application of PRP. *In vitro*, PRP has shown to induce proliferation of bone marrow stem cells and promote osteogenic differentiation [174]. *In vivo* studies have demonstrated various outcomes, with most improving the histological appearance of bone but some reporting harmful or non-significant effects [173].

Drawbacks to using recombinant growth factors in general are their roles in tumor formation or negative immune reactions, which has been demonstrated for BMP2 and VEGF [146, 175]. As with all growth factors, the design of the delivery system can greatly affect the outcome of the surgery. This adds another element to designing a biomaterial implant. If the biomaterial includes the release of a growth factor, then further consideration on the kinetics of release needs to be tailored to the wound of interest, whether it be a short or sustained release. Interestingly, combinations of scaffolds, cells, and growth factors have been shown both positive and negative results when compared to combinations of scaffolds and cells or growth factors [5].

8.2 Application of Growth Factors to Tissue Engineering

In addition to printing unique structures and multiple cell types, growth factors can be combined with bioprinting. Growth factors, like cells, can be added to the printing medium in order to drive cellular responses. Hydrogels have been effectively loaded with BMP-2 and VEGF in order to induce bone regeneration. In one study, BMP-2 was loaded into collagen hydrogels for a sustained release and VEGF was loaded into alginate and gelatin hydrogels for a burst release [176]. In this example, multiple print heads were used to create a scaffold with two different growth factors located in different regions of the scaffold that released at different rates based on material properties [176]. Bioprinting offers a simple way to incorporate various growth factors in order to study their interactions with cells; however, the material that these growth factors are encapsulated in determines their release. Further research needs to be performed in order to optimize these materials, especially materials other than hydrogels, as bioprinting is an incredibly useful tool if optimized.

There exist a wide variety of growth factors available to promote bone regeneration, and more research needs to be investigated on how to adequately deliver these and control cell fate. Again, factors that can control the balance of osteoclasts and osteoblasts, the M1 to M2 macrophage transition, and angiogenesis need to be examined. Research has demonstrated that osteoprotegerin plays a critical role in inhibiting osteoclastogenesis, which could be potentially used as a growth factor in

order to maintain this balance between osteoclasts and osteoblasts [97, 98]. In addition to this, macrophage phenotype impacts the wound outcome and growth factors could be delivered in order to promote a more M1 or M2-like phenotype. Cytokines that can induce an M1 response include LPS and IFN-γ, while cytokines that can induce an M2 response include IL-4, IL-13, and IL-10 [13, 141, 177]. An interesting opportunity exists to combine these cytokines in 3D-printed scaffolds in order to drive a particular immune response depended on release rates and specific cytokines released. Finally, angiogenesis can be accomplished by introducing VEGF to scaffolds, and more research should involve examining blood vessel formation with and without this growth factor and its potential to induce vessel formation quicker in scaffolds. Overall, growth factor addition to implant materials holds promise, but more investigation must be performed on the negative outcomes of these factors, controlling delivery, and leveraging multiple growth factors in order to drive osteogenesis, wound healing, and angiogenesis.

9 Conclusions

There are many strategies to repair bones; however, no such strategy exists without its drawbacks. Autografts have the greatest potential to heal but require another surgery within the patient's body. Allografts and xenografts have shown promising results, but processing methods can destroy important components in these materials. Other scaffold types are easy to manipulate and can be patient-specific; however, their results cannot yet compare to autografts. The future of bone regeneration involves combining these various methods to heal bone in order to achieve the properties of a biomaterial implant (Fig. 3): biocompatible materials, mechanics that match the properties of bone and prevent micromotion, a pore size and orientation that guides vessel formation and cell migration, and a material that degrades and allows new bone formation to occur. 3D printing can be used to print multiple material types, unique and challenging structures, and patient-specific implants. This can be useful in combination with the various materials, cells, and growth factors discussed here, to one day create a biomaterial implant that addresses all necessary criteria. Research efforts should also focus on targeting the balance between osteoclasts and osteoblasts, macrophage phenotype transition, and angiogenesis. These can be addressed by material design, studies investigating multiple cell-type interactions, and growth factor addition. Overall, there exists a vast amount of research and development left in the area of bone repair, and many factors need to be addressed. Optimizing materials, fabrication, cell types, and growth factors included in biomaterial implants must be accomplished in order to create the optimal biomaterial for bone repair.

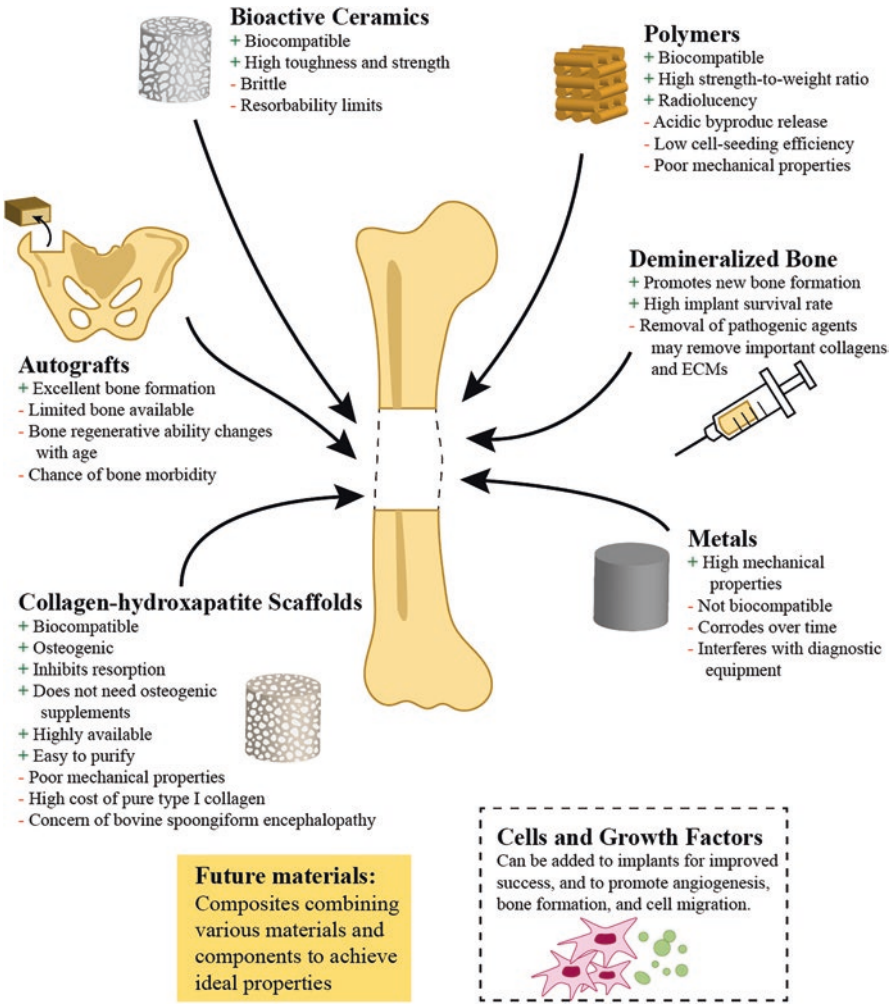

Fig. 3 Advantages and disadvantages of implant materials for bone regeneration. Future materials need to combine these advantages and supplemental materials, such as cells and growth factors, to reach optimal properties

Acknowledgements This work was supported by the Office of the Assistant Secretary of Defense for Health Affairs Broad Agency Announcement for Extramural Medical Research through the Award No. W81XWH-16-1-0566 (BACH). Opinions, interpretations, conclusions, and recommendations are those of the authors and are not necessarily endorsed by the Department of Defense. This work was also supported by the National Institute of Dental and Craniofacial Research of the National Institutes of Health under Award Number R21 DE026582 (BACH). The content is solely the responsibility of the authors and does not necessarily represent the official views of the NIH. We are grateful for the funding for this study provided by the NSF Graduate Research Fellowship DGE-1144245 (MJD). The authors would like to acknowledge Vasiliki Kolliopoulos and Andrey Nosatov for assistance with manuscript editing.

References

1. Lew T, Walker J, Wenke J, Blackbourne L, Hale R. Characterization of craniomaxillofacial battle injuries sustained by United States service members in the current conflicts of Iraq and Afghanistan. J Oral Maxillofac Surg. 2010;68(1):3–7.
2. Fong A, Lemelman B, Lam S, Kleiber G, Reid R, Gottlieb L. Reconstructive approach to hostile cranioplasty: a review of the University of Chicago experience. J Plast Reconstr Aesthet Surg. 2015;68(8):1036–43.
3. Lee J, Kleiber G, Pelletier A, Reid R, Gottlieb L. Autologous immediate cranioplasty with vascularized bone in high-risk composite cranial defects. Plast Reconstr Surg. 2013;132(4):967–75.
4. Lee E, Chao A, Skoracki R, Yu P, DeMonte F, Hanasono M. Outcomes of calvarial reconstruction in cancer patients. Plast Reconstr Surg. 2014;133(3):675–82.
5. Roffi A, Krishnakumar GS, Gostynska N, Kon E, Candrian C, Filardo G. The role of three-dimensional scaffolds in treating long bone defects: evidence from preclinical and clinical literature — a systematic review. Biomed Res Int. 2017;2017:13.
6. Staff MC. Spinal fusion. Mayo Clinic. https://www.mayoclinic.org/tests-procedures/spinal-fusion/about/pac-20384523. Accessed on 23 Jan 2020
7. Trampuz A, Zimmerli W. Diagnosis and treatment of implant-associated septic arthritis and osteomyelitis. Curr Infect Dis Rep. 2008;10(5):394–403.
8. Rodan GA. Bone homeostasis. PNAS. 1998;95(23):13361–2.
9. Thompson E, Matsiko A, Farrell E, Daniel JK, O'Brien F. Recapitulating endochondral ossification: a promising route to in vivo bone regeneration. J Tissue Eng Regen Med. 2015;9:889–902.
10. Kruijt Spanjer EC, Bittermann GKP, van Hooijdonk IEM, Rosenberg AJWP, Gawlitta D. Taking the endochondral route to craniomaxillofacial bone regeneration: a logical approach? J Craniomaxillofac Surg. 2017;45(7):1099–106. https://doi.org/10.1016/j.jcms.2017.03.025.
11. Scott CK, Hightower JA. The matrix of endochondral bone differs from the matrix of intramembranous bone. Calcif Tissue Int. 1991;49(5):349–54.
12. Ribeiro M, Monteiro FJ, Ferraz MP. Infection of orthopedic implants with emphasis on bacterial adhesion process and techniques used in studying bacterial-material interactions. Biomatter. 2012;2(4):176–94.
13. Spiller KL, Freytes DO, Vunjak-Novakovic G. Macrophages modulate engineered human tissues for enhanced vascularization and healing. Ann Biomed Eng. 2015;43(3):616–27.
14. Kim YK, Chen EY, Liu WF. Biomolecular strategies to modulate the macrophage response to implanted materials. J Mater Chem B. 2016;4(9):1600–9.
15. Gibon E, Lu LY, Nathan K, Goodman SB. Inflammation, ageing, and bone regeneration. J Orthop Transl. 2017;10:28–35. https://doi.org/10.1016/j.jot.2017.04.002.
16. Lee J, Byun H, Madhurakkat Perikamana SK, Lee S, Shin H. Current advances in immunomodulatory biomaterials for bone regeneration. Adv Healthc Mater. 2019;8:1–20.
17. Runyan CM, Gabrick KS. Biology of bone formation, fracture healing, and distraction osteogenesis. J Craniofac Surg. 2017;28(5):1380–9.
18. Elsalanty M, Genecov D. Bone grafts in craniofacial surgery. Craniomaxillofac Trauma Reconstr. 2009;2(03):125–34.
19. Pogrel M, Podlesh S, Anthony J, Alexander J. A comparison of vascularized and nonvascularized bone grafts for reconstruction of mandibular continuity defects. J Oral Maxillofac Surg. 1997;55(11):1200–6.
20. Abuzayed B, Aydin S, Aydin S, Kucukyuruk B, Sanus G. Cranioplasty: review of materials and techniques. J Neurosci Rural Pract. 2011;2(2):162.
21. Depeyre A, Touzet-Roumazeille S, Lauwers L, Raoul G, Ferri J. Retrospective evaluation of 211 patients with maxillofacial reconstruction using parietal bone graft for implants insertion. J Craniomaxillofac Surg. 2016;44(9):1162–9. https://doi.org/10.1016/j.jcms.2016.06.034.

22. Ghanaati S, Barbeck M, Booms P, Lorenz J, Kirkpatrick CJ, Sader RA. Potential lack of "standardized" processing techniques for production of allogeneic and xenogeneic bone blocks for application in humans. Acta Biomater. 2014;10(8):3557–62. https://doi.org/10.1016/j.actbio.2014.04.017.
23. Bae H, Zhao L, Kanim L, Wong P, Delamarter R, Dawson E. Intervariability and intravariability of bone morphogenetic proteins in commercially available demineralized bone matrix products. Spine (Phila Pa 1976). 2006;31(12):1299–306.
24. Nelson K, Fretwurst T, Stricker A, Steinberg T, Wein M, Spanou A. Comparison of four different allogeneic bone grafts for alveolar ridge reconstruction: a preliminary histologic and biochemical analysis. Oral Surg Oral Med Oral Pathol Oral Radiol. 2014;118(4):424–31. https://doi.org/10.1016/j.oooo.2014.05.020.
25. Athanasiou V, Papachristou D, Panagopoulos A, Saridis A, Scopa C, Megas P. Histological comparison of autograft, allograft-DBM, xenograft, and synthetic grafts in a trabecular bone defect: an experimental study in rabbits. Med Sci Monit. 2010;16(1):BR24–31.
26. Hartl A, Bitzan P, Wanivenhaus A, Kotz R. Faster integration of human allograft bone than of the bovine substitute Lubboc: non-randomized evaluation of 20 cases with benign tumors or tumor-like conditions. Acta Orthop Scand. 2004;75(2):217–20.
27. Bose S, Roy M, Bandyopadhyay A. Recent advances in bone tissue engineering scaffolds. Trends Biotechnol. 2012;30(10):546–54.
28. Dimitriou R, Babis GC. Biomaterial osseointegration enhancement with biophysical stimulation. J Musculoskelet Neuronal Interact. 2007;7(3):253–65.
29. Dewey MJ, Johnson EM, Weisgerber DW, Wheeler MB, Harley BAC. Shape-fitting collagen-PLA composite promotes osteogenic differentiation of porcine adipose stem cells. J Mech Behav Biomed Mater. 2019;95:21.
30. Murphy CM, Haugh MG, O'Brien FJ. The effect of mean pore size on cell attachment, proliferation and migration in collagen-glycosaminoglycan scaffolds for bone tissue engineering. Biomaterials. 2010;31(3):461–6. https://doi.org/10.1016/j.biomaterials.2009.09.063.
31. Sussman EM, Halpin MC, Muster J, Moon RT, Ratner BD. Porous implants modulate healing and induce shifts in local macrophage polarization in the foreign body reaction. Ann Biomed Eng. 2014;42(7):1508–16.
32. Ratner BD. A pore way to heal and regenerate : 21st century thinking on biocompatibility. Regen Biomater. 2016;3:107–10.
33. Madden LR, Mortisen DJ, Sussman EM, Dupras SK, Fugate JA, Cuy JL. Proangiogenic scaffolds as functional templates for cardiac tissue engineering. PNAS. 2010;107(34):15211–6.
34. Seong Y, Kang I, Song E, Kim H, Jeong S. Calcium phosphate – collagen scaffold with aligned pore channels for enhanced osteochondral regeneration. Adv Healthc Mater. 2017;6:1–11.
35. Bobbert FSL, Zadpoor AA. Effects of bone substitute architecture and surface properties on cell response, angiogenesis, and structure of new bone. J Mater Chem B. 2017;5(31):6175–92.
36. Lin W, Lan W, Wu Y, Zhao D, Wang Y, He X, et al. Aligned 3D porous polyurethane scaffolds for biological anisotropic tissue regeneration. Regen Biomater. 2019;7:19–27.
37. Marcacci M, Kon E, Moukhachev V, Lavroukov A, Kutepov S, Quarto R, et al. Stem cells associated with macroporous bioceramics for long bone repair: 6- to 7-year outcome of a pilot clinical study. Tissue Eng. 2007;13(5):947.
38. Sheikh Z, Sima C, Glogauer M. Bone replacement materials and techniques used for achieving vertical alveolar bone augmentation. Materials (Basel). 2015;8:2953–93.
39. Weisgerber DW, Milner DJ, Lopez-Lake H, Rubessa M, Lotti S, Polkoff K, et al. A mineralized collagen-polycaprolactone composite promotes healing of a porcine mandibular defect. Tissue Eng Part A. 2017;24(11–12):943–54.
40. Sheikh Z, Najeeb S, Glogauer M. Biodegradable materials for bone repair and tissue engineering applications. Materials (Basel). 2015;8(9):5744–94.
41. Hutmacher D, Hurzeler MB, Schliephake H. A review of material properties of biodegradable and bioresorbable polymers and devices for GTR and GBR applications. Int J Oral Maxillofac Implants. 1996;11:667–78.

42. Chanlalit C, Shukla DR, Fitzsimmons JS, An KN, O'Driscoll SW. Stress shielding around radial head prostheses. J Hand Surg [Am]. 2012;37:2118–25.
43. Dau M, Kämmerer PW, Henkel KO, Gerber T, Frerich B, Gundlach KKH. Bone formation in mono cortical mandibular critical size defects after augmentation with two synthetic nanostructured and one xenogenous hydroxyapatite bone substitute - in vivo animal study. Clin Oral Implants Res. 2016;27(5):597–603.
44. Buser Z, Brodke D, Youssef J, Meisel H, Myhre S, Hashimoto R, et al. Synthetic bone graft versus autograft or allograft for spinal fusion: a systematic review. J Neuorosurg Spine. 2016;25(4):509–16.
45. Tatara AM, Koons GL, Watson E, Piepergerdes TC, Shah SR. Biomaterials-aided mandibular reconstruction using in vivo bioreactors. PNAS. 2019;116(14):6954–63.
46. Broggini N, Bosshardt DD, Jensen SS, Bornstein MM, Wang C, Buser D. Bone healing around nanocrystalline hydroxyapatite, deproteinized bovine bone mineral, biphasic calcium phosphate, and autogenous bone in mandibular bone defects. J Biomed Mater Res B Appl Biomater. 2015;103:1478–87.
47. Wang W, Yeung KWK. Bone grafts and biomaterials substitutes for bone defect repair: a review. Bioact Mater. 2017;2(4):224–47.
48. Ghassemi T, Shahroodi A, Moradi A. Current concepts in scaffolding for bone tissue engineering. Arch Bone Jt Surg. 2018;6(2):90–9.
49. Peterson B, Whang P, Iglesias R, Wang J, Lieberman J. Osteoinductivity of commercially available demineralized bone matrix. J Bone Jt Surg. 2004;86(10):2243–50.
50. Acarturk T, Hollinger J. Commercially available demineralized bone matrix compositions to regenerate calvarial critical-sized bone defects. Plast Reconstr Surg. 2006;118(4):862–73.
51. Oryan A, Alidadi S, Moshiri A, Maffulli N. Bone regenerative medicine: classic options, novel strategies, and future directions. J Orthop Surg Res. 2014;9:18.
52. Goa T-J, Tuominen TK, Lindholm TS, Kommonen B, Lindholm TC. Morphological and biomechanical difference in healing in segmental tibia1 defects implanted with Biocoral(R) or tricalcium phbsphate cylinders. Biomaterials. 1997;18:219–23.
53. Galli C, Guizzardi S, Passeri G, Martini D, Tinti A, Mauro G, et al. Comparison of human mandibular osteoblasts grown on two commercially available titanium implant surfaces. J Periodontol. 2005;76(3):364–72.
54. Gredes T, Kubasiewicz-Ross P, Gedrange T, Dominiak M, Kunert-Keil C. Comparison of surface modified zirconia implants with commercially available zirconium and titanium implants: a histological study in pigs. Implant Dent. 2014;23(4):502–7.
55. Bansiddhi A, Sargeant T, Stupp S, Dunand D. Porous NiTi for bone implants: a review. Acta Biomater. 2008;4(4):773–82.
56. Bai X, Gao M, Syed S, Zhuang J, Xu X, Zhang X-Q. Bioactive hydrogels for bone regeneration. Bioact Mater. 2018;3(4):401–17.
57. Sanchez-Sotelo J, Munuera L, Madero R. Treatment of fractures of the distal radius with a remodellable bone cement. J Bone Jt Surg. 2000;82:856–63.
58. Lidfors N, Heikkila J, Koski I, Mattila K, Aho A. Bioactive glass and autogenous bone as bone graft substitutes in benign bone tumors. J Biomed Mater Res B. 2008;90B(1):131–6.
59. Crovace M, Souza M, Chinaglia C, Peitl O, Zanotto E. Biosilicate® — a multipurpose, highly bioactive glass-ceramic. In vitro, in vivo and clinical trials. J Non-Cryst Solids. 2016;432:90–110.
60. Leupold J, Barfield W, Han Y, Hartsock L. A comparison of ProOsteon, DBX, and collagraft in a rabbit model. J Biomed Mater Res B. 2006;79B(2):292–7.
61. Boyd D, Towler M, Wren A, Clarkin O. Comparison of an experimental bone cement with surgical Simplex® P, Spineplex® and Cortoss®. J Mater Sci Mater Med. 2008;19:1745–52.
62. Nee D, Noyes D, Shaw M, Gwilym S, Fairlie N, Birch N. Healos and bone marrow aspirate used for lumbar spine fusion: a case controlled study comparing healos with autograft. Spine (Phila Pa 1976). 2006;31(18):E636–40.

63. Liu X, Ma P. Polymeric scaffolds for bone tissue engineering. Ann Biomed Eng. 2004;32(3):477–86.
64. Gupte MJ, Ma PX. Nanofibrous scaffolds for dental and craniofacial applications. J Dent Res. 2012;91(3):227–34.
65. Qu F, Holloway J, Esterhai J, Burdick J, Mauck R. Programmed biomolecule delivery to enable and direct cell migration for connective tissue repair. Nat Commun. 2017;8:1780.
66. Baker B, Shah R, Silverstein A, Esterhai J, Burdick J, Mauck R. Sacrificial nanofibrous composites provide instruction without impediment and enable functional tissue formation. PNAS. 2012;109(35):14176–81.
67. Abuzayed B, Tuzgen S, Canbaz B, Yuksel O, Tutunculer B, Sanus G. Reconstruction of growing skull fracture with in situ galeal graft duraplasty and porous polyethylene sheet. J Craniofac Surg. 2009;20(4):1245–9.
68. Abuzayed B, Dashti R, Turk O, Kaynar M. Aneurysmal frontal bone cyst in a child with history of acute lymphoblastic leukemia: a case of rare location and history. J Pediatr Hematol Oncol. 2010;32(1):e1–3.
69. Kucukyuruk B, Biceroglu H, Abuzayed B, Ulu M, Sanus G. Intraosseous meningioma: a rare tumor reconstructed with porous polyethylene. J Craniofac Surg. 2010;21(3):936–9.
70. Brockmeyer P, Kramer K, Krohn S, Kauffmann P, Mauth C, Dard M, et al. Influence of synthetic polyethylene glycol hydrogels on new bone formation during mandibular augmentation procedures in Goettingen minipigs. J Mater Sci Mater Med. 2015;26(6):1–7.
71. Gregor A, Filová E, Novák M, Kronek J, Chlup H, Buzgo M, et al. Designing of PLA scaffolds for bone tissue replacement fabricated by ordinary commercial 3D printer. J Biol Eng. 2017;11(1):1–21.
72. Zhang H, Mao X, Zhao D, Jiang W, Du Z, Li Q, et al. Three dimensional printed polylactic acid-hydroxyapatite composite scaffolds for prefabricating vascularized tissue engineered bone: an in vivo bioreactor model. Sci Rep. 2017;7:15255.
73. Park SA, Lee H-J, Park S-Y. In vivo evaluation of 3D-printed polycaprolactone scaffold implantation combined with β-TCP powder for alveolar bone augmentation in a beagle defect model. Materials (Basel). 2018;11(2):238.
74. Weisgerber DW, Milner DJ, Lopez-Lake H, Rubessa M, Lotti S, Polkoff K, et al. A mineralized collagen-polycaprolactone composite promotes healing of a porcine mandibular ramus defect. Tissue Eng Part A. 2017;24(11–12):943–54.
75. Gredes T, Kunath F, Gedrange T, Kunert-Keil C. Bone regeneration after treatment with covering materials composed of flax fibers and biodegradable plastics: a histological study in rats. Biomed Res Int. 2016;2016:1–8.
76. Athanasiou K, Niederauer G, Agrawal CM. Sterilization, toxicity, biocompatibility and clinical applications of polylactic acid/polyglycolic acid copolymers. Biomaterials. 1996;17(2):93–102.
77. Athanasiou K, Agrawal C, Barber F, Burkhart S. Orthopaedic applications for PLA-PGA biodegradable polymers. Anthrosc J Arthrosc Relat Surg. 1998;14(7):726–37.
78. Kroeze RJ, Helder MN, Smit TH. Biodegradable polymers in bone tissue engineering. Materials (Basel). 2009;2(3):833–56.
79. Mai R, Hagedorn MG, Gelinsky M, Werner C, Turhani D, Spath H, et al. Ectopic bone formation in nude rats using human osteoblasts seeded poly(3)hydroxybutyrate embroidery and hydroxyapatite-collagen tapes constructs. J Craniomaxillofac Surg. 2006;34(2):101–9.
80. Harley BA, Leung JH, Silva ECCM, Gibson LJ. Mechanical characterization of collagen-glycosaminoglycan scaffolds. Acta Biomater. 2007;3(4):463–74.
81. O'Brien FJ, Harley BA, Yannas IV, Gibson LJ. The effect of pore size on cell adhesion in collagen-GAG scaffolds. Biomaterials. 2005;26(4):433–41.
82. Florent D, Levingstone T, Schneeweiss W, de Swartw M, Jahns H, Gleeson J, et al. Enhanced bone healing using collagen– hydroxyapatite scaffold implantation in the treatment of a large multiloculated mandibular aneurysmal bone cyst in a thoroughbred filly. J Tissue Eng Regen Med. 2015;9:1193–9.

83. Cunniffe G, Dickson G, Partap S, Stanton K, O'Brien FJ. Development and characterisation of a collagen nano-hydroxyapatite composite scaffold for bone tissue engineering. J Mater Sci Mater Med. 2010;21:2293–8.
84. Al-Munajjed A, Gleeson J, O'Brien F. Development of a collagen calcium-phosphate scaffold as a novel bone graft substitute. Stud Heal Technol Inf. 2008;133:11–20.
85. Ren X, Bischoff D, Weisgerber DW, Lewis MS, Tu V, Yamaguchi DT, et al. Osteogenesis on nanoparticulate mineralized collagen scaffolds via autogenous activation of the canonical BMP receptor signaling pathway. Biomaterials. 2015;50:107–14.
86. Caliari SR, Harley BAC. Structural and biochemical modification of a collagen scaffold to selectively enhance MSC tenogenic, chondrogenic, and osteogenic differentiation. Adv Healthc Mater. 2014;3:1086–96.
87. Caliari SR, Harley BAC. Composite growth factor supplementation strategies to enhance tenocyte bioactivity in aligned collagen-GAG scaffolds. Tissue Eng Part A. 2012;19(9–10):1100–12.
88. Kanungo BP, Gibson LJ. Density-property relationships in collagen-glycosaminoglycan scaffolds. Acta Biomater. 2010;6(2):344–53. https://doi.org/10.1016/j.actbio.2009.09.012.
89. O'Brien FJ, Harley BA, Yannas IV, Gibson L. Influence of freezing rate on pore structure in freeze-dried collagen-GAG scaffolds. Biomaterials. 2004;25(6):1077–86.
90. Murphy CM, O'Brien FJ. Understanding the effect of mean pore size on cell activity in collagen-glycosaminoglycan scaffolds. Cell Adhes Migr. 2010;4(3):377–81.
91. Weisgerber DW, Caliari SR, Harley BAC. Mineralized collagen scaffolds induce hMSC osteogenesis and matrix remodeling. Biomater Sci. 2015;3(3):533–42.
92. Yamaguchi DT, Lee JC, Tu V, Ren X, Harley BAC, Weisgerber DW, et al. Osteogenesis on nanoparticulate mineralized collagen scaffolds via autogenous activation of the canonical BMP receptor signaling pathway. Biomaterials. 2015;50:107–14. https://doi.org/10.1016/j.biomaterials.2015.01.059.
93. Kanungo BP, Silva E, Van Vliet K, Gibson LJ. Characterization of mineralized collagen-glycosaminoglycan scaffolds for bone regeneration. Acta Biomater. 2008;4(3):490–503.
94. Harley BA, Lynn AK, Wissner-Gross Z, Bonfield W, Yannas IV, Gibson LJ. Design of a multiphase osteochondral scaffold. II. Fabrication of a mineralized collagen-glycosaminoglycan scaffold. J Biomed Mater Res A. 2010;92(3):1066–77.
95. Lyons FG, Gleeson JP, Partap S, Coghlan K, O'Brien FJ. Novel microhydroxyapatite particles in a collagen scaffold: a bioactive bone void filler? Clin Orthop Relat Res. 2014;472(4):1318–28.
96. Ren X, Tu V, Bischoff D, Weisgerber DW, Lewis MS, Yamaguchi DT, et al. Nanoparticulate mineralized collagen scaffolds induce in vivo bone regeneration independent of progenitor cell loading or exogenous growth factor stimulation. Biomaterials. 2016;89:67–78.
97. Ren X, Dewey MJ, Bischoff D, Miller TA, Yamaguchi DT, Harley BAC, et al. Nanoparticulate mineralized collagen glycosaminoglycan materials directly and indirectly inhibit osteoclastogenesis and osteoclast activation. J Tissue Eng Regen Med. 2019;13:823–34.
98. Ren X, Zhou Q, Foulad D, Tiffany AS, Dewey MJ, Bischoff D, et al. Osteoprotegerin reduces osteoclast resorption activity without affecting osteogenesis on nanoparticulate mineralized collagen scaffolds. Sci Adv. 2019;5:1–12.
99. Dewey MJ, Weisgerber DW, Johnson E, Wheeler MB, Harley BAC. Shape-fitting collagen-PLA composite promotes osteogenic differentiation of porcine adipose stem cells. J Mech Behav Biomed Mater. 2019;95:21.
100. Weisgerber DW, Erning K, Flanagan CL, Hollister SJ, Harley BAC. Evaluation of multiscale mineralized collagen-polycaprolactone composites for bone tissue engineering. J Mech Behav Biomed Mater. 2016;61:318–27. https://doi.org/10.1016/j.jmbbm.2016.03.032.
101. Hortensius RA, Ebens JH, Dewey MJ, Harley BAC. Incorporation of the amniotic membrane as an immunomodulatory design element in collagen scaffolds for tendon repair. ACS Biomater Sci Eng. 2018;4(12):4367–77.

102. Hortensius RA, Ebens JH, Harley BAC. Immunomodulatory effects of amniotic membrane matrix incorporated into collagen scaffolds. J Biomed Mater Res A. 2016;104(6):1332–42.
103. Tiffany AS, Gray DL, Woods TJ, Subedi K, Harley BAC. The inclusion of zinc into mineralized collagen scaffolds for craniofacial bone repair applications. Acta Biomater. 2019;93:86–96. https://doi.org/10.1016/j.actbio.2019.05.031.
104. Dewey M, Johnson E, Slater S, Milner D, Wheeler M, Harley B. Mineralized collagen scaffolds fabricated with amniotic membrane matrix increase osteogenesis under inflammatory conditions. Regen Biomater. 2020;7:247.
105. Dewey M, Nosatov A, Subedi K, Harley B. Anisotropic mineralized collagen scaffolds accelerate osteogenic response in a glycosaminoglycan-dependent fashion. RSC Adv. 2020;10:15629.
106. Offeddu GS, Ashworth JC, Cameron RE, Oyen ML. Multi-scale mechanical response of freeze-dried collagen scaffolds for tissue engineering applications. J Mech Behav Biomed Mater. 2015;42:19–25.
107. Klaumünzer A, Leemhuis H, Schmidt-Bleek K, Schreivogel S, Woloszyk A, Korus G, et al. A biomaterial with a channel-like pore architecture induces endochondral healing of bone defects. Nat Commun. 2018;9(1):4430. https://doi.org/10.1038/s41467-018-06504-7.
108. Radzi S, Cowin G, Schmutz B. Metal artifacts from titanium and steel screws in CT, 1.5T and 3T MR images of the tibial Pilon: a quantitative assessment in 3D. Quant Imag Med Surg. 2014;4(3):163–72.
109. Terjesen T, Nordby A, Arnulf V. Bone atrophy after plate fixation: compute tomography of femoral shaft fractures. Acta Orthop Scand. 1985;56(5):416–8.
110. Alvarez K, Nakajima H. Metallic scaffolds for bone regeneration. Materials (Basel). 2009;2(3):790–832.
111. Moghaddam NS, Andani MT, Amerinatanzi A, Haberland C, Huff S, Miller M, et al. Metals for bone implants: safety, design, and efficacy. Biomanufact Rev. 2016;1:1.
112. Assad M, Jarzem P, Leroux M, Coillard C, Chernyshov AV, Charette S, et al. Porous titanium-nickel for intervertebral fusion in a sheep model: Part 1. Histomorphometric and radiological analysis. J Biomed Mater Res Part B Appl Biomater. 2003;64B(2):107.
113. Bohner M. Physical and chemical aspects of calcium phosphates used in spinal surgery. Eur Spine J. 2001;10:S114–21.
114. Durgalakshmi D, Subhathirai S, Balakumar S. Nano-bioglass: a versatile antidote for bone tissue engineering problems. Proc Eng. 2014;92:2–8.
115. Scaglione S, Quarto R, Giannoni P. Stem cells and tissue scaffolds for bone repair. In: Cellular response to biomaterials. Cambridge: Woodhead Publishing Limited; 2008. p. 291–312. https://doi.org/10.1016/B978-1-84569-358-9.50012-0.
116. Werber K, Brauer R, Weiss W, Becker K. Osseous integration of bovine hydroxyapatite ceramic in metaphyseal bone defects of the distal radius. J Hand Surg [Am]. 2000;25(5):833–41.
117. Arai E, Nakashima H, Tsukushi S, Shido Y, Nishida Y, Yamada Y, et al. Regenerating the fibula with beta-tricalcium phosphate minimizes morbidity after fibula resection. Clin Orthop Relat Res. 2005;431:233–7.
118. Devendran S, Namashivayam S, Ambigapathi M, Nagarajan S, Tsai W-B, Sethu SN, et al. Nanoceramics on osteoblast proliferation and differentiation in bone tissue engineering. Int J Biol Macromol. 2017;98:67–74. https://doi.org/10.1016/j.ijbiomac.2017.01.089.
119. Roualdes O, Duclos M-E, Gutknecht D, Frappart L, Chevalier J, Hartmann D. In vitro and in vivo evaluation of an alumina–zirconia composite for arthroplasty applications. Biomaterials. 2010;31(8):2043–54.
120. Canzi P, Marconi S, Benazzo M. From CT scanning to 3D printing technology: a new method for the preoperative planning of a transcutaneous bone-conduction hearing device. Acta Otorhinolaryngol Ital. 2018;38(3):251–6.
121. Haleem A, Javaid M. Role of CT and MRI in the design and development of orthopaedic model using additive manufacturing. J Clin Orthop Trauma. 2018;9(3):213–7.

122. Brunello G, Sivolella S, Meneghello R, Ferroni L, Gardin C, Piattelli A, et al. Powder-based 3D printing for bone tissue engineering. Biotechnol Adv. 2016;34(5):740–53.
123. Bose S, Vahabzadeh S, Bandyopadhyay A. Bone tissue engineering using 3D printing. Mater Today. 2013;16(12):496–504.
124. Trombetta R, Inzana J, Schwarz E, Kates S, Awad H. 3D printing of calcium phosphate ceramics for bone tissue engineering and drug delivery. Ann Biomed Eng. 2017;45(1):23–44.
125. Maleksaeedi S, Wang JK, El-Hajje A, Harb L, Guneta V, He Z, et al. Toward 3D printed bioactive titanium scaffolds with bimodal pore size distribution for bone ingrowth. Proc CIRP. 2013;5:1558–163.
126. Scarano A, Crincoli V, Di Benedetto A, Cozzolino V, Lorusso F, Podaliri Vulpiani M, et al. Bone regeneration induced by bone porcine block with bone marrow stromal stem cells in a minipig model of mandibular "critical size" defect. Stem Cells Int. 2017;2017:9082869.
127. Walmsley GG, Ransom RC, Wan DC. Stem cells in bone regeneration. Stem Cell Rev. 2016;12(5):524–9.
128. Wilson SM, Goldwasser MS, Clark SG, Monaco E, Bionaz M, Hurley WL, et al. Adipose-derived mesenchymal stem cells enhance healing of mandibular defects in the ramus of swine. J Oral Maxillofac Surg. 2012;70(3):e193–203. https://doi.org/10.1016/j.joms.2011.10.029.
129. Ho S, Murphy K, Leach K. Increased survival and function of mesenchymal stem cell spheroids entrapped in instructive alginate hydrogels. Stem Cells Transl Med. 2016;5(6):773–81.
130. Ho S, Keown A, Leach K. Cell migration and bone formation from mesenchymal stem cell spheroids in alginate hydrogels are regulated by adhesive ligand density. Biomacromolecules. 2017;18(12):4331–40.
131. DiGirolamo C, Stokes D, Colter D, Phinney D, Class R, Prockop D. Propagation and senescence of human marrow stromal cells in culture: a simple colony-forming assay identifies samples with the greatest potential to propagate and differentiate. Br J Haematol. 2001;107(2):275–81.
132. Im GI, Shin YW, Lee KB. Do adipose tissue-derived mesenchymal stem cells have the same osteogenic and chondrogenic potential as bone marrow-derived cells? Osteoarthr Cartil. 2005;13:845–53.
133. Luby A, Ranganathan K, Lynn J, Nelson N, Donneys A, Buchman S. Stem cells for bone regeneration: current state and future directions. J Craniofac Surg. 2019;30(3):730–5.
134. Follmar K, Prichard H, DeCroos F, Wang H, Levin L, Klitzman B, et al. Combined bone allograft and adipose-derived stem cell autograft in a rabbit model. Ann Plast Surg. 2007;58(5):561–5.
135. Kubo M, Sonoda Y, Muramatsu R, Usui M. Immunogenicity of human amniotic membrane in experimental xenotransplantation. Invest Ophthalmol Vis Sci. 2001;42:1539–46.
136. Hutson E, Boyer S, Genever P. Rapid isolation, expansion, and differentiation of osteoprogenitors from full-term umbilical cord blood. Tissue Eng. 2005;11(9–10):1407.
137. Ventola CL. Medical applications for 3D printing: current and projected uses. Pharm Ther. 2014;39(10):704–11.
138. Graney PL, Zreiqat H, Spiller KL, Spiller KL. In vitro response of macrophages to ceramic scaffolds used for bone regeneration. J R Soc Interface. 2016;13:20160346.
139. Witherel CE, Yu T, Concannon M, Dampier W, Spiller K. Immunomodulatory effects of human cryopreserved viable amniotic membrane in a pro-inflammatory environment in vitro. Cell Mol Bioeng. 2017;10:451.
140. Weingarten MS, Witherel CE, Spiller KL, Graney PL, Freytes DO. Response of human macrophages to wound matrices in vitro. Wound Repair Regen. 2016;24(3):514–24.
141. Spiller KL, Anfang RR, Spiller KJ, Ng J, Nakazawa KR, Daulton JW, et al. The role of macrophage phenotype in vascularization of tissue engineering scaffolds. Biomaterials. 2014;35(15):4477–88. https://doi.org/10.1016/j.biomaterials.2014.02.012.
142. Go YY, Kim SE, Cho GJ, Chae S, Song J. Differential effects of amnion and chorion membrane extracts on osteoblast-like cells due to the different growth factor composition of the extracts. PLoS One. 2017;12(8):1–20.

143. Go YY, Kim SE, Cho GJ, Chae S-W, Song J-J. Promotion of osteogenic differentiation by amnion/chorion membrane extracts. J Appl Biomater Funct Mater. 2016;14(2):e171–80.
144. Carano R, Filvaroff E. Angiogenesis and bone repair. Drug Discov Today. 2003;8(21):980–9.
145. Ngo M, Harley B. The influence of hyaluronic acid and glioblastoma cell coculture on the formation of endothelial cell networks in gelatin hydrogels. Adv Healthc Mater. 2017;6(22)
146. Devescovi V, Leonardi E, Ciapetti G, Cenni E. Growth factors in bone repair. Chir Organi Mov. 2008;92:161–8.
147. Laflamme C, Curt S, Rouabhia M. Epidermal growth factor and bone morphogenetic proteins upregulate osteoblast proliferation and osteoblastic markers and inhibit bone nodule formation. Arch Oral Biol. 2010;55(9):689–701.
148. Yun Y-R, Jang JH, Jeon E, Kang W, Lee S, Won J-E, et al. Administration of growth factors for bone regeneration. Regen Med. 2012;7(3):369.
149. Hossain M, Irwin R, Baumann M, McCabe L. Hepatocyte growth factor (HGF) adsorption kinetics and enhancement of osteoblast differentiation on hydroxyapatite surfaces. Biomaterials. 2005;26(15):2595–602.
150. Kawasaki T, Niki Y, Miyamoto T, Horiuchi K, Matsumoto M, Aizawa M, et al. The effect of timing in the administration of hepatocyte growth factor to modulate BMP-2-induced osteoblast differentiation. Biomaterials. 2010;31(6):1191–8.
151. Deng M, Zhang B, Wang K, Liu F, Xiao H, Zhao J, et al. Mechano growth factor E peptide promotes osteoblasts proliferation and bone-defect healing in rabbits. Int Orthop. 2011;35(7):1099–106.
152. Dai Z, Wu F, Yeung E, Li Y. IGF-IEc expression, regulation and biological function in different tissues. Growth Hormon IGF Res. 2010;20(4):275–81.
153. Young CS, Bradica G, Hollinger JO. Preclinical toxicology studies of recombinant human platelet-derived growth factor-bb either alone or in combination with beta-tricalcium phosphate and type I collagen. J Tissue Eng. 2011;2010:246215.
154. Chang P-C, Seol Y-J, Cirelli J, Pellegrini G, Jin Q, Franco L, et al. PDGF-B gene therapy accelerates bone engineering and oral implant osseointegration. Gene Ther. 2010;17:95–104.
155. Andrew J, Hoyland J, Andrew S, Freemont A, Marsh D. Demonstration of TGF-β1 mRNA by in situ hybridization in normal human fracture healing. Calcif Tissue Int. 1993;52(2):74–8.
156. Bourque W, Gross M, Hall B. Expression of four growth factors during fracture repair. Int J Dev Biol. 1993;37(4):573–9.
157. Cheng H, Jiang W, Phillips F, Haydon R, Peng Y, Zhou L, et al. Osteogenic activity of the fourteen types of human bone morphogenetic proteins (BMPs). J Bone Jt Surg Am. 2003;85(8):1544–52.
158. Krishnakumar GS, Roffi A, Reale D, Kon E, Filardo G. Clinical application of bone morphogenetic proteins for bone healing: a systematic review. Int Orthop. 2017;41(6):1073–83.
159. Chen W-J, Jingushi S, Aoyama I, Anzai J, Hirata G, Tamura M, et al. Effects of FGF-2 on metaphyseal fracture repair in rabbit tibiae. J Bone Miner Metab. 2004;22(4):303–9.
160. Draenert G, Draenert K, Tischer T. Dose-dependent osteoinductive effects of bFGF in rabbits. Growth Factors. 2009;27(6):419–24.
161. Mitlak B, Finkelman R, Hill E, Li J, Martin B, Smith T, et al. The effect of systemically administered PDGF-BB on the rodent skeleton. J Bone Miner Res. 1996;11(2):238.
162. Marden L, Ran R, Pierce G, Reddi A, Hollinger J. Platelet-derived growth factor inhibits bone regeneration induced by osteogenin, a bone morphogenetic protein, in rat craniotomy defects. J Clin Inven. 1993;92(6):2897–905.
163. Chung C, Kim D, Park Y, Nam K, Lee S. Biological effects of drug-loaded biodegradable membranes for guided bone regeneration. J Peridontal Res. 1997;32:172–5.
164. Schliephake H. Bone growth factors in maxillofacial skeletal reconstruction. Int J Oral Maxillofac Surg. 2002;31:469–84.
165. Canalis E. Growth factor control of bone mass. J Cell Biochem. 2009;108:769–77.
166. Specer E, Liu C, Si E, Howard G. In vivo actions of insulin-like growth factor-I (IGF-I) on bone formation and resorption in rats. Bone. 1991;12:21–6.

167. Akeno N, Robins J, Zhang M, Czyzyk-Krzeska M, Clemens T. Induction of vascular endothelial growth factor by IGF-I in osteoblast-like cells is mediated by the PI3K signaling pathway through the hypoxia-inducible factor-2alpha. Endocrinology. 2002;143(2):420–5.
168. Meinel L, Zoidis E, Zapf J, Hassa P, Hottiger M, Auer J, et al. Localized insulin-like growth factor I delivery to enhance new bone formation. Bone. 2003;33(4):660–72.
169. Hayrapetyan A, Jansen JA, van den Beucken JJJP. Signaling pathways involved in osteogenesis and their application for bone regenerative medicine. Tissue Eng Part B Rev. 2014;21(1):75–87.
170. Hong L, Tabata Y, Miyamoto S, Yamada K, Aoyama I, Tamura M, et al. Promoted bone healing at a rabbit skull gap between autologous bone fragment and the surrounding intact bone with biodegradable microspheres containing transforming growth factor-β1. Tissue Eng. 2004;6(4):331.
171. Yamamoto M, Tabata Y, Hong L, Miyamoto S, Hashimoto N, Ikada Y. Bone regeneration by transforming growth factor β1 released from a biodegradable hydrogel. J Control Release. 2000;64(1–3):133–42.
172. Street J, Bao M, DeGuzman L, Bunting S, Peale FJ, Ferrara N, et al. Vascular endothelial growth factor stimulates bone repair by promoting angiogenesis and bone turnover. Proc Natl Acad Sci U S A. 2002;99(15):9656–61.
173. Oryan A, Alidadi S, Moshiri A. Platelet-rich plasma for bone healing and regeneration. Expert Opin Biol Ther. 2016;16:213.
174. Zou J, Yuan C, Chunshen W, Cao C, Yang H. The effects of platelet-rich plasma on the osteogenic induction of bone marrow mesenchymal stem cells. Connect Tissue Res. 2014;55(4):304.
175. Raida M, Heymann A, Gunther C, Niederwieser D. Role of bone morphogenetic protein 2 in the crosstalk between endothelial progenitor cells and mesenchymal stem cells. Int J Mol Med. 2006;18:735–9.
176. Park JY, Shim JH, Choi S-A, Jang J, Kim M, Lee SH, et al. 3D printing technology to control BMP-2 and VEGF delivery spatially and temporally to promote large-volume bone regeneration. J Mater Chem B. 2015;2:5415–25.
177. Spiller KL, Nassiri S, Witherel CE, Anfang RR, Ng J, Nakazawa KR, et al. Sequential delivery of immunomodulatory cytokines to facilitate the M1-to-M2 transition of macrophages and enhance vascularization of bone scaffolds. Biomaterials. 2015;37:194–207.